

Lawrence Berkeley National Laboratory

Recent Work

Title

A NUMERICAL INVESTIGATION OF CONFINED TURBULENT SHEAR FLOWS

Permalink

<https://escholarship.org/uc/item/41j7z94t>

Author

Bernard, Peter Simon.

Publication Date

1976-12-01

U 0 0 0 4 6 0 0 2 4 7

LBL-5582

c.1

A NUMERICAL INVESTIGATION OF CONFINED
TURBULENT SHEAR FLOWS

Peter Simon Bernard
(Ph. D. thesis)

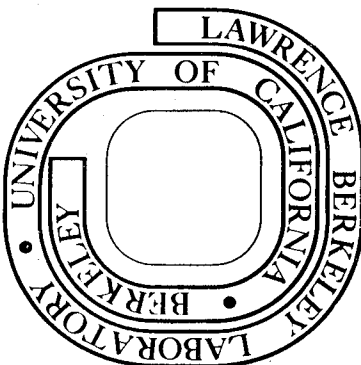
December 1976

RECEIVED
LIBRARY
DEC 22 1977
PHYSICS SECTION

Prepared for the U. S. Energy Research and
Development Administration under Contract W-7405-ENG-48

For Reference

Not to be taken from this room



LBL-5582
c.1

DISCLAIMER

This document was prepared as an account of work sponsored by the United States Government. While this document is believed to contain correct information, neither the United States Government nor any agency thereof, nor the Regents of the University of California, nor any of their employees, makes any warranty, express or implied, or assumes any legal responsibility for the accuracy, completeness, or usefulness of any information, apparatus, product, or process disclosed, or represents that its use would not infringe privately owned rights. Reference herein to any specific commercial product, process, or service by its trade name, trademark, manufacturer, or otherwise, does not necessarily constitute or imply its endorsement, recommendation, or favoring by the United States Government or any agency thereof, or the Regents of the University of California. The views and opinions of authors expressed herein do not necessarily state or reflect those of the United States Government or any agency thereof or the Regents of the University of California.

0 0 0 0 4 6 0 6 2 4 8

A NUMERICAL INVESTIGATION OF CONFINED TURBULENT SHEAR FLOWS

(Ph.D. Thesis)

Peter Simon Bernard

Lawrence Berkeley Laboratory
University of California
Berkeley, California 94720

December 1976

TABLE OF CONTENTS

I.	Introduction.....	1
II.	Historical Survey of Turbulence Closures.....	9
III.	The Method of Coarse Graining.....	16
	A. Turbulent Transport.....	17
	B. Mean Vorticity Equation.....	31
	C. The Equation for Mean Squared Fluctuating Vorticity...	32
	D. The Closure.....	38
IV.	The Turbulent Flow in a Channel.....	46
	A. Mean Vorticity Equation.....	48
	B. Equation for Mean Squared Fluctuating Vorticity.....	58
	C. Stream Function.....	70
	D. Computation of the Velocity Moments.....	71
	E. Results of Computations.....	74
V.	Flow in a Cylinder.....	89
	A. Difference Equations.....	95
	B. Computation of Stream Function, Mean Velocities and Velocity Moments.....	105
	C. Results of Computations.....	120
VI.	Conclusions and Future Work.....	127
VII.	Bibliography.....	130
VIII.	Figures.....	134

ACKNOWLEDGEMENT

I would like to express my appreciation to Professor Alexandre Chorin for the obvious and the intangible ways in which he has been a source of inspiration, illumination, and encouragement to me during the course of this work.

Also I wish to thank Professor Giles Corcos for his genuine interest in the success of this work and for his willing participation in some very helpful and stimulating conversations.

This work was performed under the auspices of the U.S. Energy Resources and Development Administration.

A NUMERICAL INVESTIGATION OF CONFINED TURBULENT SHEAR FLOWS

Peter Simon Bernard

ABSTRACT

The first objective of this work is to present a new derivation of the method of coarse graining for the computation of turbulent flows; one which strengthens and clarifies its theoretical foundation. Secondly, we show by the application of this method to the study of the turbulent flow in a channel and behind a piston in compressive motion that a promising start has been made toward acquiring the ability to predict the mean properties of turbulent flows. The work presented here is primarily concerned with two dimensional flow.

The principal improvement in the method of coarse graining consists of the establishment of a new general law of turbulent diffusion which applies to any scalar that is passively convected in a turbulent flow. The law is in the form of an expansion in roughly the Lagrangian integral time scale. The transport law is used to derive a closed set of equations for the mean vorticity and mean squared fluctuating vorticity. Other innovations include a more precise accounting of the effects of the local turbulence on the velocity moments and the use of an explicit equation for mean squared fluctuating vorticity instead of mean squared vorticity.

ACKNOWLEDGEMENT

I would like to express my appreciation to Professor Alexandre Chorin for the obvious and the intangible ways in which he has been a source of inspiration, illumination, and encouragement to me during the course of this work.

Also I wish to thank Professor Giles Corcos for his genuine interest in the success of this work and for his willing participation in some very helpful and stimulating conversations.

This work was performed under the auspices of the U.S. Energy Resources and Development Administration.

and the generation of turbulence at the piston face. The flow at two different stroke to bore ratios is studied, and an analysis is made of the flow environments that would exist at ignition.

I. INTRODUCTION

The advent of computers has brought hope that a "computational" answer may be found to the problem of finding a means of predicting the average behavior of a fluid in turbulent motion. The numerical methods that the computer has spawned, however, cannot be better than the theoretical foundations on which they are based. Thus, it is a sad fact that most numerical methods of computing the mean properties of turbulent flows in use today rely on theoretical notions about turbulent diffusion as manifested in the Reynolds stresses which have been known to be incorrect since before the first computer was built. Equally disturbing are some of the most recent numerical methods which rely on purely mathematical hypotheses and make no pretense of being based on a theory of turbulence at all.

It is ironic that such a state of affairs should exist at a time when many significant new advances have been made by experimentalists in revealing the nature of turbulent motion. One would hope that eventually this new knowledge would find its way into a mathematical form that would be useful in predicting the properties of a turbulent flow.

In point of fact, however, a rudimentary example of this procedure was performed by G. I. Taylor over sixty years ago in his vorticity transport theory. His idea, unfortunately was largely ignored, until a couple of years ago when Chorin (1974) showed how a numerical method of computing turbulent flows could be based on it. This method known as "the coarse grained approximation to turbulent motion" is innovative in both its respect for physical theory and for mathematical rigor.

This thesis will attempt to enrich the theory begun by Chorin and then apply it to the study of the turbulent flow in a channel and behind a piston in compressive motion. We hope to show that a promising start has been made toward acquiring an ability to predict the mean properties of turbulent flows.

The theory presented here will be concerned with two dimensional flows. A general theory of coarse graining which is applicable to three dimensional flows is currently under development. The study of two dimensional turbulence is useful because it is a model problem that contains many of the features of three dimensional flow yet is considerably easier to solve. Furthermore, the physical phenomena and mathematical difficulties that one encounters in two dimensions are either equivalent to or are simpler versions of the same problems that one encounters in three dimensions. Thus the application of a theory of turbulence to two dimensional flows is a useful first step in demonstrating its soundness.

In the method of coarse graining the average state of the (two dimensional) turbulent fluid is described by the mean vorticity, $\bar{\xi}$ and mean squared fluctuating vorticity, $\overline{\xi'^2}$. $\xi = \bar{\xi} + \xi'$ is the component of vorticity orthogonal to the plane of motion. A closed set of equations describing the evolution of the $\bar{\xi}$ and $\overline{\xi'^2}$ fields is derived using a simple statistical hypothesis involving certain functionals of the vorticity field. These equations may then be solved numerically.

Among the major theoretical improvements of the theory of coarse graining that are accomplished here are:

(i) The turbulent transport law has been derived in such a manner as to permit the computation of higher order terms and to give a physical interpretation of the parameters appearing in it.

(ii) The use of an explicit equation for $\overline{\xi^2}$ has been instituted replacing one for $\overline{\xi^2} + \overline{\xi'^2}$ used by Chorin. This allows an assessment to be made of the various factors contributing to the balance of $\overline{\xi^2}$.

(iii) The closure scheme is derived so as to now include the effect of the local turbulence intensity on the velocity moments.

(iv) An essentially exact boundary condition to the $\overline{\xi}$ equation is derived using the linear law of the wall.

(v) An extensive analysis of the balance of $\overline{\xi^2}$ in the wall region is made and is subsequently used to formulate a physically plausible difference equation for $\overline{\xi^2}$ near the wall.

With these improvements a fairly complete picture of the extent to which coarse graining can predict the mean properties of a two dimensional turbulent flow will emerge. The ways in which our theory is limited by the complexity of the small scale turbulent motion will be made apparent throughout this work. However each of these problems will be sharply defined and will provide an indication of the directions to which future work should be directed.

The restriction of two dimensionality has affected our numerical solution of the channel problem by giving predictions that are only partially in keeping with experiments. The results are closest, e.g. the mean vorticity distribution, (or mean velocity distribution) when the two dimensional equation does not exclude any important physical

process from being represented. They are poor when such a process is left out of the equations, e.g. our predictions of $\overline{\epsilon^2}$ is inaccurate and most likely because the production of $\overline{\epsilon^2}$ from vortex stretching and transfer is not included in the two dimensional equations.

On the whole, though, our restriction to two dimensions leaves enough of the physics of the flow in a channel intact so that we are still able to obtain some striking results. In particular is the friction law shown in Figure 8 which clearly displays a drag crisis at small Reynolds numbers and a bifurcation at a Reynolds number of approximately 6500 which separates the laminar from the turbulent flow regimes.

In the next chapter we will briefly describe the other approaches toward computing turbulent flows that may be found in use today. We will pay particular attention to the fundamental principles on which they are based and show how they differ from those of the present method.

In Chapter III we present a complete derivation of the method of coarse graining. The object of Section III.A. will be to derive the following turbulent diffusion law:

$$\begin{aligned} \overline{u_i \phi} = & - \left[\overline{u_i u_j} T_{ij} + \overline{u_i u_k} (S_{ik} - \tau T_{ik}) \frac{\partial u_j}{\partial x_k} \right] \frac{\partial \overline{\phi}}{\partial x_j} + \\ & \tau T_{ij} \overline{u_i u_j} \left[\frac{\partial^2 \overline{\phi}}{\partial x_j \partial t} + u_k \frac{\partial^2 \overline{\phi}}{\partial x_j \partial x_k} \right] + \\ & \frac{1}{2} \overline{u_i u_j u_k} T_{ijk} \frac{\partial^2 \overline{\phi}}{\partial x_j \partial x_k} \end{aligned} \quad (1.1)$$

where: ϕ is an arbitrary property of the fluid that satisfies the condition

$$\frac{D\phi}{Dt} = \frac{\partial\phi}{\partial t} + \vec{u} \cdot \nabla\phi = 0 ; \quad (1.2)$$

$\vec{u} = (u_1, u_2)$ is the velocity field; \vec{U} is the mean and \vec{u}' is the fluctuating part of the velocity field, so $\vec{u} = \vec{U} + \vec{u}'$; T_{ij} is a Lagrangian integral time scale; and τ , S_{ij} and T_{ijk} are other time scales which will be defined later. The right side of (1.1) is the first two terms of a series expansion in (roughly) the time scale T_{ij} .

It will be shown later that part of the special significance of the diffusion law (1.1) is that it accounts for the fact that the length and time scales of the small scale turbulent motion may be of the same order of magnitude as the scales at which the mean flow field varies significantly. (1.1) is most useful when the mean field is quasi-steady and quasi-homogeneous for then it is possible that we will only have to keep a small number of terms in the expansion to approximate the flux accurately.

At points sufficiently far from a boundary in a two dimensional flow both ξ and ξ^2 approximately satisfy (1.2) and thus the transport law (1.1) may be used to compute the turbulent fluxes $\overline{u'_i \xi}$ and $\overline{u'_i \xi^2}$. These fluxes arise naturally in the formation of equations for $\overline{\xi}$ and $\overline{\xi^2}$ from the vorticity equation. In Sections III.B. and III.C. we will derive equations for $\overline{\xi}$ and $\overline{\xi^2}$, respectively, which use the lowest order form of (1.1):

$$\overline{u_i^1 \phi} = -T_{ij} \overline{u_i^1 u_j^1} \frac{\partial \overline{\phi}}{\partial x_j} \quad (1.3)$$

to represent the fluxes $\overline{u_i^1 \xi}$ and $\overline{u_i^1 \xi^2}$.

The closure of the system of equations derived in III.B. and III.C. is completed in Section III.D. when we show how the velocity moments $\overline{u_i^1 u_j^1}$ may be computed from a knowledge of the $\overline{\xi^2}$ field. The closed set of equations for $\overline{\xi}$ and $\overline{\xi^2}$ that are derived in this chapter may be approximated by finite difference equations which may in turn be solved numerically for a large class of two dimensional turbulent flows.

In Chapter IV we apply the method which is described in Chapter III to a study of the fully developed turbulent flow in a channel. For this flow all of the second order terms in the transport law (1.1) are identically equal to zero so our use of the first order form of the transport law is well justified in this case.

We obtain equations for $\overline{\xi}$ and $\overline{\xi^2}$ by specializing those derived in Chapter III to this flow and then construct difference approximations to them which relate the values of $\overline{\xi}$ and $\overline{\xi^2}$ at a discrete set of points spanning the channel. To find the proper form of the difference equations near the boundary we study the physics of the turbulent flow in a channel and show that this flow may be separated into two distinct regions: a thin dissipation zone near the wall where no production of $\overline{\xi^2}$ takes place and a core region where $\overline{\xi^2}$ is produced. We conclude that for the $\overline{\xi}$ equation at the boundary we must specify the average

flux of vorticity from the wall and compute it from the relation

$$\frac{1}{R} \frac{\partial \bar{\xi}}{\partial y} \Big|_{y=0} = \frac{1}{R} \frac{U_{\infty}^2}{\delta - \delta^2} \quad (1.4)$$

where y is a coordinate normal to the wall, R is a Reynolds number, δ is the distance from the wall of an arbitrary point within the viscous sublayer and U_{∞} is the mean velocity at δ . We also find that the proper boundary condition to the $\bar{\xi}^{\prime 2}$ equation is the specification of the rate at which $\bar{\xi}^{\prime 2}$ diffuses from the core region and into the dissipation region.

In the process of forming a closed system of equations for $\bar{\xi}$ and $\bar{\xi}^{\prime 2}$ it is necessary to introduce a small number of undetermined parameters, (for example the time scale T_{ij} in (1.3)), thus to solve our system of equations for the channel problem numerically we must assign values to them. We do this by fitting the computed and experimentally determined results for the flow at one particular Reynolds number. Then we are free to investigate the predictions of our numerical method for all of the remaining Reynolds numbers. We have studied the behavior of the mean velocity profiles, $\bar{\xi}$, $\bar{\xi}^{\prime 2}$ and the friction coefficient with the Reynolds number and these results are reported in Section IV.E.

In Chapter V we apply the theory of Chapter III to study the piston driven turbulent flow in a two dimensional model of an internal combustion engine cylinder. This represents the first application of

the method of coarse graining to a turbulent flow with a fully two dimensional mean velocity field. The flow we are concerned with here is even more complex than this since the mean properties are also non-steady and the fluid is undergoing a uniform compression.

To account for the changing size of the flow domain we have defined our discrete approximations to $\bar{\xi}$ and $\overline{\xi^2}$ on a grid which collapses uniformly as the fluid is compressed. The equations for $\bar{\xi}$ and $\overline{\xi^2}$ derived in Chapter III were purposefully kept general enough so as to accomodate the particular flow we encounter in this problem. Thus to form difference equations for $\bar{\xi}$ and $\overline{\xi^2}$ here we may directly use these equations.

The results of our computation of the flow during the compression stroke described in Chapter V are to be viewed as giving a qualitative description of this flow. As expected, large amounts of vorticity and turbulence are generated next to the wall as the piston moves and are subsequently magnified by the compressive motion. We give predictions of the mean state of the fluid in the cylinder at the time of ignition for two different stroke-to-bore ratios. It is seen that a considerably different combustion process would be expected to occur in each of these different flow environments.

II. HISTORICAL SURVEY OF TURBULENCE CLOSURES

The mean velocity field of a turbulent flow evolves in part due to the action of apparent stresses which arise from the random eddying motion of the fluid. These are the Reynolds stresses, a typical component of which, $-\overline{\rho u_i' u_j'}$ expresses the average flux of the i th component of momentum in the j th direction. The Reynolds' stresses appear as additional unknowns in the equations of motion, creating the need to either relate them to the other dependent variables or to introduce an additional set of equations which describe their change. The means by which a closed system of equations is obtained is termed a turbulence closure.

In this Chapter we will present a sketch of the history of the major trends in closure formation in use today, so as to show the origin of the present method and its relationship to the other approaches. Comprehensive surveys of many particular examples of closures, giving some indication of their merits and limitations may be found in Reynolds (1974) and (1976), Cebeci and Smith (1974), Mellor and Herring (1973) and Bradshaw (1972).

The turbulence closures that are found in use today may be separated into two broad categories: Those that, in loose analogy to the viscous stresses, relate the Reynolds stresses to the gradients of the mean velocity field through a constitutive relationship involving an eddy diffusivity, and those that do not. Most closures are of the first type, and part of what is distinctive about the closure that we will present in this paper, is, that it does not belong to this group.

The first type of closure apparently originated with Boussinesq (1877), in his proposal that for a unidirectional mean flow field $U(y)$, the Reynolds stress $-\overline{\rho u'v'}$ could be approximated in analogy to the viscous stress $\mu \frac{\partial U}{\partial y}$, viz:

$$-\rho \overline{u'v'} = A_T \frac{\partial U}{\partial y} \quad (2.1)$$

The "mixing coefficient" or "eddy diffusivity" A_T remained to be determined by some unspecified means.

A theory which purported to give a plausible value to the eddy diffusivity A_T appearing in (2.1) was subsequently developed by Prandtl (1925). His idea, known as the mixing-length theory, was based on the assumption that small particles of fluid in a turbulent flow would conserve their momentum while traveling a short distance, called a mixing-length. Using this physical model of turbulent momentum exchange, he was able to deduce an analytical expression for A_T . However, his result was incomplete in that it depended explicitly on the mixing length, which was yet to be determined.

The mixing-length theory was followed by the similarity hypothesis of von Karman (1930) which supposed that the velocity fluctuations at any point in a turbulent flow depended exclusively on the values of a local length and time scale. He was able to derive an expression for A_T identical to that of Prandtl, and in addition, give a formula for the mixing length. Left undetermined in von Karman's theory was one universal constant. An account of this theory and that of Prandtl's may be found in Schlichting (1968).

In the period in which the momentum based model (2.1) was on the ascendancy, an alternative closure not of the first category, was developed by G.I. Taylor (1915). Unaware of the work of Prandtl, he considered and then rejected the idea that a closure could be based on the assumption of momentum transport which was at the heart of the mixing-length theory. He could find no justification for the belief that the pressure variations in the flow would not have a considerable effect in altering the momentum of fluid particle when they moved, even over very short distances. Thus no appeal to an analogy with the molecular transport of momentum could be made.

Taylor instead proposed that in circumstances in which the turbulent fluid motion is preponderantly two dimensional, as is the case in a unidirectional flow, one could use the fact that the vorticity of fluid particles is preserved in two dimensional inviscid motion to form a closure to the mean flow equations. He showed that the term containing the Reynolds stress - $\overline{\rho u'v'}$ in the mean momentum equation could be rewritten as the turbulent vorticity flux, $\overline{v'\xi}$. Introducing the concept of a vorticity mixing-length, say d , he derived for $\overline{v'\xi}$ the expression

$$\overline{v'\xi} = - \frac{1}{2} d \overline{|v'|} \frac{\partial \xi}{\partial y} \quad (2.2)$$

Though (2.2) is incomplete in that a means of estimating $\overline{|v'|}$ and d must still be found, in contrast to (2.1) the physical model behind it is much less open to criticism.

Later, Taylor (1932) generalized his vorticity transport theory so that it would apply to arbitrary three dimensional turbulent flows. Though the equations he derived were not in a form that could be used in practical applications, it is clear however, that at this time Taylor had a definite notion of the direction that should be pursued in obtaining a general turbulence closure.

Taylor (1932) had also learned of Prandtl's work with the mixing-length theory and made the first of several comparisons (see Taylor (1935b) and (1937)) between the predictions of his own vorticity transport theory and the theories of Prandtl and von Karman. He also provided new arguments, in addition to restating the one of 1915, which helped to cast doubt on the wisdom of postulating any similarity between turbulent and molecular transport of momentum.

In spite of the criticism by Taylor, the use of the expression (2.1) continued, though through his arguments, in part, it became increasingly clear that the justification for its use could no longer be obtained from the mixing-length theory. Perhaps the final words on the merits of the mixing-length theory, which laid it permanently to rest, (or should have), were made by Batchelor (1950) in a particularly cogent analysis. In this paper he established the principle that one must first understand the physics of the momentum exchange responsible for the Reynolds' stresses before deriving an analytical expression to gauge their magnitude. It is thus idle to speculate as to the correct analytical form of a closure based on a clearly erroneous physical model. Such has been the case with the mixing-length theory.

As we have suggested, closures of the type to which (2.1) belongs, are commonly found in use today. In particular, for general turbulent flows the use of the constitutive relationship

$$\overline{u_i' u_j'} = \frac{1}{3} \overline{u_k' u_k'} \delta_{ij} - K \frac{1}{2} \left(\frac{\partial U_i}{\partial x_j} + \frac{\partial U_j}{\partial x_i} \right) \quad (2.3)$$

where K is a function of various turbulent scales and flow variables, has become popular. Among those using either relationship (2.1) or (2.3) are Patankar and Spalding (1970), Cebeci and Smith (1974), Smagorinsky, et. al. (1965), Deardorff (1970), Saffman (1974) and Schumann (1975). Considering the widespread use of this type of closure there has continued to be a need to find a justification for it. Some attempts have been made up by Harlow (1968), Hirt (1969) and Daly and Harlow (1970). Perhaps the best approach toward giving credence to (2.1) but one which also limits the circumstances in which it is valid, is that discussed in Tennekes and Lumley (1972) p. 47. The idea behind their justification is roughly, that an expression like (2.1) is a necessary dimensional consequence of supposing that the characteristic times of the turbulent eddies and the mean flow are of the same order of magnitude. This is, incidentally, a simple example of the type of phenomenological reasoning which has been used to justify the more ambitious closure relation (2.3).

Accompanying the current use of relations (2.1) and (2.3) has been criticism of their use. Unfortunately, the arguments put forward against them have been generally much more convincing than those given

for them, e.g. see the criticisms of Tennekes and Lumley (1972) and Corrsin (1974).

The other types of closures, i.e., those that do not make an assumption such as (2.1) or (2.3) are not large in number. The approach which is most actively being pursued today is that of Reynolds stress equation modeling, see Launder, et.al. (1975), Hanjalic and Launder (1976) and Lumley and Khajeh-Nouri (1974), in which equations for the Reynolds stresses themselves are derived from the Navier-Stokes equations with the use of additional assumptions.

The exact equations for the Reynolds stresses involve triple velocity moments and pressure-velocity correlations which have to be approximated in terms of the Reynolds stresses and other mean quantities. The result is that a multitude of assumptions are now necessary to close the set of equations instead of just the one major assumption for the Reynolds stresses such as (2.3). Further, in current practice these new terms are approximated by mathematical expressions which are rarely, if ever, tied to any precise conception of the physical process which they are modeling. In view of the principle laid down by Batchelor that we have mentioned, the method of Reynolds stress equation modeling as it now stands is less justifiable than, say, the mixing-length theory, since at least the latter theory is based on some physical model, albeit an erroneous one.

The method of coarse graining which we will derive and put into practice in this paper was originated by Chorin (1974) and is related to the ideas of Taylor (1915) as expressed in his equation (2.2). We will

see that the closure used in this method is based on expressing mathematically two precise ideas about the physics of turbulent flow. The first of these concerns the transport of vorticity in a turbulent fluid and the second is the picture of a turbulent flow as being composed of many vortical structures. The major advance of Chorin was to show how these two ideas could be used to find an ingenious means of completing relation (2.2) by giving a new coefficient to the vorticity gradient $\frac{\partial \bar{\xi}}{\partial y}$, i.e. one which could be determined up to a constant from the equations of motion. This thesis will generalize the closure of Taylor and Chorin, and also clarify and improve the novel approach taken by Chorin to completing this closure.

III. THE METHOD OF COARSE GRAINING

In this chapter we consider the derivation of the method of coarse graining as it applies to an arbitrary two dimensional turbulent flow. The principal result of Section III.A is the derivation of eqn. (3.18) which is the general formula for the rate of turbulent diffusion of an arbitrary extensive property of a fluid that is preserved during the course of motion of fluid particles, and was written previously as eqn. (1.1). The simplified form, (3.19) or (1.3) of this relation is then used in Section III.B to aid us in deriving eqn. (3.25) which describes the balance of the mean vorticity field and in Section III.C to derive (3.36) for $\overline{\xi^2}$.

Section III.D explains how the velocity moments $\overline{u_i' u_j'}$ which are used in the transport law may be computed from a knowledge of the mean squared fluctuating vorticity field, thus forming a closure to our two coupled equations (3.25) and (3.36). The principle result of this section is the derivation of the three equations (3.46), (3.47) and (3.48) for $\overline{u'^2}$, $\overline{v'^2}$ and $\overline{u'v'}$ respectively.

Before beginning with the presentation of the method, we must establish some of the notation we will consistently use throughout this work. The spatial coordinates (x_1, x_2) will at times be denoted as (x, y) and similarly (u, v) is equivalent to (u_1, u_2) . Vectors are identified by an arrow overhead, and we will frequently use the notation $\vec{u}(x, y, t) = \vec{u}(\vec{x}, t)$, etc.

The mean or expected value of random flow variables is indicated either with a bar overhead or, when necessary, by use of the symbol

E[.]. The mean velocity field, however, will be indicated by the use of capitals, thus $\vec{u} = \vec{U} = (U, V)$. The fluctuating part of a random field is indicated by a prime, thus for example the velocity field \vec{u} may be written as the sum $\vec{U} + \vec{u}'$. The mean squared fluctuating vorticity field will henceforth be called $\zeta(\vec{x}, t)$, thus $\zeta = \overline{\xi'^2}$.

Vector operations will sometimes be indicated in symbols such as $\nabla \cdot \vec{u}$, and on other occasions as sums over indices, e.g. $\frac{\partial u_i}{\partial x_i}$, the summation convention always being in effect. Also, at times partial differentiation will be denoted in the manner: $u_t = \frac{\partial u}{\partial t}$ or $u_x = \frac{\partial u}{\partial x}$ etc.

All equations will be written in a nondimensional form in which a characteristic velocity and length have been used to scale the variables. R will denote a Reynolds number formed from this velocity and length. Dimensioned variables, when needed, will be defined as they arise, and usually are denoted by an asterisk.

A. Turbulent Transport

If $\phi(\vec{x}, t)$ represents the density of an arbitrary extensive property, ϕ , of an incompressible fluid, then $\overline{u'_i \phi}$ is the mean flux of ϕ due to the turbulent motion. This flux arises naturally in the process of forming an equation which describes the mean field $\overline{\phi}$, from a conservation equation for ϕ of the form

$$\frac{D\phi}{Dt} = \frac{\partial \phi}{\partial t} + \vec{u} \cdot \nabla \phi = \dots$$

The best known example of this is the case $\phi = \rho \vec{u}$ where $\rho \vec{u}$ is the density of momentum, for then the flux of momentum is $\overline{\rho \vec{u} \vec{u}}$ which is (minus) the Reynolds stress. Another example, occurring in a two dimensional flow, is $\phi = \xi$ the vorticity which is the "density" of circulation. Here, $\overline{u_i \xi}$ is the flux of circulation, conventionally called the flux of vorticity.

In some turbulent flow situations it may happen that the total amount of a property ϕ in any volume of fluid will not change as this clump of fluid moves in the velocity field \vec{u} . In this case

$$\frac{D\phi}{Dt} = 0 \quad (3.1)$$

and this relation may be used to derive a formula for the turbulent flux $\overline{u_i \phi}$, which is used in predicting the behavior of the mean field $\bar{\phi}$, as we shall now show.

Let $\vec{x}(\vec{x}_0, t)$ represent the trajectory of a fluid particle known to be at a position \vec{x}_0 at the time t_0 , i.e.

$$\vec{x}(\vec{x}_0, t_0) = \vec{x}_0 \quad (3.2)$$

Using $\vec{x}(\vec{x}_0, t)$, we may form the following equivalent, integrated, version of (3.1):

$$\phi(\vec{x}(\vec{x}_0, t), t) = \phi(\vec{x}_0, t_0). \quad (3.3)$$

$\vec{x}(\vec{x}_0, t)$ by its definition satisfies the integral equation

$$\vec{x}(\vec{x}_0, t) = \vec{x}_0 + \int_{t_0}^t \vec{u}(\vec{x}(\vec{x}_0, s), s) ds \quad (3.4)$$

For each realization of the field $\vec{u}(\vec{x}, t)$ the path $\vec{x}(\vec{x}_0, t)$ will be different, thus $\vec{x}(\vec{x}_0, t)$ is a random function. For definitions of a random function and its realizations, see Gikhman and Skorohod (1965).

Let τ represent a small time interval and let the position of the particle at $t_0 - \tau$ be \vec{a} , i.e. $\vec{x}(\vec{x}_0, t_0 - \tau) = \vec{a}$. \vec{a} is thus a random point. Using (3.3) evaluated at $t_0 - \tau$ we have for the flux $\overline{u_i \phi}$

$$\begin{aligned} \overline{u_i \phi} &= \overline{u_i \phi(\vec{a}, t_0 - \tau)} \\ &= \overline{u_i \phi(\vec{a}, t_0 - \tau)} + \overline{u_i \phi'(\vec{a}, t_0 - \tau)} \end{aligned} \quad (3.5)$$

where all variables are evaluated at the point (\vec{x}_0, t_0) unless otherwise indicated, thus e.g. $u_i = u_i(\vec{x}_0, t_0)$ in (3.5). The first term on the right of (3.5) does not drop out owing to the randomness of \vec{a} . We now

will explain, in turn, the nature of the contributions that are being made to the flux of ϕ by each of the two terms in (3.5).

The first term arises from the correlation between the fluctuating velocity at (\vec{x}_0, t_0) and the value of ϕ at the point in space-time convected there during the interval τ . The diffusive properties of this term may be revealed by the following construction:

Define $\vec{u}(t) = \vec{u}(\vec{x}(\vec{x}_0, t), t)$ and similarly for $U(t)$ and $u'(t)$.

Further, let

$$\vec{L} \equiv \int_{t_0 - \tau}^{t_0} \vec{u}(s) ds$$

Using \vec{L} and the definition of \vec{a} , (3.4) evaluated at $t_0 - \tau$ gives $\vec{a} = \vec{x}_0 - \vec{L}$. Substituting this expression for \vec{a} into $\bar{\phi}(\vec{a}, t_0 - \tau)$ and partially expanding in Taylor's series about (\vec{x}_0, t_0) we attain

$$\overline{u'_i \bar{\phi}(\vec{a}, t_0 - \tau)} = -\overline{u'_i L_j} \frac{\partial \bar{\phi}}{\partial x_j} + \tau \overline{u'_i L_j} \frac{\partial^2 \bar{\phi}}{\partial x_j \partial t} + \frac{1}{2} \overline{u'_i L_j L_k} \frac{\partial^2 \bar{\phi}}{\partial x_j \partial x_k} + O(\tau^3)$$

(3.6)

From this point on we will refrain from indicating the presence of terms of order higher than τ^2 , and will drop them without comment as they arise in the ensuing equations. These higher order terms may be computed also, though beyond the point we have gone this becomes a

rather tedious undertaking. We keep as many terms as we do, because, as we shall see, τ will be chosen to be not very much smaller than unity.

To put (3.6) into usable form we must examine the quantities $\overline{u'_i L_j}$ and $\overline{u'_i L_j L_k}$. Define

$$\overline{L_j} = \int_{t_0 - \tau}^{t_0} U_j(s) ds$$

and

$$L'_j = \int_{t_0 - \tau}^{t_0} u'_j(s) ds$$

thus $L_j = \overline{L_j} + L'_j$. Note that $\overline{L_j}$ is random owing to its dependence on the random path $\vec{x}(\vec{x}_0, t)$. Substituting for L_j in $\overline{u'_i L_j}$ we find

$$\overline{u'_i L_j} = \overline{u'_i \overline{L_j}} + \overline{u'_i L'_j} \quad (3.7)$$

Using the definition of L'_j the second term on the right hand side of (3.7) becomes

$$\begin{aligned} \overline{u'_i L'_j} &= E \left[u'_i \int_{t_0 - \tau}^{t_0} u'_j(s) ds \right] = \overline{u'_i u'_j} \int_{t_0 - \tau}^{t_0} R_{ij}(s - t_0) ds \\ &= \overline{u'_i u'_j} \int_0^{\tau} R_{ij}(s) ds \end{aligned} \quad (3.8)$$

where

$$R_{ij}(s) \equiv \frac{u_i'(t_0)u_j'(t_0+s)}{u_i'(t_0)u_j'(t_0)}$$

$R_{ij}(s)$ is a Lagrangian auto-correlation function, a special case of which was originally defined by Taylor (1921), see also Hinze (1959) p. 47. The final step in obtaining (3.8) required making the assumption that $R_{ij}(-t) = R_{ij}(t)$ for $0 \leq t \leq \tau$ which holds if the turbulence may be considered to be approximately stationary over a time period of $O(\tau)$.

For τ large enough, say $\tau \geq \tau^*$, $R_{ij}(\tau)$ is approximately zero, implying that $\int_0^\tau R_{ij}(s)ds$, $\tau \geq \tau^*$, is independent of τ . If we define the Lagrangian integral time scale

$$T_{ij} \equiv \int_0^\infty R_{ij}(s)ds \quad (3.9)$$

then for $\tau \approx \tau^*$, $T_{ij} \approx \int_0^\tau R_{ij}(s)ds$ and (3.8) becomes

$$\overline{u_i' L_j'} = T_{ij} \overline{u_i' u_j'} \quad (3.10)$$

Note that no summation is implied in (3.10) or in similar relations to follow which involve T_{ij} or other time constants still to be defined. Note also that it is possible that T_{ij} varies in space or time in a particular flow if the turbulence is nonuniform or nonstationary.

Returning to the first term on the right side of (3.7) we have

$$\overline{u_i' \bar{L}_j} = E \left[u_i' \int_{t_0 - \tau}^{t_0} U_j(s) ds \right]$$

and Taylor's expansion of $U_j(s)$ about (\vec{x}_0, t_0) yields

$$\begin{aligned} \overline{u_i' \bar{L}_j} &= E \left[u_i' U_j + u_i' \int_{t_0 - \tau}^{t_0} (x_k(s) - x_k) ds \frac{\partial U_j}{\partial x_k} + u_i' \int_{t_0 - \tau}^{t_0} (s - t_0) ds \frac{\partial U_j}{\partial t} \right] \\ &= \frac{\partial U_j}{\partial x_k} E \left[u_i' \int_{t_0 - \tau}^{t_0} ds (x_k(s) - x_k) \right] \end{aligned} \quad (3.11)$$

where x_k is the k th component of \vec{x}_0 . Through the use of (3.4) for $x_k(s) - x_k$, the integral in (3.11) becomes

$$\int_{t_0 - \tau}^{t_0} (x_k(s) - x_k) ds = \int_{t_0 - \tau}^{t_0} ds \int_{t_0}^s ds' u_k(s') = - \int_{t_0 - \tau}^{t_0} ds' \int_{t_0 - \tau}^{s'} ds u_k(s')$$

$$= - \int_{t_0 - \tau}^{t_0} ds' (s' - t_0 + \tau) u_k(s')$$

Substituting (3.12) into (3.11) after replacing $u_k(s')$ by $U_k(s') + u'_k(s')$ gives

$$\begin{aligned}
 \overline{u'_i L_j} &= -\frac{\partial U_j}{\partial x_k} E \left[u'_i \int_{t_0-\tau}^{t_0} ds' (s'-t_0+\tau) u'_k(s') + u'_j \int_{t_0-\tau}^{t_0} ds' (s'-t_0+\tau) U_k(s') \right] \\
 &= -\overline{u'_i u'_k} \frac{\partial U_j}{\partial x_k} \int_{t_0-\tau}^{t_0} ds' (s'-t_0+\tau) R_{ik}(s'-t_0) \\
 &= -\overline{u'_i u'_k} \frac{\partial U_j}{\partial x_k} \int_0^\tau (\tau-s) R_{ik}(s) ds
 \end{aligned} \tag{3.13}$$

In light of our assumption on τ , (3.13) becomes

$$\overline{u'_i L_j} = \overline{u'_i u'_k} (S_{ik} - \tau T_{ik}) \frac{\partial U_j}{\partial x_k} \tag{3.14}$$

where

$$S_{ik} \equiv \int_0^\infty s R_{ik}(s) ds$$

Combining (3.10) and (3.14) yields the result

$$\overline{u'_i L'_j} = \overline{u'_i u'_j} T_{ij} + \overline{u'_i u'_k} (S_{ik} - \tau T_{ik}) \frac{\partial U_j}{\partial x_k} \quad (3.15)$$

The analysis of $\overline{u'_i L'_j L'_k}$ is considerably longer than that of $\overline{u'_i L'_j}$, so we will only quote the result: To third order,

$$\overline{u'_i L'_j L'_k} = \tau U_j \overline{u'_i u'_k} T_{ik} + \tau U_k \overline{u'_i u'_j} T_{ij} + \overline{u'_i u'_j u'_k} T_{ijk} \quad (3.16)$$

where

$$T_{ijk} \equiv \int_0^\infty ds_1 \int_0^\infty ds_2 R_{ijk}(s_1, s_2)$$

and

$$R_{ijk}(s_1, s_2) \equiv \frac{\overline{u'_i(t_0) u'_j(t_0 + s_1) u'_k(t_0 + s_2)}}{\overline{u'_i u'_j u'_k}}$$

We have made use of the additional assumption that the condition

$R_{ijk}(-s_1, -s_2) = R_{ijk}(s_1, s_2)$ holds.

(3.6) is completed by substituting (3.15) and (3.16) into it, though we will not write out this intermediate result. To obtain our

final expression for the flux $\overline{u'_i \phi}$ we must look into the second term on the right of (3.5).

In view of our hypothesis about τ , we must have $R_{ij}(\tau) \approx 0$ which implies that $\overline{u'_i(\vec{x}_0, t_0) u'_j(\vec{a}, t_0 - \tau)} \approx 0$. We then suppose that the absence of a significant correlation between velocity components at (\vec{x}_0, t_0) and $(\vec{a}, t_0 - \tau)$ implies that u'_i at (\vec{x}_0, t_0) and ϕ' at $(\vec{a}, t_0 - \tau)$ are similarly uncorrelated. This is, of course, not a rigorously derived statement, but it is very reasonable if one considers that velocity-velocity correlations are usually the most enduring ones. The difficulty we face here is one that will encounter again and is due to our lack of understanding of the action of the small scale turbulent motion. This ignorance is actually a blessing in this case because if we cannot conceive of a physical mechanism which would result in a non-negligible correlation between $u'_i(\vec{x}_0, t_0)$ and $\phi'(\vec{a}, t_0 - \tau)$, then there is no reason to doubt our conclusion that

$$\overline{u'_i(\vec{x}_0, t_0) \phi'(\vec{a}, t_0 - \tau)} = 0 \quad (3.17)$$

We may also eliminate the possibility that viscosity promotes a strong correlation, because for all the cases we consider, the distance $|\vec{L}| \gg \sqrt{\tau/R}$, where $\sqrt{\tau/R}$ is the distance over which it is reasonable to assume that the viscosity exerts a strong influence during the time interval τ .

We are now in a position to assemble our various results and state the general diffusion law:

$$\begin{aligned} \overline{u_i \phi} = & \left[\overline{u_i u_j'} T_{ij} + \overline{u_i u_k'} (S_{ik} - \tau T_{ik}) \frac{\partial u_j}{\partial x_k} \right] \frac{\partial \overline{\phi}}{\partial x_j} + \\ & \tau T_{ij} \overline{u_i u_j'} \left[\frac{\partial^2 \overline{\phi}}{\partial x_j \partial t} + U_k \frac{\partial^2 \overline{\phi}}{\partial x_j \partial x_k} \right] + \\ & \frac{1}{2} \overline{u_i u_j u_k'} T_{ijk} \frac{\partial^2 \overline{\phi}}{\partial x_j \partial x_k} \end{aligned} \quad (3.18)$$

which is valid for any field ϕ satisfying (3.1). It may easily be seen that (3.18) is invariant under a Galilean transformation.

The time scale T_{ij} is characteristic of the typical eddies in the turbulent flow. If the time over which the mean properties of the turbulent flow varies significantly is comparable to T_{ij} then the higher order terms on the right of (3.18) will make a significant contribution to the transport law and must be included. A similar conclusion should also hold for the length scales of the mean and eddying motion. That the transport law we have derived can accommodate these situations is a strong point in its favor.

The right side of (3.18) depends on the parameter τ which must only satisfy the condition $\tau \geq \tau^*$ and thus is largely arbitrary. Since the left side of (3.18) is independent of τ so too must the right side. This apparent contradiction can be explained by realizing that the larger τ is, the more terms in the expression on the right must be included. The sum of these terms always remains constant.

To first order (3.18) gives a simple mean gradient diffusion law:

$$\overline{u_i \phi} = -T_{ij} \overline{u_i u_j} \frac{\partial \bar{\phi}}{\partial x_j} \quad (3.19)$$

In our applications of the method we will only use this lowest order term. This will not introduce serious errors into the results as long as the second and higher order derivatives of the mean field $\bar{\phi}$ are not large.

For the special case in which ϕ is the vorticity, ξ , and $\bar{\xi}$ and U depend only on y , and $V = 0$, e.g. in fully developed channel flow, then (3.18) reduces to

$$\overline{v \xi} = -T_{22} \overline{v^2} \frac{\partial \bar{\xi}}{\partial y} + \frac{1}{2} T_{222} \overline{v^3} \frac{\partial^2 \bar{\xi}}{\partial y^2} \quad (3.20)$$

If we assume that $\overline{v^3} = 0$, for this flow then this further reduces to

$$\overline{v \xi} = -T_{22} \overline{v^2} \frac{\partial \bar{\xi}}{\partial y} \quad (3.21)$$

which is accurate to third order in τ .

For the piston problem it will be necessary to generalize our diffusion law slightly so as to accommodate the diffusion of vorticity and squared vorticity in the type of compressible flow which occurs there. We will assume for that problem that the density is a sure

function which varies with time, uniformly throughout the flow field. The dilatation $\theta = \nabla \cdot \vec{u}$ in this case depends on the time, and from the continuity equation we have

$$\theta(t) = \frac{-1}{\rho} \frac{d\rho}{dt}$$

The vorticity equation without the viscous term is then,

$$\frac{D\xi}{Dt} + \xi\theta = 0$$

and the integrated version of this relation, which corresponds to (3.3) is

$$\xi(\vec{x}_0, t_0) = \frac{\rho(t_0)}{\rho(t)} \xi(\vec{x}(\vec{x}_0, t), t) \quad (3.22)$$

which may easily be verified by differentiation. It is clear that (3.22) will yield the same diffusion law as before, except for an additional factor of $\rho(t_0)/\rho(t_0 - \tau)$. However

$$\frac{\rho(t_0)}{\rho(t_0 - \tau)} = 1 + \tau\theta + O(\tau^2)$$

thus if only first order terms are to be kept in (3.18) we may still use the diffusion law (3.19) in this case.

Similarly, the equation comparable to (3.3) for the squared vorticity will be (3.22) squared, thus implying that the additional factor $(\rho(t_0)/\rho(t_0-\tau))^2$ appears in the diffusion law and again exerts no influence on the lowest order terms.

The machinery we have developed to examine the turbulent flux $\overline{u'_1 \phi}$, might also be profitably applied to finding out if there is any justification for the Boussinesq approximation, (2.1), to the Reynolds stress $-\overline{\rho u' v'}$. Thus, consider a unidirectional mean flow $(U(y), 0)$ for which we wish to find an expression for the flux of momentum in the y direction due to the fluctuations v' . The density ϕ is in this case ρu which satisfies Euler's equation

$$\frac{D(\rho u)}{Dt} = -\frac{\partial p}{\partial x}$$

and not an equation like (3.1), so we must make special account of this difference. In analogy to (3.3) ρu also satisfies the relation

$$\rho u(\vec{x}_0, t_0) = \rho u(\vec{x}(\vec{x}_0, t), t) + \int_{t_0}^t \frac{\partial p}{\partial x}(\vec{x}(\vec{x}_0, s), s) ds$$

0 0 0 0 4 6 0 0 2 6 5

Following the same sequence of steps as before we will arrive at

$$-\overline{\rho u'v'} = \rho T_{22} \overline{v'^2} \frac{\partial U}{\partial y} + \int_{t_0-\tau}^{t_0} \overline{v'(\vec{x}_0, t_0) \frac{\partial p}{\partial x}(\vec{x}(\vec{x}_0, s), s)} ds \quad (3.23)$$

where the term $\overline{v'(\vec{x}_0, t_0) u'(\vec{a}, t_0 - \tau)}$ was dropped since as already described it is essentially zero. (3.23) will provide some justification for (2.1) if one could show that the last term involving the pressure is much smaller than the first.

The technique of this section can provide no justification for the use of the general constitutive relationship (2.3) since the correlation one wishes to compute will also appear as a coefficient of some of the derivatives of the mean velocity field found in the transport law.

B. Mean Vorticity Equation

The vorticity equation for a two dimensional flow in which the density of the fluid is spatially uniform but may vary in time is

$$\xi_t + \vec{u} \cdot \nabla \xi + \xi \theta = \frac{1}{R} \nabla^2 \xi$$

An equation for the mean vorticity may be derived by substituting into this relation $\bar{\xi} + \xi'$ for ξ , $\vec{U} + \vec{u}'$ for \vec{u} and then averaging. The result is

$$\overline{\xi_t} + \vec{U} \cdot \nabla \overline{\xi} + \theta \overline{\xi} + \nabla \cdot \overline{u' \xi} = \frac{1}{R} \nabla^2 \overline{\xi} \quad (3.24)$$

where $\overline{u' \xi}$ is the flux of vorticity due to the turbulent motion. After transformation of this expression through use of the diffusion law (3.19), (3.24) becomes

$$\frac{\partial \overline{\xi}}{\partial t} = - \vec{U} \cdot \nabla \overline{\xi} - \theta \overline{\xi} + \frac{\partial}{\partial x_i} \left[\frac{1}{R} \frac{\partial \overline{\xi}}{\partial x_i} + T_{ij} \overline{u'_i u'_j} \frac{\partial \overline{\xi}}{\partial x_j} \right] \quad (3.25)$$

which is the general mean vorticity equation that will be used as the basis for difference equations in our applications.

C. The Equation for Mean Squared Fluctuating Vorticity

In the original formulation of the method of Coarse Graining by Chorin (1974) the evolution of the ζ field was computed from a set of difference equations which approximated the equation of conservation of mean squared vorticity, $\overline{\xi^2} = \overline{\xi}^2 + \zeta$. This approach obscures the relative magnitudes of the factors contributing to the balance of ζ . To remedy this we will formulate an explicit relation for ζ which will be used subsequently in the applications to derive difference equations.

The squared vorticity equation is obtained from the vorticity equation by multiplying it throughout by ξ , thus

$$\frac{1}{2} \frac{\partial \overline{\xi^2}}{\partial t} + \frac{1}{2} \vec{u} \cdot \nabla \overline{\xi^2} + \overline{\xi^2} \theta = \frac{1}{R} \overline{\xi \nabla^2 \xi}$$

Taking the average we find

$$\frac{1}{2} \frac{\partial}{\partial t} (\overline{\xi^2} + \zeta) + \frac{1}{2} \vec{U} \cdot \nabla (\overline{\xi^2} + \zeta) + \theta (\overline{\xi^2} + \zeta) + \frac{1}{2} \nabla \cdot \overline{\vec{u}' \xi'^2} = \frac{1}{R} \overline{\xi \nabla^2 \xi} + \frac{1}{R} \overline{\xi' \nabla'^2 \xi'}$$
(3.26)

Subtraction of $\overline{\xi}$ times the equation for mean vorticity (3.24), from this relation yields

$$\zeta_t = - \vec{U} \cdot \nabla \zeta - 2\theta \zeta - \overline{2\vec{u}' \xi \cdot \nabla \xi} - \overline{\nabla \cdot \vec{u}' \xi'^2} + \frac{1}{R} \nabla^2 \zeta - \frac{2}{R} \overline{\left(\frac{\partial \xi'}{\partial x_j} \right)^2}$$
(3.27)

which describes the evolution of the ζ field.

The physical interpretation of each of the terms on the right side of (3.27) is as follows: The first is the convection of ζ in the mean velocity field \vec{U} , and the next represents an increase or decrease of ζ corresponding to a similar change in the density of the fluid. The next two, as mentioned in Tennekes and Lumley (1972) p. 87 contribute respectively, to the production of ζ from the mean vorticity field, and to the diffusion of ζ due to the turbulent motion. The next to the last term represents molecular diffusion of ζ and the final term gives the dissipation of ζ due to the viscosity of the fluid.

The production and turbulent diffusion terms must be transformed using our diffusion law if they are to be in a usable form. The application of (3.19) to each of these terms will also have the pleasant

consequence of displaying their physical meaning directly. Thus, for the production term:

$$-\overline{2u'_i \xi} \frac{\partial \bar{\xi}}{\partial x_i} = 2 T_{ij} \overline{u'_i u'_j} \frac{\partial \bar{\xi}}{\partial x_i} \frac{\partial \bar{\xi}}{\partial x_j} \quad (3.28)$$

If we suppose that T_{ij} is roughly the same for each (i, j) , then

$$-\overline{2u'_i \xi} \frac{\partial \bar{\xi}}{\partial x_i} = 2 T_{ij} \overline{\left(u'_i \frac{\partial \bar{\xi}}{\partial x_i}\right)^2}$$

which is always positive and thus strictly represents production of ζ .

To transform the turbulent diffusion term we substitute the identity $\xi'^2 = \bar{\xi}^2 - 2\bar{\xi}\xi' - \bar{\xi}^2$ into it to obtain

$$-\nabla \cdot \overline{\vec{u}' \xi'^2} = -\nabla \cdot \overline{\vec{u}' \xi^2} + 2\nabla \cdot \overline{\xi \vec{u}' \xi} \quad (3.29)$$

Applying (3.19) to $\overline{\vec{u}' \xi^2}$ and $\overline{\vec{u}' \xi}$, (3.29) becomes

$$-\nabla \cdot \overline{\vec{u}' \xi'^2} = \frac{\partial}{\partial x_j} T_{ij} \overline{u'_i u'_j} \frac{\partial}{\partial x_j} (\bar{\xi}^2 + \zeta) - 2 \frac{\partial}{\partial x_i} \bar{\xi} T_{ij} \overline{u'_i u'_j} \frac{\partial \bar{\xi}}{\partial x_j} = \frac{\partial}{\partial x_j} T_{ij} \overline{u'_i u'_j} \frac{\partial \zeta}{\partial x_j} \quad (3.30)$$

which clearly reveals the diffusive nature of $-\nabla \cdot \overline{\vec{u}' \xi'^2}$.

The final term in (3.27) representing viscous dissipation must also be suitably transformed if we are to have a closed system of equations. We may do this only at the expense of introducing another parameter which is descriptive of the small scale turbulent motion. By definition

$$\frac{\partial \overline{\xi^2}}{\partial x}(x_0, y_0) = \lim_{x \rightarrow 0} \frac{\xi'(x_0+x, y_0) - \xi'(x_0, y_0)}{x}$$

so it is also true that

$$\begin{aligned} \overline{\xi_x^2} &= E \left[\lim_{x \rightarrow 0} \left[\frac{\xi'(x_0+x, y_0) - \xi'(x_0, y_0)}{x} \right]^2 \right] = \\ &\lim_{x \rightarrow 0} \frac{\overline{\xi^2}(x_0+x, y_0) + \overline{\xi^2}(x_0, y_0) - 2\xi'(x_0+x, y_0)\xi'(x_0, y_0)}{x^2} \end{aligned} \quad (3.31)$$

Let us define an Eulerian vorticity correlation function $R(\vec{x})$ by

$$R(\vec{x}) \equiv \frac{\overline{\xi'(x_0, y_0)\xi'(x_0+x, y_0+y)}}{\overline{\xi'^2}(x_0, y_0)} \quad (3.32)$$

where the dependence of $R(\vec{x})$ on \vec{x}_0 is to be understood. If we assume that the turbulence is locally homogeneous so that $\frac{\partial R}{\partial x}(0) = \frac{\partial R}{\partial y}(0) = 0$ then it is not hard to show that (3.31) leads to

$$\overline{\epsilon_x^2} = - \frac{\partial^2 R}{\partial x^2}(0) \overline{\epsilon^2}$$

A similar argument was used by Taylor (1935a) to derive an analogous result for the quantity $\left(\frac{\partial u_i}{\partial x_j}\right)$ which occurs as a dissipation term in the equation for turbulent kinetic energy. Taylor also initiated the practice of using $\frac{\partial^2 R}{\partial x^2}(0)$ to define a length scale λ_x , called a Taylor (vorticity) microscale. This length gives an indication of the extent of the smallest eddies that occur in the turbulent flow, and is defined as that distance from $x = 0$ at which a parabolic approximation to the function $R(x,0)$ about $x = 0$ is equal to 0. Since $R(0) = 1$ and $\frac{\partial R}{\partial x}(0) = 0$, we must have $R(x,0) \approx 1 + \frac{\partial^2 R}{\partial x^2}(0) \frac{x^2}{2}$ for very small x . Thus

$$\lambda_x^2 = \frac{-2}{\frac{\partial^2 R}{\partial x^2}(0)} \quad (3.33)$$

and then

$$\overline{\epsilon_x^2} = \frac{2\overline{\epsilon^2}}{\lambda_x^2} \quad (3.34)$$

A microscale λ_y similar to λ_x may be defined so as to allow us to express $\overline{\xi_y^2}$ by a relation analogous to (3.34). Defining a composite microscale λ_d by

$$\lambda_d^2 \equiv \frac{1}{2} \frac{\lambda_x^2 \lambda_y^2}{\lambda_x^2 + \lambda_y^2}$$

we have

$$\overline{\xi_x^2} + \overline{\xi_y^2} = \frac{\zeta}{\lambda_d^2} \quad (3.35)$$

It is clear from its definition that λ_d may vary throughout the flow field. We have as yet no means of predicting its value a priori, so its value will have to be assigned arbitrarily. It is possible that a precise connection between T_{22} and λ_d , for any particular turbulent flow does exist, but if it does, we have not found it.

Our final equation for ζ now follows from using (3.28), (3.30) and (3.35) in (3.27):

$$\begin{aligned} \frac{\partial \zeta}{\partial t} = & - \vec{U} \cdot \nabla \zeta - 2\theta \zeta + 2 T_{ij} \overline{u_i' u_j'} \frac{\partial \overline{\xi}}{\partial x_i} \frac{\partial \overline{\xi}}{\partial x_j} \\ & + \frac{\partial}{\partial x_i} \left(\frac{1}{R} \frac{\partial \zeta}{\partial x_i} + T_{ij} \overline{u_i' u_j'} \frac{\partial \zeta}{\partial x_j} \right) - \frac{2\zeta}{R \lambda_d^2} \end{aligned} \quad (3.36)$$

D. The Closure

The relations which govern the evolution of the mean vorticity and mean squared fluctuating vorticity fields, (3.25) and (3.36) depend explicitly on the velocity correlations $\overline{u_i u_j}$. In this section we will show how these may be computed in terms of the other dependent variables thus providing a closure to the turbulence equations.

The closure hinges directly on the statistical hypothesis formulated by Chorin (1974) to the effect that the averages of the vorticity over two disjoint regions of sufficient size in a turbulent flow may be considered to be independent random variables. An equivalent statement of this hypothesis is that the circulations of nonintersecting regions of a proper extent are independent. For completeness, we will mention two of the reasons why we expect this postulate to be true.

In the first place, the turbulent flow within or near boundaries is believed to be comprised of many small vortices. The positions and intensities of these vortices are correlated through the evolution of the turbulent flow as a whole. The mutual dependence between a pair of vortices, one in each of two disjoint regions is obscured when the circulation in these areas are computed by summing the circulations of their respective vortices. In this manner the composite circulations may be deemed to be independent.

A second argument in support of the statistical assumption can be seen by discussing the reason why we would not expect an analogous hypothesis to hold for the averages of the velocity field over disjoint regions. The velocity of the fluid at a particular place and time

depends on the whole vorticity field at that instant. Thus the velocities at two different points have the possibility of being highly correlated owing to their mutual dependence on the vorticity field. The vorticity, on the other hand, is purely a function of the local state of the fluid.

In the previous section we defined the vorticity micro scales λ_x and λ_y . These lengths give an indication of the distance over which the vorticity field is highly correlated. It would seem likely that if the statistical hypothesis just cited was to be applied to two adjacent regions then each of them should be of an extent greater than λ_x and λ_y . We are careful not to suggest that this must be true because it is not clear to what extent averaging the vorticity over regions will wash out the local correlations of the vorticity field.

In addition to postulating that the circulations of the non-intersecting regions are independent of one another, Chorin further assumed that they are Gaussian random variables. This is a plausible idea which was used in the original derivation of the method, but it will not be necessary to make this assumption here.

We will now use the statistical hypothesis to derive an expression for $\overline{u'^2}$ in terms of the ζ field and thus achieve closure. The other velocity correlations are computed similarly.

We will compute $\overline{u'^2}$ for a point \vec{x} situated with regard to a grid as depicted in Figure 1. This is the situation that is typically found in practice. The flow domain has been divided into N boxes, $N > 0$. We supposed without loss of generality that each of the

boxes is a square with sides of length h . \vec{x}_i will represent the center of the i th box, and D_i the region occupied by it.

For the type of flow situation we are considering the velocity component \vec{u}' is incompressible and thus may be represented by a stream function ψ' . ψ' satisfies Poisson's equation $\nabla^2 \psi' = -\xi'$ with appropriate boundary conditions, e.g. ψ' is constant on a solid boundary. The solution of this equation may be written as

$$\psi'(\vec{x}) = - \int_D G(\vec{x}|\vec{x}') \xi'(x') d\vec{x}' \quad (3.37)$$

where $G(\vec{x}|\vec{x}')$ is the Green's function, $\vec{x}' = (x', y')$ and $d\vec{x}' = dx' dy'$.

Since $u' = \frac{\partial \psi'}{\partial y}$ we have

$$u'(\vec{x}) = - \int_D G_u(\vec{x}|\vec{x}') \xi'(\vec{x}') d\vec{x}' \quad (3.38)$$

where

$$G_u(\vec{x}|\vec{x}') \equiv \frac{\partial}{\partial y} G(\vec{x}|\vec{x}')$$

$G_u(\vec{x}|\vec{x}')$ is a sure function which is smooth for all values of \vec{x} and \vec{x}' except when $\vec{x} = \vec{x}'$ where it has a singularity.

Breaking up the integral in (3.38) into a sum of integrals over the boxes D_i we have

$$u'(\vec{x}) = - \sum_{i=1}^N \int_{D_i} G_u(\vec{x}|\vec{x}') \xi'(\vec{x}') d\vec{x}' \quad (3.39)$$

For all boxes D_i , except boxes D_1 and D_2 which are adjacent to the point \vec{x} in Figure 1, we may, with good accuracy, write

$$\int_{D_i} G_u(\vec{x}|\vec{x}') \xi'(\vec{x}') d\vec{x}' \approx G_u(\vec{x}|\vec{x}_i) \int_{D_i} \xi'(\vec{x}') d\vec{x}' \quad (3.40)$$

We cannot readily make this same approximation for D_1 and D_2 because of the singularity; $G_u(\vec{x}|\vec{x}')$ varies quite rapidly within these boxes.

However, it will be unnecessary for us to make this assumption for these boxes so long as we make the following additional hypothesis:

$\int_{D_j} G_u(\vec{x}|\vec{x}') \xi'(\vec{x}') d\vec{x}'$ $j=1,2$ is independent of $\int_{D_i} \xi'(\vec{x}') d\vec{x}'$, $i \neq 1,2$.

Note that our first statistical hypothesis was to the effect that

$\int_{D_i} \xi'(\vec{x}') d\vec{x}'$ and $\int_{D_j} \xi'(\vec{x}') d\vec{x}'$ were independent if $i \neq j$, so this second one is just an extension of the first.

Using (3.40) and the statistical hypotheses we find that

$$\overline{u^2} = \int_{D_1 \cup D_2 \times D_1 \cup D_2} G_u(\vec{x}|\vec{x}') G_u(\vec{x}|\vec{x}'') \overline{\xi'(\vec{x}') \xi'(\vec{x}'')} d\vec{x}' d\vec{x}'' + \quad (3.41)$$

$$\sum_{i \neq 1, 2} G_u^2(\vec{x}|\vec{x}_i) \int_{D_i \times D_i} \overline{\xi'(\vec{x}') \xi'(\vec{x}'')} d\vec{x}' d\vec{x}''$$

Using the vorticity correlation function $R(\vec{x})$ defined in eqn. (3.32) we can write the first integral on the right side of (3.41) as

$$\int_{D_1 \cup D_2 \times D_1 \cup D_2} G_u(\vec{x}|\vec{x}') G_u(\vec{x}|\vec{x}'') \zeta(\vec{x}') R(\vec{x}'' - \vec{x}') d\vec{x}' d\vec{x}'' \quad (3.42)$$

If we assume that the implicit dependence of $R(\vec{x}'' - \vec{x}')$ on \vec{x}' is unimportant and that $\zeta(\vec{x}') \approx \zeta(\vec{x})$ for the region $D_1 \cup D_2$ then expanding $R(\vec{x}'' - \vec{x}')$ in Taylor's series about $\vec{x}'' - \vec{x}' = 0$, (3.42) becomes

$$\zeta(\vec{x}) \int_{D_1 \cup D_2 \times D_1 \cup D_2} G_u(\vec{x}|\vec{x}') G_u(\vec{x}|\vec{x}'') \left[1 + (x'' - x') \frac{\partial R}{\partial x}(0) + (y'' - y') \frac{\partial R}{\partial y}(0) + \dots \right] d\vec{x}' d\vec{x}'' \quad (3.43)$$

In an unbounded domain

$$G_u(\vec{x}|\vec{x}') = -\frac{1}{2\pi} \frac{(y-y')}{(x-x')^2 + (y-y')^2}$$

(in a bounded domain we consider $G_u(\vec{x}|\vec{x}')$ to be augmented by contributions from image vortices) and if this is substituted into (3.43), and a coordinate change is made, (3.43) becomes

$$\zeta(\vec{x}) \frac{1}{(2\pi)^2} \int_{-h/2}^{h/2} dy' \int_{-h}^h dx' \int_{-h/2}^{h/2} dy'' \int_{-h}^h dx'' \frac{y'y''}{(x'^2+y'^2)(x''^2+y''^2)} \quad (3.44)$$

$$\left[1 + (x''-x') \frac{\partial R}{\partial x}(0) + (y''-y') \frac{\partial R}{\partial y}(0) + \dots \right] = \frac{2\zeta(\vec{x})h^4 c^2}{\lambda_y^2} + O(h^6)$$

where

$$c \equiv \frac{1}{2\pi h^2} \int_{-h}^h dx \int_{-h/2}^{h/2} dy \frac{y^2}{x^2+y^2} = \frac{1}{\pi} \left[\frac{5}{4} \tan^{-1} 2 + \frac{1}{2} \frac{\pi}{2} \right] = .09967542103\dots$$

and we have replaced $\frac{\partial^2 R}{\partial y^2}(0)$ by using a relation similar to (3.33).

The integrals in the second term on the right of (3.41) may be written as

$$\int_{D_i \times D_i} \xi'(\vec{x}') \xi'(\vec{x}'') d\vec{x}' d\vec{x}'' = \zeta(\vec{x}_i) h^4 + O(h^6) \quad (3.45)$$

after using an argument analagous to the one leading to (3.44). Substituting (3.44) and (3.45) into (3.41) and neglecting terms of $O(h^6)$ and higher we get

$$\overline{u^2} = \frac{2h^4 c^2 \zeta(\vec{x})}{\lambda_y^2} + \sum_{i \neq 1,2} G_u^2(\vec{x}|\vec{x}_i) \zeta(\vec{x}_i) h^4 \quad (3.46)$$

In practice we need to compute $\overline{v^2}$ at points situated with respect to the grid as represented by the point \vec{x}_0 in Figure 1. Following the same steps as was used for $\overline{u^2}$ we find

$$\overline{v^2} = \frac{2h^4 c^2 \zeta(\vec{x})}{\lambda_x^2} + \sum_{i \neq 1,2} G_v^2(\vec{x}|\vec{x}_i) \zeta(\vec{x}_i) h^4 \quad (3.47)$$

The correlations $\overline{u'v'}$ are in general required at both points like \vec{x} and like \vec{x}_0 in Figure 1. In either case one finds that:

$$\overline{u'v'} = -h^4 c c' \zeta(\vec{x}) \frac{\partial^2 R}{\partial x \partial y}(0) + \sum_{i \neq 1, 2} G_u(\vec{x} | \vec{x}_i) G_v(\vec{x} | \vec{x}_i) \zeta(\vec{x}_i) h^4 \quad (3.48)$$

where

$$c' = \frac{1}{\pi} \left(\frac{5}{4} \tan^{-1} \frac{1}{2} + \frac{1}{2} - \frac{\pi}{8} \right) = .2186345 \dots$$

Apart from values for the parameters, λ_x , λ_y , λ_d , T_{ij} , and $\frac{\partial^2 R}{\partial x \partial y}(0)$ and a specification of the boundary conditions, which we will do in the next chapter, we now have a complete closed system of equations in (3.25), (3.36), (3.46), (3.47) and (3.48) which may be solved numerically for a wide range of two dimensional turbulent flow problems. The next two chapters will take up the application of this method to the two different flow situations we shall consider.

IV. THE TURBULENT FLOW IN A CHANNEL

In this chapter we will use the method of coarse graining to investigate the fully developed turbulent flow in a channel. In section IV.A. we derive the difference equations (4.13) and (4.20) which approximate the mean vorticity equation in the core region and the wall region respectively. To derive (4.20) which uses the boundary condition (1.4) previously discussed in Chapter I, we will use the linear law of the wall. We also show in IV.A. how the distance δ and velocity $U_\infty = U(\delta)$ which appear in (4.20) may be estimated using the computed stream function.

In section IV.B. we analyze the physics of the overall balance of ζ in the channel and conclude that there must exist a distance from the wall, say y' , which separates the flow domain into the two regions mentioned in Chapter I: A pure dissipation region next to the wall and a core region where ζ is produced. We show that for sufficiently large Reynolds numbers y' is very small and then use this fact to formulate a boundary condition to the ζ equation in the wall region. We then construct the difference approximations to the ζ equation: (4.32) for the wall region and (4.33) for the core region.

In section IV.C. we show how the stream function, (and then U) may be computed from the known values of $\bar{\xi}$. In IV.D. we specialize the general results of III.D. on our closure scheme to the present case and derive equation (4.40) which gives the velocity moment $\overline{v^2}$ in terms of the ζ field.

We present the results of our numerical computations of the flow in a channel in section IV.E. Our first task here is the determination of the various parameters which must be assigned values before we can find the solutions of our difference equations. We determine these parameters by fitting the computed and experimental predictions of the mean flow in a channel for a Reynolds number of 57,000 which was studied by Comte-Bellot (1965). Then keeping these parameters fixed we investigate the variation with Reynolds number of the friction coefficient, mean velocity distribution, mean vorticity distribution, and ζ .

Our requirement that the flow in the channel be "fully developed" implies that the x component of the mean velocity field, U , is assumed to be uniform in the x direction, steady, and symmetrical about the centerline of the channel. If lengths are scaled using the channel width, $2D$, then it follows from the assumptions on U that $V=0$, $\bar{\xi}(y) = -\bar{\xi}(1-y)$ and $\zeta(y) = \zeta(1-y)$.

Velocities will be scaled by U_m , the average mass flow velocity, so that

$$\int_0^1 U(y) dy = 1 \quad (4.1)$$

If we define a stream function $\bar{\psi}$ from the relation $U = 1 + \bar{\psi}_y$ and if $\bar{\psi} = 0$, at $y = 0$, then (4.1) and the symmetry condition imply that $\bar{\psi}(y) = -\bar{\psi}(1-y)$. $\bar{\psi}$ is related to $\bar{\xi}$ by

$$\frac{d^2\bar{\psi}}{dy^2} = -\bar{\omega}$$

Since conditions are uniform in the x direction, we will only have to solve for the values of $\bar{\xi}$, ζ and $\bar{\psi}$ at one x position along the channel, which we choose to be $x=0$. The set of points $(0, (j-\frac{1}{2})h)$, $j=1, \dots, M$ with $h = 1/M$ forms a staggered grid, on which we will define discrete approximations $\bar{\xi}_j$, ζ_j and $\bar{\psi}_j$ to $\bar{\xi}((j-\frac{1}{2})h)$, $\zeta((j-\frac{1}{2})h)$ and $\bar{\psi}((j-\frac{1}{2})h)$ respectively. These grid functions will be related by difference equations, the solutions of which for $\bar{\xi}_j$ and ζ_j are found by allowing $\bar{\xi}_j$ and ζ_j to depend on time, and integrating the equations until a steady time independent solution is found. A superscript 'n' will refer to the time step $n\Delta t$ where Δt is the interval of time between integration steps.

A. Mean Vorticity Equation

The mean vorticity equation for the flow in a channel is

$$0 = -\frac{\partial}{\partial y} \overline{v'\xi} + \frac{1}{R} \frac{\partial^2 \bar{\xi}}{\partial y^2} \quad (4.2)$$

which is a special case of the general equation (3.25). The average flux of vorticity due to the molecular motion is $-\frac{1}{R} \frac{\partial \bar{\xi}}{\partial y}$. The minus sign is necessary to satisfy the condition that the flux be positive

if it acts to increase the vorticity lying on the + side of the surface through which the flux occurs. $\overline{v'\xi}$ is the average flux of vorticity due to the turbulent motion and if we define the total mean flux of vorticity as $Q(y)$ then $Q(y) = -\frac{1}{R} \overline{\xi_y} + \overline{v'\xi}$. (4.2) implies that $\frac{\partial Q(y)}{\partial y} = 0$ i.e. the total flux of vorticity is constant across the channel, (or more generally a function of x).

The constant mean rate at which vorticity diffuses across the channel may be determined by transformation of the x momentum equation:

$$\frac{\partial}{\partial y} \overline{u'v'} = -\frac{\partial \overline{p}}{\partial x} + \frac{1}{R} \frac{\partial^2 U}{\partial y^2} \quad (4.3)$$

through use of the relations $u'_x + v'_y = 0$ and $\overline{\xi} = -U_y$. We find that

$$Q(y) = + \frac{\partial \overline{p}}{\partial x} \quad (4.4)$$

Let us define a friction coefficient, λ , through

$$\lambda = \frac{\tau_w^*}{\frac{1}{2} \rho U_m^2} \quad (4.5)$$

where

$$\tau_w^* = \mu \left. \frac{dU^*}{dy^*} \right|_{y^*=0}$$

is the dimensioned shear stress at the wall and $U^* = U_m U$ and $y^* = 2Dy$ are dimensioned variables. We will show that

$$\lambda = - \frac{\partial \bar{p}}{\partial x} \quad (4.6)$$

and therefore that (4.4) may be written as

$$Q(y) = -\lambda \quad (4.7)$$

If the nondimensionalization of τ_w^* is carried out in (4.5) we find that

$$\lambda = \frac{1}{R_e} U'(0) \quad (4.8)$$

where $R_e = U_m D / \nu = R/2$. The y momentum equation,

$$\frac{\partial}{\partial y} (\bar{p} + \overline{v'^2}) = 0$$

implies that $\frac{\partial \bar{p}}{\partial x}$ is independent of y since $\frac{\partial \overline{v'^2}}{\partial x} = 0$, so (4.3) may be integrated across the channel from $y = 0$ to 1 to give

$$\frac{\partial \bar{p}}{\partial x} = \frac{1}{R} \left(U'(1) - U'(0) \right) = \frac{-U'(0)}{R_e} \quad (4.9)$$

where the symmetry of $U(y)$ was used. (4.8) and (4.9) then imply that $\frac{\partial \bar{p}}{\partial x} = -\lambda$ and therefore (4.7) holds.

It is known that the mean flow fields such as U , $\bar{\xi}$, $\bar{\xi}_y$ and $\overline{v'\xi}$ vary sharply in a thin region near the wall in a high Reynolds number flow. (4.7) shows that in spite of this $Q(y)$ is a constant across this region. We will show now that this fact may be used to advantage in forming a difference approximation to the mean vorticity equation for the box adjacent to the wall.

For the purposes of constructing difference equations we pretend that $\bar{\xi}_t$ is not identically zero, so that in approximating $\bar{\xi}_t$ by a finite difference we create a means of iterating to the steady state solution. The equation we are to difference is thus

$$\frac{\partial \bar{\xi}}{\partial t} = - \frac{\partial Q}{\partial y}(y) \quad (4.10)$$

and we approximate this at any grid point $j = 1, \dots, M/2$ (because of symmetry we do not need difference equations for $j > M/2$) as

$$\frac{\bar{\xi}_j^{n+1} - \bar{\xi}_j^n}{\Delta t} = \frac{Q(jh) - Q((j-1)h)}{h} + O(h^2) \quad (4.11)$$

We may have complete confidence in the order of magnitude of the truncation error for all grid points, including, in particular, $j = 1$ near the wall since $Q(y)$ according to (4.7) will be constant across the wall region after the numerical solution has converged.

For points sufficiently far from the wall so that we may suppose that our transport law is valid we have

$$Q(y) = \left(\frac{1}{R} + T_{22} \overline{v^2} \right) \frac{\partial \bar{\xi}}{\partial y} \quad (4.12)$$

If we suppose that the point $y = h$ is in this region then our difference approximations to (4.10) are for $j = 2, \dots, M/2$:

$$\frac{\bar{\xi}_j^{n+1} - \bar{\xi}_j^n}{\Delta t} = \left(\frac{1}{R} + T_{22} \overline{v_j^2} \right) \left(\frac{\bar{\xi}_{j+1}^n - \bar{\xi}_j^n}{h^2} \right) - \left(\frac{1}{R} + T_{22} \overline{v_{j-1}^2} \right) \left(\frac{\bar{\xi}_j^n - \bar{\xi}_{j-1}^n}{h^2} \right) \quad (4.13)$$

which follows from (4.11) using (4.12) and where $\overline{v_j^2} = \overline{v^2}(jh)$.

For the grid point $j = 1$ at the wall we have

$$\frac{\bar{\xi}_1^{n+1} - \bar{\xi}_1^n}{\Delta t} = \left(\frac{1}{R} + T_{22} \frac{\sqrt{12}}{v_1} \right) \left(\frac{\bar{\xi}_2^n - \bar{\xi}_1^n}{h^2} \right) - \frac{1}{hR} \left. \frac{\partial \bar{\xi}}{\partial y} \right|_{y=0} \quad (4.14)$$

since $\left. \sqrt{12} \bar{\xi} \right|_{y=0} = 0$. If (4.14) is to be useful we must find an alternative expression for $\left. \frac{\partial \bar{\xi}}{\partial y} \right|_{y=0}$; one that we are able to compute. We will show using the linear law of the wall that

$$\left. \frac{\partial \bar{\xi}}{\partial y} \right|_{y=0} = \frac{U_\infty}{\delta} \frac{2}{\delta} \quad (4.15)$$

where δ is a point in the viscous sublayer and $U_\infty \equiv U(\delta)$. Later we will show how δ and U_∞ may be computed (approximately) using the stream function.

First let us recall what the content of the linear law of wall is. This law is the experimental observation that the mean velocity field $U(y)$ varies approximately linearly in the viscous sublayer. This has been found to occur in both pipes and channels, (see Comte-Bellot (1965) and Schlichting (1968) Chapter XX).

Though the distribution of U in the viscous sublayer appears in experiment to be linear, it does in fact vary parabolically, though so slightly as to be easily overlooked. This may be seen by

evaluating the momentum equation (4.3) at the wall. We find, after using (4.6) that

$$U''(0) = R \frac{\partial \bar{p}}{\partial x} = -2\lambda R_e \quad (4.16)$$

which shows that $U''(0) \neq 0$ and therefore U cannot be purely linear at the wall. If we expand $U(y)$ in Taylor's series about $y = 0$ we find, since $U(0) = 0$ that

$$U(y) = \lambda R_e (y - y^2) + O(y^3)$$

We may take the linear law of the wall as suggesting that $U(y) = \lambda R_e y$ in the viscous layer or equivalently

$$U(y) = \lambda R_e (y - y^2) \quad (4.17)$$

since the contribution of the term with y^2 to $U(y)$ is negligible in the viscous sublayer.

(4.17) shows that if δ is a point in the viscous sublayer then

$$\lambda = \frac{U_\infty}{(\delta - \delta^2) R_e} \quad (4.18)$$

Furthermore since $\bar{\xi} = -U_y$,

$$\left. \frac{\partial \bar{\xi}}{\partial y} \right|_{y=0} = -U''(0) \quad (4.19)$$

and therefore (4.15) follows from using (4.16) and (4.18) in (4.19).

If we substitute (4.15) into (4.14) we attain

$$\frac{\bar{\xi}_1^{n+1} - \bar{\xi}_1^n}{\Delta t} = \left(\frac{1}{R} + T_{22} \frac{v_1^2}{1} \right) \left(\frac{\bar{\xi}_2^n - \bar{\xi}_1^n}{h^2} \right) - \frac{2}{Rh} \frac{U_\infty}{\delta - \delta^2} \quad (4.20)$$

which is the difference equation to be used for the grid point $j=1$.

As we have seen the boundary condition (4.15) to the mean vorticity equation that is used in (4.20) may be justified by a combination of theoretical and experimental facts. This situation is to be contrasted with the heuristically derived boundary conditions used by Deardoff (1970) and Schumann (1976) in their large eddy simulations of the flow in a channel. Both of them rely on making a crude connection between their filtered variables and the logarithmic law of the wall. We have found in our computations of the flow in a channel, that an accurate accounting of the boundary condition is crucial toward obtaining the correct solution. It is, therefore, not evident that the results of their computations will have any meaning until such time as a rigorous justification of the boundary conditions they use is found.

The usefulness of our boundary condition, however, depends on there being available to us a means of determining the velocity U at a point δ within the viscous sublayer. Clearly we would have such a means if we were to use an extremely fine mesh (and supposing that we were able to adopt our numerical method to such a grid) that had at least one grid point within the viscous sublayer. We do not propose to use such a grid, though, and will in fact use a very coarse grid which has $h = 1/16$. This will result in our having to devise a crude method of finding a pair of values (δ, U_∞) . We found that the determination of a value of δ within the sublayer for the full range of Reynolds numbers that we have studied is rather easily accomplished, but to compute the value of U at this point is a much more difficult task and will force us to introduce a parameter that must be found by using the experimental data.

Our method of computing δ relies on the construction shown in Figure 2 which is a crude approximation to the behavior of the stream function in the region near the wall. In this figure we have drawn a straight line with slope -1 leaving the origin and a parabolic arc through the values of the computed stream function at the three grid points closest to the wall, i.e. $y=h/2, 3h/2$ and $5h/2$. The first line, the one leaving the origin, satisfies the boundary conditions that the stream function must satisfy at the wall. We have found that the point of intersection of these two lines always occurs in the viscous sublayer and so we have let δ be this point.

After some simple algebra, one may ascertain that

$$\delta = \frac{1+B - \sqrt{(1+B)^2 - 4AC}}{2A} \quad (4.21)$$

where

$$A = \frac{1}{2h^2} (\bar{\psi}_1 - 2\bar{\psi}_2 + \bar{\psi}_3)$$

$$B = \frac{1}{h} (-2\bar{\psi}_1 + 3\bar{\psi}_2 - \bar{\psi}_3)$$

and

$$C = \frac{15}{8}\bar{\psi}_1 - \frac{5}{4}\bar{\psi}_2 + \frac{3}{8}\bar{\psi}_3$$

As we have suggested, without more information about the flow within the wall region the evaluation of U at the value of δ given in (4.21) can only be done crudely. We have found nonetheless that the following artifice works surprisingly well as we shall see in section IV.E: We know that $U(y) = 1 + \bar{\psi}_y$, so as to compute $U(\delta)$ we must find an approximation to $\bar{\psi}_y(\delta)$. We can estimate the order of magnitude of $\bar{\psi}_y(\delta)$ from the slope at the point δ , ($= B + 2A\delta$), of the parabolic curve used to compute δ , and then suppose that $\bar{\psi}_y(\delta)$ is proportional to this slope. Therefore,

introducing a parameter C_1 , we have

$$U(\delta) = 1 + C_1(B+2A\delta) \quad (4.22)$$

where C_1 remains to be determined using experimental data.

B. Equation for Mean Squared Fluctuating Vorticity

To aid us in formulating the correct difference equations for ζ in the wall region we must discuss at length the distribution of the ξ field throughout the whole channel. We will show that two fundamentally different regions, so far as the ζ dynamics are concerned, may be distinguished. The first will be a thin dissipation region near the wall where no production of ζ from the mean flow takes place, and the other is an outer zone where ζ is produced.

Our first job will be to predict the behavior $\bar{\xi}$ across the channel. From differentiating (4.17) we find that

$$\bar{\xi}(y) = -\lambda R_e(1-2y) \quad (4.23)$$

in the viscous sublayer. We can find the distribution of $\bar{\xi}(y)$ throughout the remainder of the channel by considering what is known about the typical mean velocity profiles that have been measured in turbulent channel flows. For example, it has been experimentally observed that the turbulent mean velocity profiles in a channel are considerably flatter in the center of the channel than the parabolic velocity

distribution which exists in a laminar flow. As a consequence, $|\bar{\xi}| = \left| \frac{dU}{dy} \right|$ must be smaller in the core region of the channel in a turbulent flow than it is in a laminar one.

We also know from experiments that $\frac{dU}{dy} = -\bar{\xi}$ monotonically increases going from the center of the channel where it is zero to the wall $y = 0$ where it is λR_e . Using this fact and our knowledge of $\bar{\xi}$ at the boundary contained in (4.23) we expect the distribution of $\bar{\xi}$ to appear similar to the form given in figure 3, where the length scale near the wall has been greatly exaggerated.

Using the curve for $\bar{\xi}$ in Figure 3 we can predict the general behavior of $\bar{\xi}_y$ across the channel. First of all, we know from (4.17) that $\bar{\xi}_y = 2\lambda R_e$ throughout the viscous sublayer. Figure 3 then shows that $\bar{\xi}_y$ must increase immediately outside of this region reaching a maximum at the place where $\bar{\xi}$ has a point of inflection and then rapidly fall to the much smaller value it has throughout most of the core region. The distribution of $\bar{\xi}_y$ across the channel is plotted in Figure 4, (actually $\frac{1}{R} \bar{\xi}_y$ is shown, for later convenience).

It follows then that there must exist a point outside of the viscous sublayer, say y' , where $\bar{\xi}_y$ is again equal to the value $2\lambda R_e$ which it has at the wall. We will show that the point y' has several physical interpretations (as far as a two dimensional flow is concerned) and that its location in the channel is of major importance to us in our effort to numerically solve for the mean properties of this flow.

The first interpretation of y' has to do with the direction of the mean turbulent flux of vorticity. The mean vorticity equation (4.7) is

$$Q(y) = -\frac{1}{R} \frac{d\bar{\xi}}{dy} + \overline{v'\xi} = -\lambda \quad (4.7)$$

which implies that when $\bar{\xi}_y = 2\lambda R_e = \lambda R$, $\overline{v'\xi} = 0$. Therefore $\overline{v'\xi} = 0$ at y' . We see from Figure 4 that for $y < y'$, $\frac{1}{R}\bar{\xi}_y > \lambda$ and that for $y > y'$ (more precisely $1 - y' > y > y'$, but we will assume throughout this discussion that we are only referring to the half channel $0 \leq y < y'$), $\frac{1}{R}\bar{\xi}_y < \lambda$. (4.7) then implies that $\overline{v'\xi} > 0$ for $y < y'$ and that $\overline{v'\xi} < 0$ for $y > y'$. Since the vorticity is negative in this half of the channel $\overline{v'\xi} > 0$ here corresponds to a flux of - vorticity in the -y direction. We have thus seen that the point y' separates the flow in the channel into a region $0 \leq y < y'$ where the mean turbulent flux of vorticity is towards the wall and a region $y > y'$ where it is away from the wall. At the point y' this flux is 0.

y' may be interpreted in another way, as the point which separates the flow into zones of production of ζ , when $y > y'$, and pure 'dissipation' or destruction of ζ when $y < y'$. This may be seen by considering the exact equation which governs the evolution of the ζ field for the channel problem, which is, from a reduction of (3.27):

$$0 = \frac{\partial}{\partial y} \left(\frac{1}{R} \frac{\partial \zeta}{\partial y} - \overline{v'\xi'^2} \right) - 2 \overline{v'\xi} \frac{\partial \zeta}{\partial y} - \frac{2}{R} \left(\overline{\xi_x'^2} + \overline{\xi_y'^2} \right) \quad (4.24)$$

The term in the middle of the right side is the one that we previously indicated in Chapter III is responsible for the production of ζ from the mean flow. However, it is clear that it can only lead to production of ζ when $\overline{v'\xi} < 0$ and this only occurs, based on our previous discussion, in the wall region $y' > 0$. In the wall region where $\overline{v'\xi} > 0$, this term represents a loss of ζ by a reversion to the mean field $\overline{\xi}^2$. The overall dynamics of ζ may be seen by integrating (4.24) over the regions $0 \leq y \leq y'$ and $y' \leq y \leq \frac{1}{2}$ in turn.

For the wall region $0 \leq y \leq y'$ we find that

$$\left(\frac{1}{R} \frac{\partial \zeta}{\partial y} + \overline{v'\xi^2} \right)_{y=y'} = - \int_0^{y'} 2\overline{v'\xi} \overline{\xi}_y dy - \int_0^{y'} \frac{2}{R} \left(\overline{\xi_x^2} + \overline{\xi_y^2} \right) dy - \frac{1}{R} \frac{\partial \zeta}{\partial y} \Big|_{y=0}$$

The first term on the right, which is negative, is the previously considered loss of ζ by reversion to $\overline{\xi}^2$, while the next term represents viscous dissipation of ζ . Since it doesn't make physical sense that ζ would be produced at the wall by the molecular motion, we expect that $\zeta_y > 0$ at the wall, and thus the final term on the right represents an additional loss of ζ by its diffusion into the highly viscous sublayer. These three losses on the right are balanced by the term on the left, which is the total flux of ζ at the position $y = y'$. Since the right side of the equation is negative, we must conclude that the left hand side represents a flux of ζ into the wall region from the outer flow. All of the ζ which diffuses into the wall region is then lost due to the various phenomena listed on the right side.

Now let us explore the region $y' < y$, by integrating (4.24) between these limits. We find that

$$0 = \int_{y'}^{\frac{1}{2}} -2\overline{v'\xi} \overline{\xi}_y dy - \int_{y'}^{\frac{1}{2}} \frac{2}{R} \left(\overline{\xi_x'^2} + \overline{\xi_y'^2} \right) dy + \left(\frac{1}{R} \frac{\partial \zeta}{\partial y} + \overline{v'\xi^2} \right)_{y=y'} \quad (4.25)$$

Since $\overline{v'\xi} < 0$ in this region, the first term on the right represents the total production of ζ taking place in (half) the channel. The next term represents the dissipation taking place here and the last term represents, as we just saw, a loss of ζ from the core region by its diffusion into the wall region. The only way in which a balance can be maintained in (4.25) is if the production term exceeds the middle term representing viscous dissipation. Therefore a net production of ζ takes place in the core region which is in turn balanced by a net loss of ζ occurring through its dissipation in the wall region.

Since $\overline{v'\xi} = 0$ at $y = y'$ the sole contribution to the flux of vorticity at this point comes from the molecular motion. Thus, it is evident that the effects of viscosity on the vorticity dynamics extend out at least the distance y' into the flow. This implies that there is no justification for believing that the vorticity approximately satisfies (3.1) in this zone, i.e. that the viscous terms in the vorticity equation can be neglected here. We are then not surprised to find that the transport law (3.21) does break down in the region

$y < y'$ as is obvious from the fact that both $\overline{v^2 \xi}$ and $T_{22} \overline{v^2 \xi_y}$ are greater than zero here.

In deriving our difference approximation to the mean vorticity equation at the first grid box, in the previous section, we applied the transport law (3.21) at the point h . We had assumed then that the point h was far enough from the wall so that (3.21) was valid there. If we can now show that $y' < h$, then we will have some justification for that assumption. Fortunately we can do even better than this and can show that $y' = o(h)$ if R_e is sufficiently high. The fact that the region $0 \leq y \leq y'$ occupies only a small portion of the first grid box will also be helpful to us in forming a difference equation for ζ there.

To show that y' is exceedingly small (for sufficiently large Reynolds numbers) we first establish that y' has yet another interpretation as the point where $\overline{u'v'}$ has a minimum. The distribution of $\overline{u'v'}$ across the channel may be found by integrating the momentum equation (4.3) between $y = 0$ and y , and using the definition of λ . We get

$$\overline{u'v'} = \lambda(y - \frac{1}{2}) - \frac{\overline{\xi}}{R} \quad (4.26)$$

$\overline{\xi}/R$ is a significant term in this equation only for a region very close to the wall. Thus we expect $\overline{u'v'}$ to have the behavior shown in Figure 3, which is a well known result. We see from this figure that $\overline{u'v'}$ has

a minimum at a point near the wall. At this point $\frac{\partial}{\partial y} \overline{u'v'} = 0$. But, for an incompressible flow in a channel, $\overline{v'\xi} = -\frac{\partial}{\partial y} \overline{u'v'}$, and since $\overline{v'\xi} = 0$ at y' , so must $\frac{\partial}{\partial y} \overline{u'v'} = 0$. This proves that $\overline{u'v'}$ is a minimum here.

The point where $\overline{u'v'}$ is a minimum has been measured in experiments of turbulent flow past walls and in channels and pipes. It is generally found (see Tennekes and Lumley (1972) p. 161), that this occurs at $y^*u_\tau/\nu \approx 30$, where $u_\tau = \sqrt{\tau_w^*/\rho}$ is the friction velocity and τ_w^* is the dimensional shear stress at the wall. This point also coincides with the lower limit of the range of y values in which the log law of the wall holds, see Tennekes and Lumley (1972) and Comte-Bellot (1965). After nondimensionalization we have

$$y' \approx \frac{30}{R} \sqrt{\frac{2}{\lambda}} \quad (4.27)$$

When $R_e = 57,000$, $\lambda \approx .00366$ and therefore $y' \approx .00615$. h , however for our computations = .0625, and thus it is true for this value of R_e that $y' \ll h$. However, as $R \rightarrow 0$, this assumption becomes progressively less true and in fact for $R_e \leq 7500$, it appears from our computations that $h < y'$.

As a sidelight of this discussion it is interesting to note from Figure 3 that the molecular diffusion of momentum is much less than its turbulent flux, (i.e. the Reynolds stress) at the distance y' from the wall. The molecular diffusion of vorticity, however, as we

just mentioned is still comparatively large at $y = y'$, thus it is clear that the influence of the viscosity on the diffusion of vorticity extends considerably further into the flow than its influence on the momentum transport. This might explain, in part, why Taylor (1935b) saw that his vorticity transport theory was not as accurate as the momentum transport theory in the wall region.

Another interesting aspect of the wall region and one which will have a bearing on our formulation of a difference approximation for ζ_1 is the location of the point of greatest production of ζ and the magnitude of the production there. Using (4.7) the production term in the ζ equation (4.24) may be written as

$$-2 \overline{v'\xi} \overline{\xi}_y = -2R \overline{v'\xi} (\lambda + \overline{v'\xi}) \quad (4.28)$$

We saw in Figure 4 that $-\overline{v'\xi}$ goes from 0 at y' to a value near λ further from the wall. Consequently (4.28) will vary from 0 at y' to a maximum $\frac{1}{2}\lambda^2 R$ when $-\overline{v'\xi} = \lambda/2$ and then back down to a smaller value throughout the rest of the core region. The point where the production rate is a maximum most likely lies close to the point y' since $\overline{\xi}_y$ is known to be comparatively small a short distance into the log law region.

Though the production rate of ζ is much less than $\frac{1}{2}\lambda^2 R$ for most of the flow field, its contribution to the total amount of production is just as significant as the intense production coming from the wall region, since this latter region is quite thin. It might be helpful

if we demonstrate this fact with some numbers. Suppose that the maximum production in the wall region occurred over a distance $\approx h/2$. Then the total production here is $\approx \frac{\lambda^2 R h}{4}$, which for $R_e = 57,000$ is $\approx .024$. A typical value of $\bar{\xi}_y$ in the core region of the channel is $\frac{1}{2}h$, so the total production term of (half) the core region is $\approx (2\lambda\bar{\xi}_y) = \frac{1}{2} \frac{\lambda}{h} \approx .015$. It is thus clear that they are comparable.

It is a curious fact that a similar conclusion cannot be drawn for the production of mean turbulent kinetic energy $\overline{q^2}$ where $q^2 = \frac{1}{2}(u'^2 + v'^2)$ i.e. virtually all of the production of $\overline{q^2}$ takes place in a thin region next to the wall. To see this fact consider the equation describing the balance of q^2

$$0 = -\overline{u'v'} U_y - \frac{\partial}{\partial y} \overline{v'p'} + \frac{\partial}{\partial y} \left(\frac{1}{R} \frac{\partial \overline{q^2}}{\partial y} - \overline{v'q^2} \right) - \frac{1}{R} \left(\overline{u_x'^2} + \overline{u_y'^2} + \overline{v_x'^2} + \overline{v_y'^2} \right) \quad (4.29)$$

The term $-\overline{u'v'} U_y$ which is always positive for the flow in a channel, represents production of $\overline{q^2}$ from the mean flow field. This term reaches a maximum of $\approx \frac{1}{16} \lambda^2 R$ at the point in Figure 3 where $R \overline{u'v'} = \bar{\xi}$.

Making similar estimates as before, i.e. supposing the maximum production rate occurs over the distance $h/2$ and the core region is of an extent $\frac{1}{2}$, we find that for the wall zone the total production is approximately $\frac{h}{2} \cdot \frac{1}{16} \lambda^2 R \approx .003$, while in the core region it is $\frac{1}{2} \overline{u'v'} U_y = \frac{1}{2} \frac{\lambda}{4} \cdot \frac{1}{2} \approx .0002$, since $U_y = -\bar{\xi} \approx \frac{1}{2}$ and $\overline{u'v'} \approx \frac{\lambda}{4}$ here. Our claim is thus clearly substantiated.

Part of the intriguing complexity of the turbulent flow past a wall is the fact that while the wall region is a place of large production of both $\overline{q^2}$ and ζ , it is also the place where a great deal of the dissipation or destruction of $\overline{q^2}$ and ζ takes place. It has been sometimes conjectured, see Townsend (1961), that the wall region may be considered to be in an equilibrium where the production of $\overline{q^2}$ is balanced by its loss. To aid us in deriving a difference equation for ζ in the grid box adjacent to the wall we will extend this assumption to also include the case of $\overline{q^2}$. Specifically, we suppose that to a good approximation, the ζ which is produced in the high production region just outside of y' , is lost by its diffusion into the dissipation zone $y < y'$ as well as its dissipation in the vicinity of where it was made.

Though this assumption seems equally plausible for the $\overline{q^2}$ field as it does for ζ , it has drastically different consequences on a hypothetical numerical method which hopes to compute $\overline{q^2}$ throughout the flow field by incorporating this hypothesis. Thus, if the production of $\overline{q^2}$ in the boundary region is left out of the difference equation for $\overline{q^2}$ by virtue of its supposed cancellation by the dissipation term, then the part of the production that one is left with to compute, is just a small part of the total production, therefore it is likely that small errors in the computations would have a considerable effect on the calculated solutions. Such behavior is clearly not expected in the case of the ζ equation if a similar approximation is made, since a goodly portion of the ζ production is being computed.

We now are finally in a position where we can present the difference equations that we will use to approximate (4.24). In the region $y > y'$, we presume that ζ satisfies the equation

$$0 = \frac{\partial}{\partial y} \left(\frac{1}{R} + T_{22} \overline{v'^2} \right) \frac{\partial \zeta}{\partial y} + 2 T_{22} \overline{v'^2} \overline{\xi_y^2} - \frac{2\zeta}{\lambda_d^2 R} \quad (4.30)$$

which makes use of our transport law. To form a difference equation for the box $j = 1$ we difference the diffusion term in (4.30) between $y = y'$ and $y = h$ and suppose that $h - y' \approx h$. The evaluation of $(1/R + T_{22} \overline{v'^2}) \zeta_y$ at $y = h$ is no trouble but at $y = y'$ it is. To be more precise, we actually must compute $\frac{1}{R} \zeta_y - \overline{v'^2} \overline{\xi_y^2}$ at $y = y'$ since we have a right to be suspicious of the transport law here. In view of the limitations arising from our coarse grid we will make the following crude approximation:

$$\left(\frac{1}{R} \frac{\partial \zeta}{\partial y} - \overline{v'^2} \overline{\xi_y^2} \right)_{y=y'} \approx C_2 \left(\frac{1}{R} + T_{22} \overline{v'^2}_1 \right) \frac{\zeta_1}{h} \quad (4.31)$$

where C_2 is another constant to be determined empirically.

In view of our supposition as to the existence of a partial equilibrium in the production and dissipation of ζ in the wall region about $y = y'$, we will suppose that an adequate approximation to the production term for the first box is

$$-2 \sqrt{v} \bar{\xi} \bar{\xi}_y \approx 2 T_{22} \sqrt{v} \left(\frac{\bar{\xi}_2 - \bar{\xi}_1}{h} \right)^2$$

Incorporating this approximation as well as (4.31), the difference equation for ζ_1 may now be written as

$$\begin{aligned} \frac{\zeta_1^{n+1} - \zeta_1^n}{\Delta t} &= \left(\frac{1}{R} + T_{22} \sqrt{v} \right) \left(\frac{\zeta_2^n - \zeta_1^n}{h^2} \right) - c_2 \left(\frac{1}{R} + T_{22} \sqrt{v} \right) \frac{\zeta_1^n}{h^2} \\ &+ 2 T_{22} \sqrt{v} \left(\frac{\bar{\xi}_2^n - \bar{\xi}_1^n}{h} \right)^2 - \frac{2}{R \lambda_d^2} \zeta_1^n \end{aligned} \quad (4.32)$$

For the remaining boxes $j=2, \dots, M/2$ we will use the following difference equation which is a straight forward approximation to (4.30)

$$\begin{aligned} \frac{\zeta_j^{n+1} - \zeta_j^n}{\Delta t} &= \left(\frac{1}{R} + T_{22} \sqrt{v} \right) \left(\frac{\zeta_{j+1}^n - \zeta_j^n}{h^2} \right) - \left(\frac{1}{R} + T_{22} \sqrt{v} \right) \left(\frac{\zeta_j^n - \zeta_{j-1}^n}{h^2} \right) \\ &+ T_{22} \sqrt{v} \left(\frac{\bar{\xi}_{j+1}^n - \bar{\xi}_j^n}{h} \right)^2 + T_{22} \sqrt{v} \left(\frac{\bar{\xi}_j^n - \bar{\xi}_{j-1}^n}{h} \right)^2 - \frac{2}{R \lambda_d^2} \zeta_j^n \end{aligned} \quad (4.33)$$

C. Stream Function

The stream function $\bar{\psi}$ is determined uniquely for a known vorticity field, $\bar{\xi}$, as the solution of the equation

$$\frac{d^2\bar{\psi}}{dy^2} = -\bar{\xi} \quad (4.34)$$

with the boundary conditions $\bar{\psi} = 0$ at $y = 0$ and 1 . The discrete stream function $\bar{\psi}_j$ is similarly determined from the $\bar{\xi}_j$ by a finite difference analogue to (4.34). At the grid points $j=2, \dots, M/2$, which are distant from the boundary, we may form the consistent approximation to (4.34):

$$\frac{\bar{\psi}_{j+1} - 2\bar{\psi}_j + \bar{\psi}_{j-1}}{h^2} = -\bar{\xi}_j \quad (4.35)$$

which is accurate to $O(h^2)$.

When $j=1$, (4.35) cannot be used because this would necessitate the use of a point outside of the flow domain. We may, however, use the approximation

$$\frac{-5\bar{\psi}_1 + 2\bar{\psi}_2 - 1/5\bar{\psi}_3}{h^2} = -\bar{\xi}_1 \quad (4.36)$$

which may be easily verified to also be of second order accuracy in h .

If the equation in (4.35) when $j=2$ is multiplied by $1/5$ and then added to (4.36) we get

$$\frac{-\frac{24}{5}\bar{\psi}_1 + \frac{8}{5}\bar{\psi}_2}{h^2} = -\bar{\xi}_1 - \frac{1}{5}\bar{\xi}_2 \quad (4.37)$$

The system of equations (4.35) $j=2, \dots, M/2$ and (4.36) have the same solution if (4.36) is replaced by (4.37). This latter system is a tri-diagonal system of equations which is easily solved using the standard algorithm.

Once the $\bar{\psi}_j$ are known we can find approximations U_j to $U(jh)$, $j=1, \dots, M/2$ from

$$U_j = 1 + \frac{\bar{\psi}_{j+1} - \bar{\psi}_j}{h}$$

In section IV.E. we will compare the computed value of U_j with those found experimentally.

D. Computation of the Velocity Moments

In this section we will show how the $\overline{v_j^2}$ may be computed using the technique of section III.D. We will evaluate $\overline{v_j^2}$ at the point $(0, jh)$ shown in Figure 5. The channel has been partitioned into boxes with M of them spanning the channel. It is seen that each $\overline{v_j^2}$ is situated with respect to the grid in the same manner as was required for the

development of section III.D. Thus we may apply the results of that section to the present case and find that

$$\overline{v_j^2} = \frac{h^4 C^2}{\lambda_x^2} (\zeta_j + \zeta_{j+1}) + h^4 \sum_{\ell=1}^M \left(\sum_{k=-\infty}^{+\infty} G_V^2(\vec{x}_j | \vec{x}_{k\ell}) \zeta_{\ell} \right) \quad (4.38)$$

where

$$G_V(\vec{x}_j | \vec{x}_{k\ell}) \equiv -\frac{\partial G}{\partial x}(\vec{x}_j | \vec{x}_{k\ell})$$

$\vec{x}_j = (0, jh)$ and $\vec{x}_{k\ell} = (x_k, y_\ell) = (kh, (\ell - \frac{1}{2})h)$. Since all of the functions $G_V(\vec{x} | \vec{x}_{0\ell})$ are equal to zero, we do not have to remove from the sum on the right the contribution from the boxes $(0, j)$ and $(0, j+1)$ to $\overline{v_j^2}$ which are already being accounted for by the first term on the right. Note also that the constant C appearing in (4.38) should depend on j , but exact computations of it show that the variation is so slight that it may be neglected.

$G_V(\vec{x}_j | \vec{x}_{k\ell})$ represents the y component of velocity induced at a point \vec{x}_j due to a vortex of circulation one sitting at $\vec{x}_{k\ell}$. For a vortex placed in a channel, $G_V(\vec{x}_j | \vec{x}_{k\ell})$ may be computed exactly by setting up an array of image vortices: Plus vortices are situated at the points $(x_k, y_\ell + 2m)$, $-\infty < m < +\infty$ and negative vortices at $(x_k, 2m - y_\ell)$, $-\infty < m < +\infty$. The velocity at any point x in the channel

due to the vortex at $\vec{x}_{k\ell}$ is then the sum of the velocities induced at \vec{x}_j as if no boundaries are present, by this vortex plus all of the image vortices.

The velocity at \vec{x}_j arising from this infinite collection of vortices may be written in closed form using the velocity field induced by a row of vortices, given in Lamb (1932). We have

$$G_V(\vec{x}_j | \vec{x}_{k\ell}) = -\frac{1}{4} \frac{\sinh(\pi x_k)}{(\cosh \pi x_k - \cos \pi(jh - y_\ell))} + \frac{1}{4} \frac{\sinh(\pi x_k)}{(\cosh \pi x_k - \cos \pi(jh + y_\ell))}$$

the first term coming from the column of + vortices and the second from the - vortices.

The use of (4.38) in practice is much simplified if we define a function $A(j, \ell)$ which gives the contribution to $\overline{v_j^2}$ from all the boxes with center at $y = (\ell - \frac{1}{2})h$. Thus

$$A(j, \ell) = \sum_{k=-\infty}^{+\infty} G_V^2(\vec{x}_j | \vec{x}_{k\ell})$$

Using this function (4.38) becomes

$$\overline{v_j^2} = \frac{h^4 c^2}{\lambda_x^2} (\zeta_j + \zeta_{j+1}) + \sum_{\ell=1}^M \zeta_\ell A(j, \ell) \quad (4.39)$$

Since $\zeta_{M+1-l} = \zeta_l$ (4.39) may be simplified further to

$$\overline{v_j^{\prime 2}} = \frac{h^4 c^2}{\lambda_x^2} (\zeta_j + \zeta_{j+1}) + \sum_{\ell=1}^{M/2} B(j,\ell) \zeta_\ell \quad (4.40)$$

where $B(j,\ell) = A(j,\ell) + A(j,M+1-\ell)$. The $M/2 \times M/2$ array $B(j,\ell)$ may be computed once and for all and stored, making the computation of $\overline{v_j^{\prime 2}}$ a trivial operation at each time step.

E. Results of Computations

Before discussing the results of our computations let us collect together the system of difference equations we intend to solve numerically and the equations which they approximate. The mean vorticity equation is

$$\frac{\partial \bar{\xi}}{\partial t} = \frac{\partial}{\partial y} \left(\frac{1}{R} + T_{22} \overline{v^{\prime 2}} \frac{\partial \bar{\xi}}{\partial y} \right) \quad (4.10)$$

which we approximate at the grid points $j=2, \dots, M/2$ by

$$\frac{\bar{\xi}_j^{n+1} - \bar{\xi}_j^n}{\Delta t} = \left(\frac{1}{R} + T_{22} \overline{v_j^{\prime 2}} \right) \left(\frac{\bar{\xi}_{j+1}^n - \bar{\xi}_j^n}{h^2} \right) - \left(\frac{1}{R} + T_{22} \overline{v_{j-1}^{\prime 2}} \right) \left(\frac{\bar{\xi}_j^n - \bar{\xi}_{j-1}^n}{h^2} \right) \quad (4.13)$$

and at $j=1$ by

$$\frac{\bar{\xi}_1^{n+1} - \bar{\xi}_1^n}{\Delta t} = \left(\frac{1}{R} + T_{22} \frac{\bar{v}_1^2}{v} \right) \left(\frac{\bar{\xi}_2^n - \bar{\xi}_1^n}{h^2} \right) - \frac{2}{Rh} \frac{U_\infty}{\delta - \delta^2} \quad (4.20)$$

where δ is evaluated from (4.21), U_∞ from (4.22) and \bar{v}_j^2 from (4.40).

The stream function used in (4.21) and (4.22) is computed from equations (4.35) and (4.37).

The equation for ζ is

$$\frac{\partial \zeta}{\partial t} = \frac{\partial}{\partial y} \left(\frac{1}{R} + T_{22} \frac{\bar{v}^2}{v} \right) \frac{\partial \zeta}{\partial y} + 2 T_{22} \frac{\bar{v}^2}{v} \left(\frac{\partial \bar{\xi}}{\partial y} \right)^2 - \frac{2\zeta}{\lambda_d^2 R} \quad (4.30)$$

which is approximated by

$$\begin{aligned} \frac{\zeta_j^{n+1} - \zeta_j^n}{\Delta t} = & \left(\frac{1}{R} + T_{22} \frac{\bar{v}_j^2}{v} \right) \left(\frac{\zeta_{j+1}^n - \zeta_j^n}{h^2} \right) - \left(\frac{1}{R} + T_{22} \frac{\bar{v}_{j-1}^2}{v} \right) \left(\frac{\zeta_j^n - \zeta_{j-1}^n}{h^2} \right) \\ & + T_{22} \frac{\bar{v}_j^2}{v} \left(\frac{\bar{\xi}_{j+1}^n - \bar{\xi}_j^n}{h} \right)^2 + T_{22} \frac{\bar{v}_{j-1}^2}{v} \left(\frac{\bar{\xi}_j^n - \bar{\xi}_{j-1}^n}{h} \right)^2 - \frac{2\zeta_j^n}{R\lambda_d^2} \end{aligned} \quad (4.33)$$

at the grid points $j=2, \dots, M/2$ and by

$$\begin{aligned} \frac{\zeta_1^{n+1} - \zeta_1^n}{\Delta t} = & \left(\frac{1}{R} + T_{22} \frac{\sqrt{1/2}}{v_1} \right) \left(\frac{\zeta_2^n - \zeta_1^n}{h^2} \right) - C_2 \left(\frac{1}{R} + T_{22} \frac{\sqrt{1/2}}{v_1} \right) \frac{\zeta_1^n}{h^2} \\ & + 2 T_{22} \frac{\sqrt{1/2}}{v_1} \left(\frac{\bar{\xi}_2^n - \bar{\xi}_1^n}{h} \right)^2 - \frac{2}{R\lambda_d^2} \zeta_1^n \end{aligned} \quad (4.32)$$

at the grid point $j=1$.

After values have been assigned to the various parameters in the difference equations, we will then have a complete system of equations with which to solve for the grid functions $\bar{\xi}_j$ and ζ_j . As mentioned earlier, the equations are to be solved by iteration from initial values $\bar{\xi}_j^0$ and ζ_j^0 until $\bar{\xi}_j^n$ and ζ_j^n have converged to a solution of the time independent equations. Our criterion for deciding that convergence has occurred is the condition that $\sup_j |\bar{\xi}_j^{n+1} - \bar{\xi}_j^n| < 10^{-10}$ and $\sup_j |\zeta_j^{n+1} - \zeta_j^n| < 10^{-10}$.

The integration time step Δt , must be chosen to be small enough so that the difference equations are stable. We may set an upper bound to Δt by the requirement that

$$\frac{\Delta t}{h^2} \left(\frac{1}{R} + T_{22} \sup_j \frac{\sqrt{1/2}}{v_j} \right) < \frac{1}{2}$$

which generally must be satisfied for numerical approximations to the heat equation such as (4.13). Since we only seek steady solutions of our difference equations, we will also find out a posteriori from the fact of convergence of the iterations, that the value of Δt was small enough.

For the time step and initial conditions we have used, the convergence is in general quite rapid, requiring < 3000 iterations and less than a second of CDC 7600 computer time. The only exception to this is at Reynolds numbers within the range separating the turbulent solutions from the laminar solutions. Here, convergence may take considerably longer, on the order of 40,000 iterations.

The solutions we have found are independent of initial conditions so long as all of the ζ_j^0 are not equal to 0, for in that case, as is apparent from equations (4.32) and (4.33), the solution cannot help but be the non-turbulent parabolic flow. The iteration scheme advances by using the known values of $\bar{\xi}_j^n$ to compute $\bar{\psi}_j^n$ by inverting equations (4.35) and (4.37), and then using (4.21) and (4.22) to find values of δ and U_∞ to be used in (4.20). The values of ζ_j^n are used to compute the \bar{v}_j^2 from (4.40) and then the new values of $\bar{\xi}_j^{n+1}$ and ζ_j^{n+1} are obtained from (4.13), (4.20), (4.32), and (4.33) and the cycle is repeated again.

It is worthwhile at this point, before going into the numerical results, to recapitulate what are the failings of the system of equations that we hope to solve numerically for the mean properties of the flow in a channel. These limitations are:

(i) The transport law introduces the Lagrangian integral time scale T_{22} , which is as yet indeterminable from theory.

(ii) The dissipation term in the equation for ζ and the local term in the equation for $\overline{v'^2}$ introduce the Taylor vorticity microscales λ_x and λ_y which are a property of the small scale motion and again are not yet amenable to theoretical prediction.

(iii) For modest Reynolds numbers, just outside of the laminar range, the distance y' may be comparable to h , and in that event our use of the transport law in deriving the difference equations for the first two boxes would be unjustified.

(iv) The production term in (4.32) which is for the box adjacent to the wall has only been estimated roughly.

(v) The rate of diffusion of ζ into the region $y < y'$ has been modeled crudely in (4.32) and this has resulted in the introduction of a constant C_2 which must be determined empirically.

(vi) The need to compute U at a point δ within the sublayer has introduced another unknown parameter C_1 , in equation (4.22).

The problems listed in (iv)-(vi) are those that we hope may be solved one day by a more sophisticated mathematical treatment of the wall region. (i)-(iii) on the other hand, present much more fundamental difficulties and will require extensive new theoretical development before they are resolved.

We will determine values for the unknown parameters by using the experimental results of the flow in a channel at $R_e = 57,000$ which were obtained by Comte-Bellot (1965). This will keep our reliance on

experiment to a minimum, but also will necessitate making the assumption that none of our parameters change with Reynolds number. Since we obtain generally good results with these parameters for the two other Reynolds numbers, i.e. 120,000 and 230,000 that Comte-Bellot studied, we may suppose that, in fact, these parameters do not change greatly for large R_e .

We should point out that there have been at least three other published experimental studies of the flow in a channel, one by Laufer (1953), one by Clark (1968) and one by Eckelmann (1970). We have not yet seen this last one, and the work of Clark will not be of much use to us because it does not provide us with sufficient detail on the quantities we will need. The work of Laufer does, but we found it to be in serious disagreement with that of Comte-Bellot, forcing us to choose between the one or the other to use. We chose to use the data of Comte-Bellot because it is more recent than that of Laufer and is from a channel which is longer and has a higher aspect ratio than the one used by Laufer.

The first kind of data that we will use is the experimentally determined friction coefficient. Actually, the quantity which is measured is $\Delta\bar{p}^*/\frac{1}{2}\rho U_0^{*2}$, where U_0^* is the (dimensioned) centerline velocity and $\Delta\bar{p}^* = \bar{p}^*(x) - \bar{p}^*(x_0)$ is the absolute mean pressure drop between a fixed position x_0 in the channel and the variable point x . When $R_e = 57,000$ we see from the experimental data that

$$\frac{\bar{p}^*(70D) - \bar{p}^*(120D)}{\frac{1}{2}\rho U_0^{*2}} = .150$$

Since

$$\left[\bar{p}^*(70D) - \bar{p}^*(120D) \right] 2D = 2\tau_w^*(120D - 70D)$$

we must have

$$\frac{\tau_w^*}{\frac{1}{2}\rho U_0^{*2}} = \frac{\lambda}{U_0^2} = \frac{.15}{50} = .003$$

where U_0 is the dimensionless centerline velocity. We thus have the result that for $R_e = 57,000$,

$$\lambda = .003 U_0^2 \quad (4.41)$$

If we use (4.41) in place of

$$\lambda = \frac{U_\infty}{R_e(\delta - \delta^2)} \quad (4.42)$$

in (4.20) then we may determine all of the parameters except C_1 by adjusting them until the computed and experimental predictions of the velocity profile at $R_e = 57,000$ coincide. After this is done, C_1 may be

determined from the requirement that (4.41) and (4.42) are equal.

The selection of a value of λ_d is governed by the following considerations: The sole source of production of ζ in our two dimensional model comes from the term $2 T_{22} \overline{v'^2} \overline{\xi_y^2}$ in (4.30). In the core region of the channel where $\frac{1}{R} \overline{\xi_y}$ is small, the mean vorticity equation (4.7) implies that $T_{22} \overline{v'^2} \overline{\xi_y} \approx \lambda$. Therefore the local rate of production of ζ in the channel is $2 \lambda \overline{\xi_y}$. For a given Reynolds number λ and $\overline{\xi_y}$ are determined and thus the rate of production is fixed and is essentially independent of the value of T_{22} . As a result of this we are limited in the choice of λ_d that we may make because we do not wish it to be so small that the dissipation rate is too much for the fixed production rate and therefore prevent us from finding a solution to the equations.

We also believe that most of the dissipation of ζ takes place in the dissipation zone $y < y'$ that we have discussed. Therefore we wish to choose a value of λ_d that will allow most of the dissipation to occur by its diffusion into the wall region. A typical value of $\frac{1}{\lambda_d^2}$ which satisfies this conditions and also does not cause the dissipation rate to be too large is $\frac{1}{\lambda_d^2} = 10$. This value of $\frac{1}{\lambda_d^2}$ implies that λ_x and λ_y are considerably larger than h and thus the condition that λ_x and λ_y be $< h$ which was suggested in section III.D. is violated. If we were to set $\lambda_x = \lambda_y \approx h/2$ so as to satisfy this condition then we would find that even with $C_2 = 0$ which implies that no ζ diffuses into the wall region, the dissipation far exceeds the production of ζ and hence no solutions may be found.

The cause of this difficulty apparently is our restriction to two dimensions. By going into three dimensions we would then be able to include the production of ζ arising from vortex stretching and other causes, which would in turn allow us to significantly increase the dissipation rate by decreasing λ_x and λ_y .

We will arbitrarily assign T_{22} the value .4 which insures that $\overline{v^2}$ is the right order of magnitude. This value is also of the magnitude of some Eulerian integral scales which have been measured by Comte-Bellot (1965). The value of C_2 will be found by a comparison of the computed results with experiments. Before showing how this is done we will show that the computed solutions for $\bar{\xi}$ and hence U only depend (roughly) on the ratio $\frac{C_2}{1/\lambda_d^2} = C_2 \lambda_d^2$ which is reflective of the relative amounts of dissipation which occur in the wall region as against the core region and on the ratio $T_{22}/(1/\lambda_d^2) = T_{22} \lambda_d^2$ which is suggestive of the strength of the production term in comparison to the dissipation terms in the core region.

To see this, suppose that λ and U are fixed. Thus $\bar{\xi}_y$ is set and the $\bar{\xi}$ equation is unaffected if T_{22} is replaced by $K T_{22}$ and $\overline{v^2}$ by $\frac{1}{K} \overline{v^2}$ where K is a constant. Now consider the equation for ζ (4.30). To preserve $T_{22} \lambda_d^2$ we must substitute $\frac{1}{K} \lambda_d^2$ for λ_d^2 , and to preserve $C_2 \lambda_d^2$ we must then use $K C_2$ for C_2 . Also, (4.40) implies that we can change $\overline{v^2}$ to $\frac{1}{K} \overline{v^2}$ by replacing ζ by $\frac{1}{K} \zeta$. We have just established that with $T_{22} \lambda_d^2$ and $C_2 \lambda_d^2$ held constant but with T_{22} , $1/\lambda_d^2$ and C_2 all multiplied by a factor K , we will obtain, (modulo the diffusion term $\frac{\partial}{\partial y} \left(\frac{1}{R} + T_{22} \overline{v^2} \right) \frac{\partial \zeta}{\partial y}$ in (4.30) whose effect on this argument

turns out not to be major in practice) the same solution for U but with the ζ field approximately equal to $\frac{1}{K} \zeta$. From computations we have performed we have found that U will experience a change of less than 2.5% for factors K such that $\frac{1}{2} \leq K \leq 2$.

This argument shows that T_{22} may be adjusted later if we so desire (and thus also λ_d^2 and C_2) to insure that $\overline{v'^2}$ is equal to its experimentally determined value. However, as we will show later, there is some disagreement between the shape of the computed distribution of $\overline{v'^2}$ across the channel with that of the experimentally determined one, making it pointless to adjust T_{22} .

We are now left with the determination of C_2 . C_2 will be found by adjusting it until the velocity profile found experimentally at $R_e = 57,000$ matches the computed one. We found that this occurred when $C_2 = 1.25$. The closeness of fit is shown in Figure 6. As mentioned we now can determine C_1 and we found that it is equal to 3.28.

We have presumed in this analysis that T_{22} and λ_d are constant throughout the channel. There is some experimental justification for the belief that this is approximately true. Comte-Bellot (1965) and Laufer (1953) have measured the integral scale

$$L_y \equiv \frac{1}{\overline{v'^2}} \int_{r=0}^{\infty} \overline{v'(x,y)v'(x,y+r)} dr$$

and velocity microscales similar to our λ_x and λ_y , and found that they do not vary greatly across most of the channel. We will take these facts to mean that the character of the turbulence does not

radically change throughout the core region and that it is not unwarranted to presume that T_{22} and λ_d are constants.

We now have our parameters specified and we can investigate the predictions of the theory for the full range of Reynolds numbers. We first must make a comparison of the computed and experimental results for the Reynolds numbers 120,000 and 230,000 which were also studied in detail by Comte-Bellot. For $R_e = 120,000$ the experimentally determined value of λ/U_0^2 was .0026 and our computed result was .0023. Similarly for $R_e = 230,000$ experiment found $\lambda/U_0^2 = .00206$ and our computed result was .00172. Figure 6 shows a comparison for each of these Reynolds numbers of the computed and experimentally determined mean velocity profiles. It is seen that the agreement is quite good. Figure 7 shows a comparison of the velocity profiles of the 3 Reynolds numbers studied by Comte-Bellot with our numerical predictions of these curves.

Figure 8 shows our prediction of the friction law, i.e. the dependence of λ on R_e , for R_e up to 1,000,000. This result must be viewed with some caution in the lower range of Reynolds number in light of the questionable validity of our difference equations there. A drag crisis is clearly evident in Figure 8 at low Reynolds numbers where the values of λ suddenly increase from the laminar friction law $\lambda = 6/R_e$, which is represented by the straight line on the left. A distinct bifurcation in the computed results is observed at $R_e \approx 6500$. This is a critical Reynolds number, below which the solutions are laminar and above which they are turbulent. We cannot actually compute a smooth transition from the laminar solution to the turbulent ones because

our method of computing U and δ breaks down for the parabolic case. This could be easily corrected by a suitable artifice in our computer program but the only gain in doing this would be aesthetic. The collapse of our computed solutions to the laminar case is manifested quite clearly in practice and is equivalent to actually giving a prediction of the parabolic curve.

There has been at least one experimental study of the instability of a flow in a channel, that of Kao and Park (1970). They found that the critical Reynolds number at which all small amplitude disturbances were damped was $R_e \approx 5850$. They also observed that at Reynolds numbers lower than the critical value, disturbances of sufficiently large amplitude would cause subcritical neutral disturbances. Thus it is an open question as to what Reynolds number would be the upper limit at which the flow would be stable to all finite amplitude disturbances. The important point here is that the experimental and computed critical Reynolds numbers are of the same order of magnitude. That our numerical method is able to predict this qualitative behavior is a strong indication that we are doing justice to the physics of turbulent flow in a channel.

For a particular channel, i.e. D fixed, and a particular fluid, i.e. ρ and ν fixed, an engineer is interested in how much mass flow U_m can be obtained as a function of pressure gradient $\frac{\partial \bar{p}^*}{\partial x^*}$. Since $\lambda R^2 = \frac{\partial \bar{p}^*}{\partial x^*} \frac{(2D)^3}{\rho \nu^2}$ and $R = U_m 2D/\nu$, Figure 9 which is a plot of $\log \lambda R^2$ vs. $\log R$ graphically illustrates the crisis which occurs as the fluid becomes turbulent. On the left where the flow is laminar,

$\lambda = 12/R$ and thus $\lambda R^2 = 12R$ which implies that U_m will increase linearly with $\frac{\partial \bar{p}^*}{\partial x^*}$. However it is seen that when the flow becomes turbulent at $R \approx 14,000$ U_m is then barely affected by an increase in $\frac{\partial \bar{p}^*}{\partial x^*}$ until large pressure gradients are reached. This phenomenon is the drag crisis which arises from the increased ability of the turbulent fluid to deposit high momentum fluid near the wall. As the Reynolds number get very large Figure 9 shows that U_m varies with only the 2/3 power of $\frac{\partial \bar{p}^*}{\partial x^*}$ and not linearly as occurred in Poiseuille flow.

In Figure 10 is a family of computed velocity profiles covering the full range of Reynolds numbers, 4500 - 1,000,000 that we studied. For comparison a plot of the parabolic velocity profile is included. Figure 11 shows the computed mean vorticity profiles for the same range of Reynolds numbers. The straight line evident in this picture is the vorticity profile for laminar flow.

The dependence of the ζ distribution on R_e is shown in Figure 12, while Figure 13 shows a plot of $\overline{v'^2}$ for $R_e = 57,000$. It is apparent from Figure 12 that the magnitude of ζ increases with R_e to a maximum of $R_e \approx 30,000$, and then decreases subsequently. The velocity correlation $\overline{v'^2}$ has the same dependence on R_e as does ζ so the curves of $\overline{v'^2}$ also decrease with increasing R_e above 30,000. This behavior of $\overline{v'^2}$ for high R_e is qualitatively the same as has been observed experimentally by Comte-Bellot.

It is evident from Figure 13 that $\overline{v'^2}$ decreases gradually to a value of 0 at the wall. The local contributions to $\overline{v'^2}$ for the value of λ_x that we have used, are negligible, thus the shape of the distribution of $\overline{v'^2}$ is being determined by the fact that the ζ_j are smaller

near the wall than in the center and by the values of the $G_v(\vec{x}|\vec{x}')$ which are determined by the geometry of the channel. We found that the latter factor is generally much more important in determining the shape of $\overline{v'^2}$ distribution than is the values of the ζ_j .

As previously mentioned, this result for the computed shape of $\overline{v'^2}$ departs considerably from what has been observed experimentally. There it is found that $\overline{v'^2}$ is roughly constant across most of the channel and drops to zero sharply at a short distance from the wall.

One apparent explanation of this discrepancy, that can be shown to be wrong, is that we have chosen λ_x to be too large in the first few grid boxes so that the local contribution to $\overline{v'^2}$ here are much smaller than they should be. This argument can't be true, because to make λ_x small enough near the wall so that $\overline{v'^2}$ will be nearly constant across the channel, would also have the effect of driving up the total dissipation of ζ so high that it would greatly exceed the total production of ζ taking place in the channel. Also, as previously mentioned, we would not expect to find in a real flow the large variations of λ_x across the channel that this action would mandate.

The most probable cause of the anomalous distribution of $\overline{v_j'^2}$ is the fact that we have considered a purely two dimensional turbulent flow. This explanation may be made more plausible if we attempt to compute $\overline{u^i v^i}$ through the use of our formula (3.48). We find that the contributions to $\overline{u^i v^i}$ from all of the distant grid boxes cancel with one another because of our assumption of the uniformity of flow conditions up and downstream. We are then left with the relation

$$\overline{u'v'}_j = h^4 C C' \frac{\partial^2 R}{\partial x \partial y} (0) \zeta_j \quad (4.43)$$

We saw in equation 4.26) that $\overline{u'v'} \approx \lambda/4$ for part of the core region, and if the right side of (4.43) is to be of this magnitude then $\frac{\partial^2 R}{\partial x \partial y}(0)$ must be quite large, in fact $\gg \frac{\partial^2 R}{\partial x^2}(0)$ or $\frac{\partial^2 R}{\partial y^2}(0)$. This result, which is of doubtful physical validity, is a necessary consequence of presuming that purely two dimensional turbulent motion would give rise to the mean flow field that is found experimentally in a three dimensional channel. In the real flow in a channel, the major source of correlation between u' and v' arises from vorticity lying above and below and parallel to the x - y plane and aligned in the direction of the principle rate of strain, see Tennekes and Lumley (1972) p. 41. Since this contribution to $\overline{u'v'}$ is clearly left out of our two dimensional model, it explains the origin of the physically implausible relation (4.43). Further, this same vorticity may be seen to also contribute $\overline{v'^2}$ and if accounted for might bring the computed distribution of $\overline{v'^2}$ across the channel into line with experiments.

V. FLOW IN A CYLINDER

In this chapter we will apply the method of coarse graining to the study of the turbulent flow in a two dimensional idealization of an internal combustion engine cylinder. We will only consider the flow during the piston's travel from BDC (Bottom Dead Center, i.e. the furthest position the piston takes from the cylinder head, see figure 14), to TDC (Top Dead Center, i.e. the piston's closest approach to the head), with the valves shut, i.e. the compression stroke.

In section V.A. we will derive the system of difference equations with which we intend to solve for the flow in the cylinder. Our discrete approximations $\bar{\xi}_{ij}$ to $\bar{\xi}$ and ζ_{ij} to ζ are defined on a grid which collapses with the changing size of the flow domain. To obtain the difference equations (5.9) and (5.10) for $\bar{\xi}_{ij}$ and ζ_{ij} respectively, at interior grid points, we approximate the equations for $\bar{\xi}$ and ζ derived in Chapter III. We then give representative examples, eqn. (5.15) for $\bar{\xi}_{ij}$ and eqn. (5.16) for ζ_{ij} , of the type of difference equations that we use at the boundary. To derive these we borrow slightly from our experience with the channel problem.

Due to the changing size of the flow domain the Green's function used in the computation of $\overline{u_i^t u_j^t}$ must be evaluated at every time step. Our method of calculating the Green's function uses a fast direct method of solving Poisson's equation and is presented in section V.B. Equation (5.33) gives an explicit formula for $\overline{u_{ij}^t}$ in terms of the Green's function and (5.34) gives the stream function. Using the stream function the components of the mean velocity field are then computed from (5.35) and (5.36).

In section V.C. we present the results of our computations of the flow in a cylinder. We have paid particular attention to predicting the mean flow field which occurs in the cylinder at the time of ignition and have shown how these conditions change with stroke-to-bore ratio.

Lengths in this problem will be scaled using the bore B so that the nondimensional flow domain is a rectangle with constant width 1, and a length x_p which varies with time. The wall at $x = 0$ is fixed and the one at x_p represents the piston face and is in motion. To find x_p we must first define some of the technical terms used to describe engines.

The crank angle, α , is defined as the angle which the crankshaft journal, see figure 14, makes with its position at TDC, reckoning so that $\alpha = -180^\circ$ at BDC and $\alpha = 0^\circ$ at TDC. The stroke, $2r$, is the distance traveled by the piston from BDC to TDC. If L is the length of the connecting rod, then the distance between the position the piston occupies at TDC to its position when the crankangle is α is, say $d = r(1 - \cos\alpha) + L - \sqrt{L^2 - r^2 \sin^2\alpha}$. $(r/L)^2$ for many engines is near .07 so it is common practice to suppose that $L - \sqrt{L^2 - r^2 \sin^2\alpha} \approx 0$ and thus $d = r(1 - \cos\alpha)$. The compression ratio, χ , is the ratio of the volume of the flow domain when the piston is at BDC to its volume when it is at TDC. Using χ and d it is not hard to show that

$$x_p = \sigma \left(\frac{1}{\chi - 1} + \frac{1}{2}(1 - \cos\alpha) \right) \quad (5.1)$$

where $\sigma = 2r/B$ is the stroke to bore ratio.

It will be most convenient for us to define a dimensionless time t with the property that $t=0$ at BDC and $t=1$ at TDC. To do this we first relate α to a real time coordinate, t' , through $\alpha = -\pi + 2\pi\omega t'$ where ω is the rate of revolution of the crankshaft in revolutions per second. Defining $t = 2\omega t'$ we get the desired relation between α and t , i.e. $\alpha = -\pi + \pi t$. In terms of t (5.1) becomes

$$x_p(t) = \sigma \left(\frac{1}{\chi-1} + \frac{1}{2}(1 + \cos\pi t) \right) \quad (5.2)$$

For the flow conditions of a typical engine the Mach number formed from the maximum piston velocity is small enough so that compression waves formed at the face of the cylinder rapidly disperse throughout the whole domain before the piston moves appreciably. Thus the compression of the fluid may be assumed to take place instantaneously and uniformly as the piston moves. Since there will be no combustion taking place during this stroke, there is then no possibility of gradients in density arising from this cause either and hence we may then make the simplifying assumption that the density ρ depends solely on the time.

It is clear that this assumption about the density is equivalent to supposing that the thermodynamic pressure (as compared to the dynamic pressure) varies uniformly with time also. With both the density and thermodynamic pressure uniform we may also conclude that the temperature is uniform, and thus that the flow is adiabatic and reversible.

If the charge is considered to behave like a perfect gas, then from our knowledge of the density we may find the thermodynamic pressure and temperature from the relations:

$$\frac{p}{p_0} = \left(\frac{\rho}{\rho_0}\right)^\gamma \quad \text{and} \quad \frac{T}{T_0} = \left(\frac{\rho}{\rho_0}\right)^{\gamma-1}$$

where $\gamma = C_p/C_v$ is the ratio of specific heats. The conservation of mass implies that

$$\rho(t)x_p(t) = \rho(0)x_p(0)$$

thus

$$\frac{p}{p_0} = \left(\frac{x_p(0)}{x_p(t)}\right)^\gamma \quad \text{and} \quad \frac{T}{T_0} = \left(\frac{x_p(0)}{x_p(t)}\right)^{\gamma-1}$$

The dilatation

$$\Theta = -\frac{1}{\rho} \frac{d\rho}{dt} = \frac{U_p}{x_p} \quad (5.3)$$

where

$$U_p = \frac{dx_p}{dt} = \frac{-\sigma\pi}{2} \sin\pi t \quad (5.4)$$

is the velocity of the piston. θ is uniform throughout the flow field.

We will separate the velocity field \vec{u} into a compressible and irrotational component $\vec{U}_c = (U_c, V_c)$ and an incompressible and rotational component $\vec{u}_I = (u_I, v_I)$. U_c will account for the compression of the fluid due to the piston and is a pure function, while $\vec{u}_I = \vec{u} + \vec{u}'$ is random. \vec{U}_c satisfies the boundary conditions $U_c = 0$ at $x = 0$ and $U_c = U_p$ at $x = x_p$, and $V_c = 0$ at $y = 0$ and 1 , while \vec{u}_I must satisfy $u_I = 0$ at $x = 0$ and x_p , $u_I = -U_c$ at $y = 0$ and 1 , and $v_I = 0$ at $y = 0$ and 1 and $v_I = -V_c$ at $x = 0$ and 1 .

Since θ is known we may compute \vec{U}_c a priori. To satisfy the irrotational requirement on \vec{U}_c we define a potential ϕ via $\vec{U}_c = \nabla\phi$. Then ϕ satisfies $\nabla^2\phi = \theta$, with specified values of its normal derivatives at each boundary. This is a Neumann Problem which has a unique solution. Using (5.3) the solution is easily found to be $\phi = \theta x^2/2 + \text{constant}$.

Thus

$$U_c = \theta x \quad (5.5)$$

$$V_c = 0$$

Since θ is a sure function, so is U_c and as hypothesized, this part of velocity field makes no contribution to the fluctuating velocity field.

Using the previously defined length and time scales for this problem we may form the velocity scale $2B\omega$. The Reynolds number appearing in the equations of motion is then

$$R = \frac{2B^2 \omega \rho}{\mu}$$

which is time dependent due to the density and the viscosity μ . The viscosity is time dependent through its dependence on the pressure and temperature. For simplicity we will assume that the kinematic viscosity, $\nu = \mu/\rho$ is constant during the compression stroke and therefore that R is also. In application it is a simple matter to supply the proper dependence of μ on T and p .

We will assume that the mean flow pattern is symmetrical through reflection in the line $y = \frac{1}{2}$. As a consequence, $U(x,y) = U(x,1-y)$ and $V(x,y) = -V(x,1-y)$. These relations then imply that $\bar{\xi}(x,y) = -\bar{\xi}(x,1-y)$, and if we use a stream function to represent U then we must have $\bar{\psi}(x,y) = -\bar{\psi}(x,1-y)$.

At $t = 0$ we will divide the flow domain into $N \times M$ boxes of equal size with M boxes spanning the width of the cylinder and N boxes its length. Once constituted, we will consider these boxes to move with the velocity U_c , and consequently the boxes will remain uniform in size.

The boxes will have the constant width $\Delta y = 1/M$ and a variable length $\Delta x = x_p(t)/N$. The collection of centers of the boxes at any one

instant: $\left\{ \left((i-\frac{1}{2})\Delta x, (j-\frac{1}{2})\Delta y \right) : i=1, \dots, N \text{ and } j=1, \dots, M \right\}$ form a staggered grid, which collapses as t varies from 0 to 1. Our discrete representations, $\bar{\xi}_{ij}$, ζ_{ij} and $\bar{\psi}_{ij}$ of $\bar{\xi}$, ζ and $\bar{\psi}$ respectively, will be defined on this grid. We will use the superscript 'n' to denote the discretized time step which the grid variable refers to. Thus, for example $\bar{\xi}_{ij}^n$ approximates $\bar{\xi} \left((i-\frac{1}{2})\Delta x_n, (j-\frac{1}{2})\Delta y, n\Delta t \right)$ where $\Delta x_n = x_p(n\Delta t)/N$ and Δt is the integration time step.

A. Difference Equations

We saw in section IV.E. that to accurately predict the values of the velocity correlations $\overline{u'v'}$ one must make a three dimensional simulation of the flow field. Since we do not propose to do this here we will suppose instead that the qualitative features of the flow in the two dimensional cylinder will not be strongly affected if all terms in the equations for $\bar{\xi}$ and ζ containing $\overline{u'v'}$ are set equal to zero. With this assumption the equations governing $\bar{\xi}$ and ζ for the flow in a cylinder are

$$\frac{\partial \bar{\xi}}{\partial t} = -(\vec{U}_c + \vec{U}) \cdot \nabla \bar{\xi} - \bar{\xi}\theta + \frac{\partial}{\partial x} \left(\frac{1}{R} + T_{11} \overline{u'^2} \right) \frac{\partial \bar{\xi}}{\partial x} + \frac{\partial}{\partial y} \left(\frac{1}{R} + T_{22} \overline{v'^2} \right) \frac{\partial \bar{\xi}}{\partial y} \quad (5.6)$$

and

$$\begin{aligned}
\frac{\partial \zeta}{\partial t} = & -(\vec{U}_c + \vec{U}) \cdot \nabla \zeta - 2\zeta\theta + \frac{\partial}{\partial x} \left(\frac{1}{R} + T_{11} \overline{u'^2} \right) \frac{\partial \zeta}{\partial x} \\
& + \frac{\partial}{\partial y} \left(\frac{1}{R} + T_{22} \overline{v'^2} \right) \frac{\partial \zeta}{\partial y} + 2 T_{11} \overline{u'^2} \left(\frac{\partial \bar{\xi}}{\partial x} \right)^2 \\
& + 2 T_{22} \overline{v'^2} \left(\frac{\partial \bar{\xi}}{\partial y} \right)^2 - \frac{2\zeta}{\lambda_d^2 R}
\end{aligned} \tag{5.7}$$

where for simplicity we will assume that (5.6) and (5.7) may be used everywhere in the flow domain.

In forming difference equations for $\bar{\xi}_{ij}^n$ and ζ_{ij}^n which are consistent to (5.6) and (5.7) we must be careful of how we account for the collapsing grid. The index 'i' in $\bar{\xi}_{ij}^n$ refers to the point $(i-\frac{1}{2})\Delta x_n$ so that even though $\bar{\xi}_{ij}^n$ and $\bar{\xi}_{ij}^{n+1}$ may have the identical i index, i.e. they refer to the same grid box, they do not refer to the same physical point in space. Consider the finite difference approximation:

$$\frac{\bar{\xi}_{ij}^{n+1} - \bar{\xi}_{ij}^n}{\Delta t} \tag{5.8}$$

We may show that because of the movement of the grid this term actually represents an approximation to $\bar{\xi}_t + U_c \bar{\xi}_x$ and not just to $\bar{\xi}_t$: Substitute the function $\bar{\xi}$ into (5.8) to get

$$\begin{aligned}
& \frac{\bar{\xi} \left((i-\frac{1}{2})\Delta X_{n+1}, (j-\frac{1}{2})\Delta y, (n+1)\Delta t \right) - \bar{\xi} \left((i-\frac{1}{2})\Delta X_n, (j-\frac{1}{2})\Delta y, n\Delta t \right)}{\Delta t} \\
&= \frac{(i-\frac{1}{2})(\Delta X_{n+1} - \Delta X_n) \bar{\xi}_x + \Delta t \bar{\xi}_t}{\Delta t} + O(\Delta t) \\
&= \frac{(i-\frac{1}{2})}{N} \frac{(X_p(t+\Delta t) - X_p(t))}{\Delta t} \bar{\xi}_x + \bar{\xi}_t + O(\Delta t) \\
&= \frac{\Delta X_n (i-\frac{1}{2}) U_p}{X_p} \bar{\xi}_x + \bar{\xi}_t + O(\Delta t) \\
&= U_c \bar{\xi}_x + \bar{\xi}_t + O(\Delta t)
\end{aligned}$$

Q.E.D.

The difference equations to follow will use this time differencing, so that to have equations consistent with (5.6) and (5.7) we will not have to further consider the term $U_c \bar{\xi}_x$ in (5.6) or $U_c \zeta_x$ in (5.7).

The difference equations for the interior boxes where $i = 2, \dots, N-1$ and $j = 2, \dots, M/2$ are

$$\begin{aligned}
\frac{\varepsilon_{ij}^{n+1} - \varepsilon_{ij}^n}{\Delta t} = & \frac{(u_{ij}^n (\varepsilon_{i+1,j}^n + \varepsilon_{ij}^n) - u_{i-1,j}^n (\varepsilon_{ij}^n + \varepsilon_{i-1,j}^n))}{2\Delta x_n} - \frac{(v_{ij}^n (\varepsilon_{ij+1}^n + \varepsilon_{ij}^n) - v_{ij-1}^n (\varepsilon_{ij}^n + \varepsilon_{ij-1}^n))}{2\Delta y} \\
& - \varepsilon_{ij}^n \theta_n + \left(\frac{1}{R} + \tau_{11} \nu_{ij}^{2n} \right) \frac{\varepsilon_{i+1,j}^n - \varepsilon_{ij}^n}{(\Delta x_n)^2} - \left(\frac{1}{R} + \tau_{11} \nu_{i-1,j}^{2n} \right) \frac{\varepsilon_{ij}^n - \varepsilon_{i-1,j}^n}{(\Delta x_n)^2} \\
& + \left(\frac{1}{R} + \tau_{22} \nu_{ij}^{2n} \right) \frac{\varepsilon_{i,j+1}^n - \varepsilon_{ij}^n}{(\Delta y)^2} - \left(\frac{1}{R} + \tau_{22} \nu_{i,j-1}^{2n} \right) \frac{\varepsilon_{ij}^n - \varepsilon_{i,j-1}^n}{(\Delta y)^2}
\end{aligned}$$

(5.9)

00104605294

$$\begin{aligned}
 \frac{c_{1j}^{n+1} - c_{1j}^n}{\Delta t} &= \frac{-\left(u_{1j}^n (c_{1+1,j}^n + c_{1j}^n) - u_{1-1,j}^n (c_{1j}^n + c_{1-1,j}^n)\right)}{2\Delta x_n} - \frac{\left(v_{1j}^n (c_{1,j+1}^n - c_{1j}^n) - v_{1,j-1}^n (c_{1j}^n + c_{1,j-1}^n)\right)}{2\Delta y} \\
 &- 2c_{1j}^n \theta_n + \left(\frac{1}{R} + \tau_{11} \frac{\tau_{1j}^n}{u_{1j}^n}\right) \frac{c_{1+1,j}^n - c_{1j}^n}{(\Delta x_n)^2} - \left(\frac{1}{R} + \tau_{11} \frac{\tau_{1j}^n}{u_{1-1,j}^n}\right) \frac{c_{1j}^n - c_{1-1,j}^n}{(\Delta x_n)^2} \\
 &+ \left(\frac{1}{R} + \tau_{22} \frac{\tau_{1j}^n}{v_{1j}^n}\right) \frac{c_{1,j+1}^n - c_{1j}^n}{(\Delta y)^2} - \left(\frac{1}{R} + \tau_{22} \frac{\tau_{1j}^n}{v_{1,j-1}^n}\right) \frac{c_{1j}^n - c_{1,j-1}^n}{(\Delta y)^2} \\
 &+ \tau_{11} \frac{\tau_{1j}^n}{u_{1j}^n} \left(\frac{\bar{\epsilon}_{1+1,j}^n - \bar{\epsilon}_{1j}^n}{\Delta x_n}\right)^2 + \tau_{11} \frac{\tau_{1j}^n}{u_{1-1,j}^n} \left(\frac{\bar{\epsilon}_{1j}^n - \bar{\epsilon}_{1-1,j}^n}{\Delta x_n}\right)^2 \\
 &+ \tau_{22} \frac{\tau_{1j}^n}{v_{1j}^n} \left(\frac{\bar{\epsilon}_{1,j+1}^n - \bar{\epsilon}_{1j}^n}{\Delta y}\right)^2 + \tau_{22} \frac{\tau_{1j}^n}{v_{1,j-1}^n} \left(\frac{\bar{\epsilon}_{1j}^n - \bar{\epsilon}_{1,j-1}^n}{\Delta y}\right)^2 - \frac{2}{\lambda_d^2 R} c_{1j}^n
 \end{aligned}$$

(5.10)

where U_{ij} and $\overline{u_{ij}^2}$ are at the point $(i\Delta x_n, (j-\frac{1}{2})\Delta y)$ and V_{ij} and $\overline{v_{ij}^2}$ are evaluated at $((i-\frac{1}{2})\Delta x_n, j\Delta y)$ and $\theta_n = \theta(n\Delta t)$. The convection term in both of these equations has been written in conservative form for ease of programming.

The special form for the boundary condition to the mean vorticity equation which was derived for the channel problem will not apply to the present case. However we may still suppose that the total vorticity flux normal to a boundary does not change rapidly across the wall region in spite of the fact that the molecular flux and the turbulent flux may individually vary greatly. Thus the boundary condition to the $\bar{\xi}$ equation will be the vorticity flux from the wall, i.e. $\frac{1}{R} \frac{\partial \bar{\xi}}{\partial y}$ at the wall $y = 0$ and $\frac{1}{R} \frac{\partial \bar{\xi}}{\partial x}$ at $x = 0$ and x_p .

We approximate this flux by, e.g. at $y = 0$:

$$\left. \frac{1}{R} \frac{\partial \bar{\xi}}{\partial y} \right|_{y=0} \approx \frac{1}{R} \left(\frac{\bar{\xi}(\Delta y/2) - \bar{\xi}_w}{\Delta y/2} \right) \quad (5.11)$$

where $\bar{\xi}_w = \bar{\xi}(0)$ and we presume here that all quantities are at a fixed value of x . The approximation in (5.11) is not unreasonable because the typical Reynolds numbers we will encounter, e.g. when an engine is rotating at 4000 rpm is only ≈ 5000 . Since $\bar{\xi}_w = - \left. \frac{\partial U}{\partial y} \right|_{y=0}$ we must estimate $\frac{\partial U}{\partial y}$ at the wall to complete (5.11). To do this we will say that

$$\left. \frac{\partial U}{\partial y} \right|_{y=0} = \left. \frac{\partial (U_c + U)}{\partial y} \right|_{y=0} = \frac{U' - (U_c + U)|_{y=0}}{\delta'} = \frac{U'}{\delta'} \quad (5.12)$$

where U' and δ' are a typical velocity and length at the outer edge of the region of rapid variation next to the wall. Using $\bar{\psi}$ we may define U' as the average mass flow velocity in the region between $y = 0$ and $y = \Delta y/2$, thus

$$U' \frac{\Delta y}{2} \equiv \int_0^{\Delta y/2} (U_c + U) dy = U_c \frac{\Delta y}{2} + \bar{\psi} \left(\frac{\Delta y}{2} \right)$$

or

$$U' = U_c + \frac{2}{\Delta y} \bar{\psi}(\Delta y/2) \quad (5.13)$$

We will define δ' as a mass displacement thickness, by the requirement that

$$U_c \frac{\Delta y}{2} + \bar{\psi} \left(\frac{\Delta y}{2} \right) = \left(U_c + U \left(\frac{\Delta y}{2} \right) \right) \left(\frac{\Delta y}{2} - \delta' \right)$$

which says that the total mass flow between 0 and $\Delta y/2$ is equal to the product of the velocity at $\Delta y/2$ and the reduced distance $\Delta y/2 - \delta'$.

If we assume that $U(\Delta y/2) \approx (\bar{\psi}_{i2} - \bar{\psi}_{i1})/\Delta y$ then we find that

$$\delta' = \frac{\frac{1}{2} \bar{\psi}_{i2} - \frac{3}{2} \bar{\psi}_{i1}}{U_c + \frac{\bar{\psi}_{i2} - \bar{\psi}_{i1}}{\Delta y}} \quad (5.14)$$

This same expression for δ' may be obtained by an argument which is similar to the one that was used to obtain δ for the channel problem in section IV.A. In the present case one may show that δ' is the value of y at the point of intersection of a line leaving the origin with slope $-U_c$, with the extension of a straight line connecting $(\Delta y/2, \bar{\psi}_{i1})$ and $(3\Delta y/2, \bar{\psi}_{i2})$. Thus instead of using a parabolic arc coming from the grid points near the wall to approximate $\bar{\psi}$ as was done in IV.A, here we are using a straight line.

Formula (5.14) gives a reasonable value of δ' when the flow near the wall has a turbulent boundary layer. In flow situations such as when the piston is near TDC, we don't necessarily expect to find the type of large gradients in U and $\bar{\psi}$ which are required for (5.14) to make sense, so in this case we will set $\delta' = \Delta y/2$.

Using the approximations (5.11) and (5.12) and similar relations for the wall $x = 0$ we may write out the $\bar{\xi}$ equation to be used at the corner box $i = 1, j = 1$:

$$\frac{\bar{\xi}_{11}^{n+1} - \bar{\xi}_{11}^n}{\Delta t} = \frac{-\bar{u}_{11}^n (\bar{\xi}_{21}^n + \bar{\xi}_{11}^n)}{2\Delta X_n} - \frac{v_{11}^n (\bar{\xi}_{12}^n + \bar{\xi}_{11}^n)}{2\Delta y}$$

$$-\bar{\xi}_{11}^n \theta_n + \left(\frac{1}{R} + T_{11} \frac{v_{11}^{2n}}{u_{11}^n} \right) \frac{\bar{\xi}_{21}^n - \bar{\xi}_{11}^n}{(\Delta X_n)^2}$$

$$\frac{-2}{R(\Delta X_n)^2} \left(\bar{\xi}_{11}^n - \frac{2V'}{\Delta X_n} \right) + \left(\frac{1}{R} + T_{22} \frac{v_{11}^{2n}}{v_{11}^n} \right) \frac{\bar{\xi}_{12}^n - \bar{\xi}_{11}^n}{(\Delta y)^2}$$

$$- \frac{2}{R(\Delta y)^2} \left(\bar{\xi}_{11}^n + U'/\delta' \right)$$

(5.15)

where V' is defined analogously to U' and we have used $\Delta X_n/2$ at the walls $x = 0$ and x_p in place of computing a length like δ' .

Note that there is no need to introduce any special arbitrary parameters, e.g. in the definitions of U' or δ' , because we have no quantitative experimental data with which to compare our results.

Similarly, we will use the following equation at the corner box $i = 1$, $j = 1$ which is also free of additional parameters:

$$\begin{aligned}
\frac{\zeta_{11}^{n+1} - \zeta_{11}^n}{\Delta t} &= -U_{11}^n \frac{(\zeta_{21}^n + \zeta_{11}^n)}{2\Delta X_n} - V_{11}^n \frac{(\zeta_{12}^n + \zeta_{11}^n)}{2\Delta y} - 2\zeta_{11}^n \theta_n \\
&+ \left(\frac{1}{R} + T_{11} \frac{u_{11}^{2n}}{u_{11}^n} \right) \frac{\zeta_{21}^n - \zeta_{11}^n}{(\Delta X_n)^2} - \left(\frac{1}{R} + T_{11} \frac{u_{11}^{2n}}{u_{11}^n} \right) \frac{\zeta_{11}^n}{(\Delta X_n)^2} \\
&+ \left(\frac{1}{R} + T_{22} \frac{v_{11}^{2n}}{v_{11}^n} \right) \frac{\zeta_{12}^n - \zeta_{11}^n}{(\Delta y)^2} - \left(\frac{1}{R} + T_{22} \frac{v_{11}^{2n}}{v_{11}^n} \right) \frac{\zeta_{11}^n}{(\Delta y)^2} \\
&+ 2 T_{11} \frac{u_{11}^{2n}}{u_{11}^n} \left(\frac{\zeta_{21}^n - \zeta_{11}^n}{\Delta X_n} \right)^2 + 2 T_{22} \frac{v_{11}^{2n}}{v_{11}^n} \left(\frac{\zeta_{12}^n - \zeta_{11}^n}{\Delta y} \right)^2 \\
&\frac{-2\zeta_{11}^n}{\lambda_d^2 R}
\end{aligned} \tag{5.16}$$

The stability analysis of the difference equations (5.9) and (5.10) et.al. is unaffected by the fact that the grid is collapsing, except as in so far as ΔX_n is changing in magnitude. The complexity of these equations is such that we will do no more than impose the stability conditions which are applicable for a linear system with constant coefficients, i.e.

$$\Delta t \left[\frac{1}{(\Delta x_n)^2} \left(\frac{1}{R} + T_{11} \sup_{ij} \overline{u_{ij}^2} \right) + \frac{1}{(\Delta y)^2} \left(\frac{1}{R} + T_{22} \sup_{ij} \overline{v_{ij}^2} \right) \right] \leq \frac{1}{4}$$

and

$$\Delta t \sup_{ij} |U_{ij}| < \Delta x_n$$

$$\Delta t \sup_{ij} |V_{ij}| < \Delta y$$

In practice these conditions pose no hardship to finding a useful value of Δt for which no instabilities appear in the computations.

B. Computation of Stream Function, Mean Velocity and Velocity Moments

The functions $G_u(\vec{x}|\vec{x}')$ and $G_v(\vec{x}|\vec{x}')$ which are used to compute $\overline{u^2}$ and $\overline{v^2}$ will have to be recomputed at every time step in this problem because of the changing size of the flow domain. The functions may be calculated exactly by setting up a lattice of image vortices in the plane and adding up their contributions to $\overline{u^2}$ and $\overline{v^2}$, as was done in the channel problem. This is, however, a very slow procedure computationally, so instead we will compute the functions G_u and G_v only approximately but by a considerably faster method.

To explain this procedure, let us consider two general functions $f(\vec{x})$ and $g(\vec{x})$ which are related through Poisson's equation $\nabla^2 f = g$ on our rectangular domain D . f , in addition, is required to be 0 on the boundaries. As we saw in eqn. (3.37) f is determined by g through the integral relation

$$f(\vec{x}) = \int_D G(\vec{x}|\vec{x}') g(\vec{x}') d\vec{x}' \quad (5.17)$$

We will find an approximation to $G(\vec{x}|\vec{x}')$ by forming an analogue to (5.17) in terms of grid functions.

Let f_{ij} and g_{ij} be approximations to f and g , respectively, at the point indicated by (i,j) on our staggered grid. We relate f_{ij} and g_{ij} through a difference approximation to Poisson's equation. For points at a distance from the boundary we use the standard five point approximation to the Laplacian:

$$\frac{f_{i+1 j} - 2f_{ij} + f_{i-1 j}}{(\Delta x)^2} + \frac{f_{i j+1} - 2f_{ij} + f_{i j-1}}{(\Delta y)^2} = g_{ij} \quad (5.18)$$

and at a wall, i.e. $i = 1$ or N and/or $j = 1$ or M , we use, e.g.

when $j = 1$, $1 < i < N$:

$$\frac{f_{i+1,1} - 2f_{i,1} + f_{i-1,1}}{(\Delta x)^2} + \frac{f_{i,2} - 3f_{i,1}}{(\Delta y)^2} = g_{i,1} \quad (5.19)$$

and e.g. in the corner $i = 1, j = 1$:

$$\frac{f_{21} - 3f_{11}}{(\Delta x)^2} + \frac{f_{12} - 3f_{11}}{(\Delta y)^2} = g_{11} \quad (5.20)$$

Equations (5.19) and (5.20) are not formally consistent with Poisson's equation, however, the use of them may be justified by a simple physical argument for the case in which f is the stream function $\bar{\psi}$: Consider the process of making a finite difference approximation to $\frac{\partial U}{\partial y} = \frac{\partial^2 \bar{\psi}}{\partial y^2}$ near the wall $y = 0$, in a turbulent flow when we expect that a sharp gradient in U exists in a small region next to the wall. We may say

$$\frac{\partial U}{\partial y} \Big|_{y=\frac{\Delta y}{2}} = \frac{\partial}{\partial y} (U_c + U) \Big|_{y=\frac{\Delta y}{2}} = \frac{(U_c + U) \Big|_{y=\Delta y} - U'}{\Delta y} \quad (5.21)$$

where U' is a typical velocity just outside the region of large variation in U and which we make take to be the average velocity U' defined in (5.13). The term $(U_c + U)_{y=\Delta y}$ may be approximated as

$$\left(U_c + U \right)_{y=\Delta y} \approx U_c + \frac{\bar{\psi}_{i2} - \psi_{i1}}{\Delta y}$$

and thus (5.21) becomes

$$\left. \frac{\partial U}{\partial y} \right|_{y=\Delta y} \approx \frac{\bar{\psi}_{i2} - 3\bar{\psi}_{i1}}{\Delta y} \quad (5.22)$$

which is used in the making of (5.19) and (5.20).

The motivation to use this special differencing at the wall comes from the fact that the relations (5.19), (5.20) et.al. will permit us to use a fast direct method of solving Poisson's equation for the staggered grid, a very important consideration. The only alternative differencing procedure we know of that also admits of a solution by a fast direct method, is to interpolate the mean vorticity field onto a non-staggered grid, and then solve a system of equations like (5.18) which relate the $\bar{\psi}_{ij}$ on this grid. We have found that for a test problem containing a turbulent-like vorticity distribution for which U and $\bar{\psi}$ could be obtained analytically the procedure we have elected

to use predicted U more accurately over more of the flow domain than the alternative procedure, and therefore we chose to use it.

Now to continue our argument, we fix indices k and l , and suppose that g_{ij} is equal to $\frac{1}{\Delta x \Delta y} \delta_{in} \delta_{jm}$ where δ_{in} is the Kronecker delta function. The solution of the difference equations (5.18) et.al. for this special function g_{ij} we call G_{ij}^{nm} . If we compute the functions G_{ij}^{nm} for each value of (n,m) , $n=1, \dots, N$ and $m=1, \dots, M$ then it is a simple matter to show that, for an arbitrary function g_{ij} :

$$f_{ij} = \sum_{n=1}^N \sum_{m=1}^M G_{ij}^{nm} g_{ij} \Delta x \Delta y \quad (5.23)$$

(5.23) is formally an approximation to (5.17) and we may suppose that $G_{ij}^{nm} \approx G \left((i-\frac{1}{2})\Delta x, (j-\frac{1}{2})\Delta y \mid (n-\frac{1}{2})\Delta x, (m-\frac{1}{2})\Delta y \right)$.

In practice we will only have to compute G_{ij}^{nm} for $n=1, \dots, N/2$ and $m=1, \dots, M/2$ because we may use the following relations which arise from the symmetry of the rectangle:

$$G_{ij}^{N+1-n, m} = G_{N+1-i, j}^{nm}$$

$$G_{ij}^{n, M+1-m} = G_{i, M+1-j}^{nm}$$

$$G_{ij}^{N+1-n, M+1-m} = G_{N+1-i, M+1-j}^{nm}$$

to compute the others.

We will now show how the system of equations (5.18), (5.19), (5.20) et.al. may be solved using a fast direct method based on numerical separation of variables: We presume, initially, that g_{ij} is a general grid function and will specialize it later to obtain the G_{ij}^{nm} . Let us define column vectors f^i and g^i through

$$f^i \equiv \begin{pmatrix} f_{i1} \\ \bullet \\ \bullet \\ \bullet \\ f_{iM} \end{pmatrix}, \quad g^i \equiv \begin{pmatrix} g_{i1} \\ \bullet \\ \bullet \\ \bullet \\ g_{iM} \end{pmatrix}$$

The system of equations (5.18) et.al. may be written concisely in terms of these vectors as

$$\frac{f^{i+1} - 2f^i + f^{i-1}}{(\Delta x)^2} + \frac{(B-2I) f^i}{(\Delta y)^2} = g^i \quad i = 2, \dots, N-1$$

$$\frac{f^{i+1} - 3f^i}{(\Delta x)^2} + \frac{(B-2I) f^i}{(\Delta y)^2} = g^i \quad i=1 \quad (5.24)$$

$$\frac{f^{i-1} - 3f^i}{(\Delta x)^2} + \frac{(B-2I) f^i}{(\Delta y)^2} = g^i \quad i=N$$

$$\phi^k = \begin{pmatrix} \phi_{k1} \\ \vdots \\ \phi_{kM} \end{pmatrix}$$

The eigenvalue corresponding to ϕ^k is $\lambda_k = 2\cos\alpha_k$. Since the ϕ^k are linearly independent and complete we may write f^i and g^i as a linear combination of them, viz:

$$f^i = \sum_{k=1}^M B_k^i \phi^k \quad (5.25)$$

and

$$g^i = \sum_{k=1}^M A_k^i \phi^k \quad (5.26)$$

The orthogonality of the ϕ^k implies that the inner product of ϕ^{k_1} and ϕ^{k_2} is

$$\langle \phi^{k_1}, \phi^{k_2} \rangle \equiv \sum_{\ell=1}^M \phi_{k_1 \ell} \phi_{k_2 \ell} = C_{k_1} \delta_{k_1 k_2}$$

where

$$C_k = \langle \phi^k, \phi^k \rangle = \begin{cases} M/2 & k \neq M \\ M & k = M \end{cases}$$

Substituting (5.25) and (5.26) into (5.24) and taking the inner product with respect to each ϕ^k in turn, $k=1, \dots, M$, gives the following system of equations for the B_k^i 's in terms of the A_k^i 's

$$\frac{B_k^{i+1} - 2B_k^i + B_k^{i-1}}{(\Delta x)^2} + \frac{(\lambda_k - 2) B_k^i}{(\Delta y)^2} = A_k^i \quad i=2, \dots, N-1$$

$$\frac{B_k^{i+1} - 3B_k^i}{(\Delta x)^2} + \frac{(\lambda_k - 2) B_k^i}{(\Delta y)^2} = A_k^i \quad i = 1 \quad (5.27)$$

$$\frac{B_k^{i-1} - 3B_k^i}{(\Delta x)^2} + \frac{(\lambda_k - 2) B_k^i}{(\Delta y)^2} = A_k^i \quad i = N$$

The A_k^i 's are computed from

$$A_k^i = \frac{1}{C_k} \langle \phi^k, g^i \rangle = \frac{1}{C_k} \sum_{j=1}^M g_{ij} \sin \frac{k\pi}{M} (j-\frac{1}{2})$$

using the known values of g_{ij} . For each k (5.27) gives a tridiagonal system of M equations for the M unknowns B_k^i , and the solution is easily obtained computationally.

With the B_k^i in hand we can compute the f_{ij} from

$$f_{ij} = \sum_{k=1}^M B_k^i \phi_{kj} = \sum_{k=1}^M B_k^i \sin \frac{k\pi}{M} (j-1/2) \quad (5.28)$$

and this completes the algorithm.

For the special case when $g_{ij} = \frac{1}{\Delta x \Delta y} \delta_{in} \delta_{jm}$ so that $f_{ij} = G_{ij}^{nm}$ we can shorten some of the steps involved in carrying out this algorithm. First of all, the evaluation of the A_k^i in this case is trivial since

$$A_k^i = \frac{1}{C_k} \sum_{j=1}^M \frac{1}{\Delta x \Delta y} \delta_{in} \delta_{jm} \sin \frac{k\pi}{M} (j-\frac{1}{2}) = \frac{1}{C_k \Delta x \Delta y} \delta_{in} \sin \frac{k\pi}{M} (m-\frac{1}{2})$$

Next, using these special values of A_k^i we can significantly reduce the amount of labor needed to solve the system of equations (5.27). To show how this may be done let us make the definitions:

$$W_k = -2 + \left(\frac{\Delta x}{\Delta y}\right)^2 (\lambda_k - 2) \tag{5.29}$$

$$D_k^m = \frac{1}{C_k \Delta y} \sin \frac{k\pi}{M} (m - \frac{1}{2}) \tag{5.30}$$

The tridiagonal equations we must solve may be written, using (5.29) and (5.30) as

$$\begin{aligned} (W_k - 1) B_1^k + B_2^k &= 0 \\ \vdots \\ B_{i-1}^k + W_k B_i^k + B_{i+1}^k &= 0 \\ \vdots \\ B_{n-1}^k + W_k B_n^k + B_{n+1}^k &= \Delta x D_k^m \\ \vdots \\ B_{N-1}^k + (W_k - 1) B_N^k &= 0 \end{aligned} \tag{5.31}$$

If we define coefficients R_i^k , $i=0,1,\dots,N$ recursively through

$$R_0^k = -1$$

$$R_i^k = \frac{-1}{W_k + R_{i-1}^k} \quad i=1,2,\dots,N$$

then the solution of the system of equations (5.31) may be obtained by first computing

$$B_n^k = \frac{\Delta x D_k^m}{W_k + R_{n-1}^k + R_{N-n}^k}$$

and then computing the rest of the B_i^k 's from the recursion relations

$$B_i^k = R_i^k B_{i+1}^k \quad i = n-1, n-2, \dots, 2, 1$$

$$B_i^k = R_{N+1-i}^k B_{i-1}^k \quad i = n+1, n+2, \dots, N-1, N$$

Since the coefficients R_i^k do not depend on n and m , they may be computed once at each time step, to be used in the computations of all the G_{ij}^{nm} . The quantities D_k^m may be computed once and for all time before the numerical integration is initiated, and held in an array.

There is no special savings to be had, arising from the special nature of the g_{ij} , for the computation of the sum in (5.28). However we may evaluate it more efficiently than doing it directly, through the use of a fast Fourier transform. The sum in (5.28) is not in the standard form that can be computed by a fast Fourier transform, but it may be put into such a form. To do this we define, for an arbitrary vector z_k with $M' = 4M$ components, the following finite Fourier transform:

$$\tilde{z}_\ell \equiv \sum_{k=1}^{M'} z_k e^{\frac{2\pi i k \ell}{M'}} \tag{5.32}$$

$\ell=1,2,\dots,M'$.

If

$$z_k = \begin{cases} B_k^i & k = 1,2,\dots,M \\ 0 & k > M \end{cases}$$

then it is easy to see that

$$f_{ij} = \sum_{k=1}^M B_k^i \sin \frac{k\pi}{M} (j-\frac{1}{2}) = \text{Im}[\tilde{Z}_{2j-1}]$$

where $\text{Im}[\quad]$ means 'the imaginary part of'.

When M is equal to a power of 2, (5.32) may be evaluated efficiently through the use of the fast Fourier transform algorithm given by Cooley and Tukey (1965). To do this, we must specify a value of M and then write a special program tailored to this M which takes advantage of the special properties of our sum, e.g. that $Z_k = 0$ for $k > M$, etc. We have done for $M = 16$ and found that a 1/3 savings in time could be had over computing (5.28) directly. Considering that this sum must be done $MN^2/4$ times for each time step this represents a considerable increase in efficiency. The fact that we are then restricted to have $M = 16$ is not a hardship because the width of the cylinder does not vary and $M = 16$ gives adequate resolution of the flow field without being unduly expensive. Also N may still be varied to account for different values of σ .

Turning now to the computations of the velocity correlations $\overline{u^2}$ and $\overline{v^2}$ we may use the computed Green's function G_{ij}^{nm} to approximate the functions $G_u(\vec{x}|\vec{x}')$ and $G_v(\vec{x}|\vec{x}')$ by finite differences. To simplify the writing of the formulas we define a function H_{ij}^{nm} as an approximation to $G(i\Delta x, j\Delta y | (n-\frac{1}{2})\Delta x, (m-\frac{1}{2})\Delta y)$, and compute it from interpolation of the G_{ij}^{nm} viz:

$$H_{ij}^{nm} = \frac{1}{4} (G_{i+1, j+1}^{nm} + G_{i, j+1}^{nm} + G_{i+1, j}^{nm} + G_{ij}^{nm})$$

Using the H_{ij}^{nm} we find e.g.

$$\begin{aligned} \overline{u_{ij}^2} = & \sum_{m=1}^{M/2} \sum_{n=1}^{N/2} \left\{ \left[\left(\frac{H_{ij}^{nm} - H_{i, j-1}^{nm}}{\Delta y} \right)^2 + \left(\frac{H_{i, M-j+1}^{nm} - H_{i, M-j}^{nm}}{\Delta y} \right)^2 \right] \zeta_{nm} \right. \\ & \left. + \left[\left(\frac{H_{N-i, j}^{nm} - H_{N-i, j-1}^{nm}}{\Delta y} \right)^2 + \left(\frac{H_{N-i, M-j+1}^{nm} - H_{N-i, M-j}^{nm}}{\Delta y} \right)^2 \right] \zeta_{N+1-n, m} \right\} \end{aligned} \quad (5.33)$$

where, for simplicity we treat the boxes making a local contribution to $\overline{u_{ij}^2}$ the same as the others. A similar formula may be obtained for $\overline{v_{ij}^2}$.

Using the computed values of G_{ij}^{nm} and (5.23) with no extra work we get the stream function from

$$\overline{\psi_{ij}} = - \sum_{m=1}^{M/2} \sum_{n=1}^{N/2} \left[\left(G_{ij}^{nm} - G_{i, M+1-j}^{nm} \right) \overline{\xi}_{ij} + \left(G_{N+1-ij}^{nm} - G_{N+1-i, M+1-j}^{nm} \right) \overline{\xi}_{N+1-ij} \right] \quad (5.34)$$

where we have used the antisymmetry of $\overline{\xi}_{ij}$.

U_{ij} and V_{ij} may then be computed from the relations

$$U_{ij} = \frac{\bar{\psi}_{i+1, j+1} + \bar{\psi}_{i, j+1} - \bar{\psi}_{i+1, j-1} - \bar{\psi}_{i, j-1}}{2\Delta y} \quad \begin{array}{l} i = 1, \dots, N-1 \\ j = 1, 2, \dots, M/2 \end{array} \quad (5.35)$$

$$V_{ij} = - \left(\frac{\bar{\psi}_{i+1, j+1} + \bar{\psi}_{i+1, j} - \bar{\psi}_{i-1, j+1} - \bar{\psi}_{i-1, j}}{2\Delta x} \right) \quad \begin{array}{l} i = 1, \dots, N \\ j = 1, 2, \dots, M/2 \end{array} \quad (5.36)$$

where we have let $\bar{\psi}_{i0} = -\bar{\psi}_{i1}$ $i = 1, \dots, N$ and $\bar{\psi}_{0j} = -\bar{\psi}_{1j}$ and $\bar{\psi}_{N+1, j} = -\bar{\psi}_{Nj}$ for $j = 1, \dots, M/2$, so as to enable (5.35) and (5.36) to apply at grid points near the boundary.

C. Results of Computations

For convenience let us collect together the basic difference equations we hope to solve for the flow in the cylinder. The $\bar{\xi}$ equation is

$$\frac{\partial \bar{\xi}}{\partial t} = -(\vec{U}_c + \vec{U}) \cdot \nabla \bar{\xi} - \bar{\xi} \Theta + \frac{\partial}{\partial x} \left(\frac{1}{R} + \tau_{11} \bar{u}^2 \right) \frac{\partial \bar{\xi}}{\partial x} + \frac{\partial}{\partial y} \left(\frac{1}{R} + \tau_{22} \bar{v}^2 \right) \frac{\partial \bar{\xi}}{\partial y}$$

(5.6)

which we approximate at all interior grid points by

$$\begin{aligned}
 & \frac{\epsilon_{1j}^{n+1} - \epsilon_{1j}^n}{\Delta t} = \dots \frac{(u_{1j}^n (\epsilon_{1+1,j}^n + \epsilon_{1j}^n) - u_{1-1,j}^n (\epsilon_{1j}^n + \epsilon_{1-1,j}^n))}{2\Delta x_n} - \frac{(v_{1j}^n (\epsilon_{1,j+1}^n + \epsilon_{1j}^n) - v_{1,j-1}^n (\epsilon_{1j}^n + \epsilon_{1,j-1}^n))}{2\Delta y} \\
 & - \epsilon_{1j}^n \theta_n + \left(\frac{1}{R} + T_{11} \overline{v_{1j}^{2n}} \right) \frac{\epsilon_{1+1,j}^n - \epsilon_{1j}^n}{(\Delta x_n)^2} - \left(\frac{1}{R} + T_{11} \overline{u_{1-1,j}^{2n}} \right) \frac{\epsilon_{1j}^n - \epsilon_{1,j-1}^n}{(\Delta x_n)^2} \\
 & + \left(\frac{1}{R} + T_{22} \overline{v_{1j}^{2n}} \right) \frac{\epsilon_{1,j+1}^n - \epsilon_{1j}^n}{(\Delta y)^2} - \left(\frac{1}{R} + T_{22} \overline{v_{1,j-1}^{2n}} \right) \frac{\epsilon_{1j}^n - \epsilon_{1,j-1}^n}{(\Delta y)^2}
 \end{aligned}$$

(5.9)

and at a boundary point by an equation similar to (5.15) which is for the corner point $i = 1, j = 1$. The \overline{u}_{ij}^2 are computed from (5.33) and \overline{v}_{ij}^2 from a similar relation that we have not written out. U' and δ' appearing in (5.15) are computed from (5.13) and (5.14) respectively. The Green's function used in the computation of \overline{u}_{ij}^2 and \overline{v}_{ij}^2 is computed by solving the system of equations (5.18), (5.19) et.al. using the method described in section V.B. In (5.34) the stream function is found from the Green's function, and U_{ij} is computed from (5.35) and V_{ij} from (5.36).

The ζ equation used in this problem is

$$\begin{aligned} \frac{\partial \zeta}{\partial t} = & -(\vec{U}_c + \vec{U}) \cdot \nabla \zeta - 2\zeta\theta + \frac{\partial}{\partial x} \left(\frac{1}{R} + T_{11} \overline{u}^2 \right) \frac{\partial \zeta}{\partial x} \\ & + \frac{\partial}{\partial y} \left(\frac{1}{R} + T_{22} \overline{v}^2 \right) \frac{\partial \zeta}{\partial y} + 2 T_{11} \overline{u}^2 \left(\frac{\partial \zeta}{\partial x} \right)^2 \\ & + 2 T_{22} \overline{v}^2 \left(\frac{\partial \zeta}{\partial y} \right)^2 - \frac{2\zeta}{\lambda_d^2 R} \end{aligned} \quad (5.7)$$

which we approximate at interior grid points by

$$\begin{aligned}
& \frac{c_{ij}^{n+1} - c_{ij}^n}{\Delta t} = \frac{\left(u_{ij}^n (c_{i+1,j}^n + c_{ij}^n) - u_{i-1,j}^n (c_{ij}^n + c_{i-1,j}^n) \right)}{2\Delta x_n} - \frac{\left(v_{ij}^n (c_{i,j+1}^n - c_{ij}^n) - v_{i,j-1}^n (c_{ij}^n + c_{i,j-1}^n) \right)}{2\Delta y} \\
& - 2c_{ij}^n \theta_n + \left(\frac{1}{R} + \tau_{11} \frac{\tau_2^n}{u_{ij}^n} \right) \frac{c_{i+1,j}^n - c_{ij}^n}{(\Delta x_n)^2} - \left(\frac{1}{R} + \tau_{11} \frac{\tau_2^n}{u_{i-1,j}^n} \right) \frac{c_{ij}^n - c_{i-1,j}^n}{(\Delta x_n)^2} \\
& + \left(\frac{1}{R} + \tau_{22} \frac{\tau_2^n}{v_{ij}^n} \right) \frac{c_{i,j+1}^n - c_{ij}^n}{(\Delta y)^2} - \left(\frac{1}{R} + \tau_{22} \frac{\tau_2^n}{v_{i,j-1}^n} \right) \frac{c_{ij}^n - c_{i,j-1}^n}{(\Delta y)^2} \\
& + \tau_{11} \frac{\tau_2^n}{u_{ij}^n} \left(\frac{\bar{c}_{i+1,j}^n - \bar{c}_{ij}^n}{\Delta x_n} \right)^2 + \tau_{11} \frac{\tau_2^n}{u_{i-1,j}^n} \left(\frac{\bar{c}_{ij}^n - \bar{c}_{i-1,j}^n}{\Delta x_n} \right)^2 \\
& + \tau_{22} \frac{\tau_2^n}{v_{ij}^n} \left(\frac{\bar{c}_{i,j+1}^n - \bar{c}_{ij}^n}{\Delta y} \right)^2 + \tau_{22} \frac{\tau_2^n}{v_{i,j-1}^n} \left(\frac{\bar{c}_{ij}^n - \bar{c}_{i,j-1}^n}{\Delta y} \right)^2 - \frac{2}{\lambda_d^2 R} c_{ij}^n
\end{aligned} \tag{5.10}$$

and at a wall we use an equation of which (5.16) for the corner $i = 1, j = 1$ is a typical example.

We will report here the results of simulations of the turbulent flow during the compression stroke in our two dimensional model of an internal combustion engine cylinder. Until such time as useful experimental measurements of the flow in a cylinder are made, an assessment of the accuracy of these computations cannot be made. In the future we hope to make a visual comparison of our computed solutions with some laser schlieren photographs of the flow in a cylinder being taken at Berkeley by A.K. Oppenheim, et.al. (1976). Also we should note that there has recently been a start at obtaining quantitative data, (see Witze (1975)) of the flow in a cylinder, but as of the moment the measurements were made at only one point in the flow and this will be of no use to us in establishing the truth of our predictions.

To initiate our solutions we will assume that $\bar{\xi}_{ij}^0 = 0$ and $\zeta_{ij}^0 = .1$ for all i,j for all of the computations reported here. These initial conditions amount to an initial low level of turbulence with no mean currents. This will allow us to clearly observe the motion generated by the piston.

To have a non-trivial solution we must also give initial values to the quantities $\bar{\xi}_{w_i}$ in (5.11). This will have the effect of putting a small amount of vorticity into the fluid while the piston moves during the first time step. We will set

$$\bar{\xi}_{w_i}^0 = U_{C_i} (\Delta t) \sqrt{\frac{R}{\pi \Delta t}}$$

which is the value it would have at the wall at time Δt in a flow impulsively moved with the velocity $U_c(\Delta t)$.

We will present the results of simulations for two cases. In the first, we have set $R = 5000$, $\chi = 8$ and $\sigma = 1$, values which are of the magnitude commonly found in engines. The second case differs from the first only in that $\sigma = 2$. Our grid will have $M = 16$ and $N = 12$, and most computations were done with $\Delta t = .01$. Also we have assumed that $T_{11} = T_{22} = .4$ and $\lambda_x = \sqrt{5} \Delta x$ and $\lambda_y = \sqrt{5} \Delta y$.

The computations proved to be largely independent of both grid size and time step. The largest source of disagreement between computations done with different time steps arose during the interval $t = .9 - 1$. when considerable amounts of ζ which had been generated previously by the piston motion were then being increased greatly by the term $-2 \theta \zeta$ in equation (5.7). Considering the precipitous drop of $\theta(t)$ shown in Figure 15 as $t \rightarrow 1$, we see that the smaller Δt is, the greater the magnification of ζ will be.

Figures 15 and 17 show a contour plot of $\bar{\psi}_{ij}$ for the first case for the times $t = .5$ & $1.$, respectively. Figure 18 shows a plot of the mean vorticity distribution for this case at $t = 1$ while Figure 19 shows the distribution of ζ at $t = 1$.

Figures 17, 18 and 19 represent our predictions of the mean flow properties existing in the cylinder at the time of ignition. It is apparent that the great amount of turbulence and vorticity generated in the corners has not diffused very far into the flow field and certainly not into the vicinity of the sparkplug. This result would mean that a spark set off in this environment would create an essentially

laminar flame which after burning sufficiently far into the flow would become turbulent.

Figure 20 shows a plot of $\bar{\psi}_{ij}$ at $t = 1$ for $\sigma = 2$ and Figure 21 shows the corresponding ζ field. When $\sigma = 2$, the piston must travel a longer distance than when $\sigma = 1$ and also attains a higher velocity. These figures show that there is quite a good deal more turbulence and vorticity generated in this case. The combustion process occurring after ignition in this environment would most likely be significantly different than the one occurring in the previous case.

VI. CONCLUSIONS AND FUTURE WORK

We have attempted in this thesis to develop and present the method of coarse graining in a manner which sharply distinguishes between what we may assert with confidence to be true about a turbulent flow and what is either an hypothesis or as yet unknown to us. It is only in this way that a precise and complete theory of turbulence may emerge. On the boundary between our knowledge and ignorance may be found well defined problems whose solution will extend the applicability of this approach. Thus we expect that coarse graining is evolutionary in nature, and will continue to be refined and improved in the future.

The transport law (3.18) that we have derived should represent a special case of a more general transport law. For example, it is conceivable that the effect of the molecular diffusion of the quantity ϕ could be incorporated into a more general version of (3.18). This would permit a more careful study to be made of the flow at the range of Reynolds numbers just above the transition to turbulence.

Another direction to proceed in generalizing (3.18) is to enable it to account for the turbulent diffusion of vorticity in a three dimensional flow. To do this it would have to account for the effect of the stretching and rotation of vortex filaments as they are diffused. This is precisely the type of problem which could benefit from the results of experiments into the nature of vorticity dynamics in a turbulent flow.

The transport law (3.18) betrays our inability to predict the small scale motion of a turbulent fluid by its inclusion of the

Lagrangian integral time scale T_{ij} and the other integral parameters. We may assume that the source of this difficulty has to do with the nature of turbulent diffusion itself and is not a quirk of our particular transport law. Thus we expect that in all turbulent diffusion models our ignorance of the small scale motion will require us to include indeterminable parameters such as T_{ij} . This phenomenon should be viewed the same as our experience with the molecular viscosity: In gases of a very special nature it may be predicted theoretically but in dense gases and liquids it must be found by experiment. So too we may imagine that in some turbulent flows T_{ij} may be predicted theoretically but in others it must be found experimentally or by analogy to similar flows where it has been determined previously. It thus seems that the search for 'flow' independent parameters in turbulence models may not be justified.

Our experience with the transport law (3.18) should teach us that in the design of a more sophisticated transport law of the types we have suggested, we should be open to the possibility that we will need to incorporate new time and length scales into it. These scales would be reflective of some aspect of the physical phenomenon that is being modeled.

Another area of investigation should be to determine the relationship of the vorticity microscales λ_x and λ_y to the size of the region for which the statistical hypothesis mentioned in section III.D. is valid. Also, the question as to whether or not a connection exists between the various lengths and time scales should be studied.

Our considerable success in solving for the mean flow in a channel shows that many of the physical processes found in a turbulent flow are being well represented by the method of coarse graining. This is an encouraging sign that if coarse graining were to be extended to three dimensions that it would be successful in predicting the mean properties of real turbulent flows.

The extension of coarse graining to three dimensional turbulent flows is complicated by the fact that we then need to follow the dynamics of all three components of vorticity. In addition, we would have to contend with modeling the process of vortex stretching which is of such major importance in the dynamics of turbulent flow.

Our work with the piston problem reported here represents a prelude to a much more extensive investigation of this flow, in which we will include the combustion process which arises after ignition. These computations will have to predict correctly the pressure pulse determined experimentally. In spite of the heavy-handedness with which we will be forced to deal with some of the aspects of the turbulent flow in the cylinder, a complete simulation of this flow and combustion by coarse graining even in 2-d would represent a great advance over any existing method.

VII. BIBLIOGRAPHY

- Batchelor, G. K., (1950), "Note on free turbulent flows, with special reference to the two-dimensional wake", J. Aero. Sci. 17 441
- Boussinesq, J., (1877), "Theorie de l'ecoulement tourbillant", Mem. pres. Acad. Sci. XXIII, 46, Paris
- Bradshaw, P. (1972), "The understanding and prediction of turbulent flow", Aero. J. 76 403
- Cebeci, T. and Smith, A.M.O. (1974) "Analysis of turbulent boundary layers," Applied Mathematics and Mechanics, 15 Academic Press.
- Chorin, A. J. (1974) "An analysis of turbulent flow with shear" College of Eng'g, UC - Berkeley Report No. FM-74-9
- Chorin, A. J. (1976) "Crude Approximations of turbulent flow", SYNSPADE 1975
- Clark, J. A. (1968) "A study of incompressible turbulent boundary layers in channel flow", J. Basic Eng'g. 90 455
- Comte-Bellot, T. (1965) "Ecoulement turbulent entre deux parois paralleles" Publications Scientifiques et Techniques du Ministere de L'air NO. 419
- Cooley, J. W. and Tukey, J. W. (1965) "An algorithm for the machine calculation of complex Fourier series." Math. Comput. 19, 297
- Corrsin, S. (1973) "Limitations of gradient transport models in random walks and in turbulence", Adv. in Geophysics, 18A, 25 (Academic Press)
- Daly, B. J. and Harlow, F. H. (1970) "Transport equations in turbulence," Phys. Fluids 13, 2634

- Deardorff, J. W. (1970) "A numerical study of three-dimensional turbulent channel flow at large Reynolds numbers," J. Fluid Mech., 41, 453
- Eckelmann, H. (1970), Experimentelle Untersuchungen in einer turbulente Kanalströmung mit starken viskosen Wandschichten. Mitt. Max-Planck Inst. f. Strömungsforschung, Göttingen no, 48
- Gear, C. W. (1969) A simple set of test matrices for eigenvalue programs" Math. Comp. 23 119
- Gikhman, I. I and Skorokhod, A. V. (1965) Introduction to the Theory of Random Processes, W. B. Saunders Co.
- Hanjalic, K. and Launder, B. E. (1976) "Contribution towards a Reynolds stress closure for low-Reynolds number turbulence", J.F.M. 74 593
- Harlow, F. H. (1968) "Transport of anisotropic or low-intensity turbulence", Los Alamos Scientific Laboratory Report No. LA-3947
- Hinze, J. O. (1959) Turbulence McGraw-Hill Book Co.
- Hirt, C. W. (1969) "Computer studies of time-dependent turbulent flows". Phys. Fluids Suppl. II 12 II-219
- Kao, T. W. and Park, C. (1970) "Experimental investigations of the stability of channel flow I", J. Fluid. Mech. 43 145
- Karman, Th. von (1930) Mechanische Ähnlichkeit und Turbulenz. Nach. Ges. Wiss. Göttingen, Math. Phys. Klasse, 58
- Lamb, H. (1932) Hydrodynamics 6th Ed. Dover
- Laufer, J. (1950) "Investigation of turbulent flow in a two-dimensional channel," NACA TN 1053
- Launder, B.E., REECE, G. J. and Rodi, W. (1975) "Progress in the development of a Reynolds-stress turbulence closure" J. Fluid Mech. 68 537

- Lumley, J. L. and Khajeh-Nouri, B. (1974) "Computational modeling of turbulent transport," Adv. in Geophysics, 18A, 169 (Academic Press)
- Oppenheim, A. K. et. al. (1976) "A cinematographic study of combustion in an enclosure fitted with a reciprocating piston", Proc. Conf. on Stratified Charge Engines Inst. Mech. Engrs. London, 11/23-25, 1976.
- Mellor, G. L. and Herring, J. J. (1973) "A survey of the mean turbulent field closure methods," AIAA Jour. 11 590
- Patankar, S. V. and Spalding, D. B. (1970) Heat and Mass Transfer in Boundary Layers, 2nd Ed., Intertext Books.
- Prandtl, L. (1925) "Uber die ausgebildeter Turbulenz. ZAMM 5 136
- Reynolds, W. C. (1974) "Recent advances in the computation of turbulent flows," Adv. in Chemical Engrg., 9, 193 (Academic Press)
- Reynolds, W. C. (1976) "Computation of Turbulent flows," Annual Rev. of Fluid Mech. 8 183 Annual Reviews Inc.
- Saffman, P. G., (1974) "Model equations for turbulent shear flow," Studies in App. Math., 53, 17
- Schlichting, H. (1968) Boundary Layer Theory 6th Ed. McGraw Hill
- Schumann, U. (1975) "Subgrid scale model for finite difference simulations of turbulent flows in plane channels & annuli". J. Comp. Phys. 18 376
- Smagorinsky, J., Manabe, S. & Holloway, J. L. (1965) "Numerical results from a nine-level general circulation model of the atmosphere" Mon. Weath. Rev. 93, 727.
- Taylor, G. I. (1915), "Eddy motion in the atmosphere," Phil. Trans. Roy. Soc. CCXV 1.

- Taylor, G. I., (1921) "Diffusion by continuous movements," Proc. Lon. Math. Soc. Ser. 2, 20 320
- Taylor, G. I. (1932) "The transport of vorticity and heat through fluids in turbulent motion", Proc. Roy. Soc. 135A 685.
- Taylor, G. I. (1935A) "Statistical theory of turbulence I" Proc. Roy. Soc. 151A 421
- Taylor, G. I. (1935b) "Distribution of velocity and temperature between concentric rotating cylinders." Pro. Roy. Soc. 151A 494
- Taylor, G. I. (1937) "Flow in pipes and between parallel planes", Proc. Roy. Soc. 159A, 496
- Tennekes, J. and Lumley, J. L. (1972) A First Course in Turbulence
MIT Press
- Townsend, A. A. (1961) "Equilibrium layers and wall turbulence".
Jour. Fluid Mech. 11 97
- Witze, P. O. (1975) "Hot-wire turbulence measurements in a motored internal combustion engine" Sandia Laboratories Report SAND75-8641

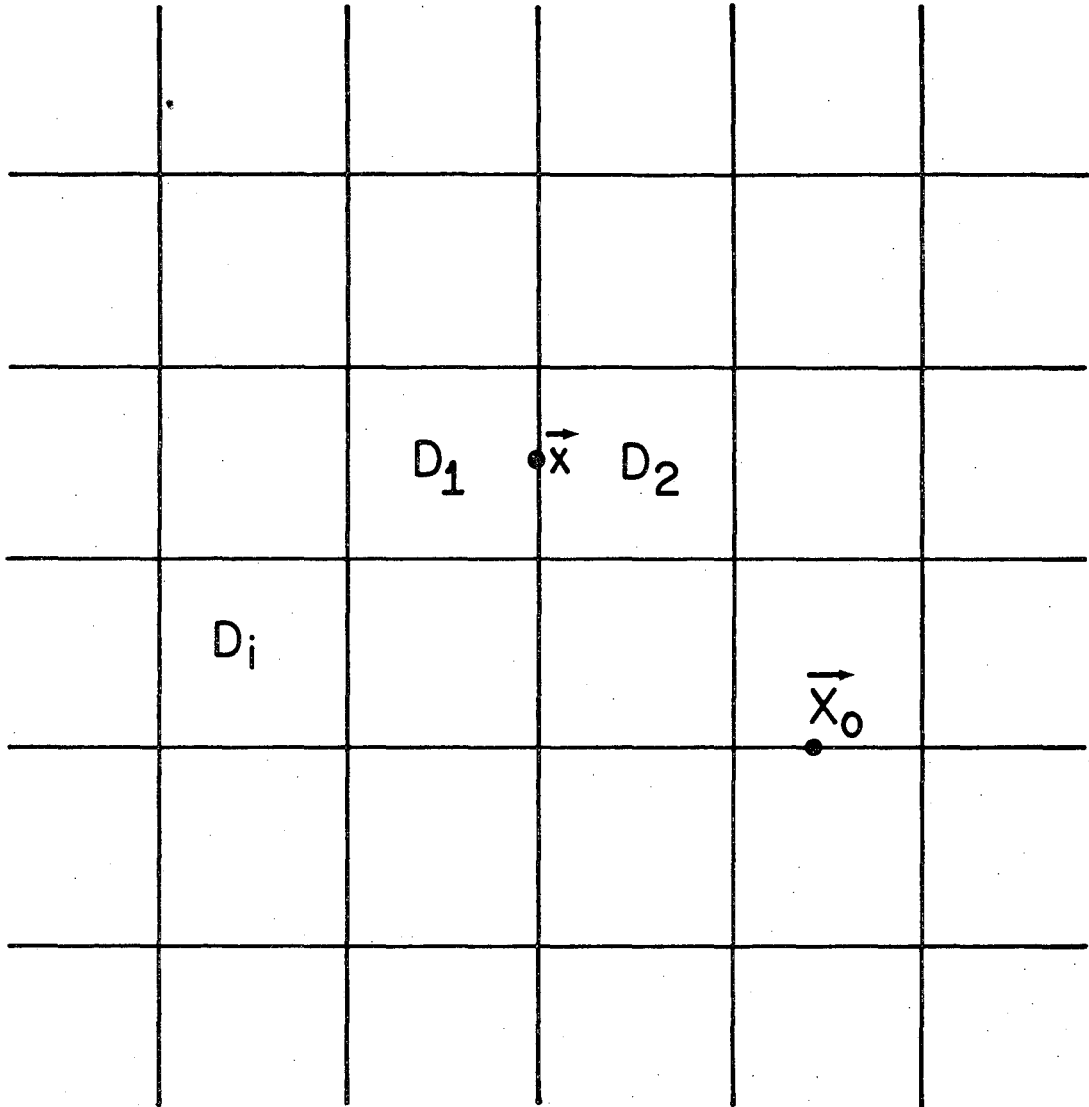


FIGURE 1

XBL 772-260

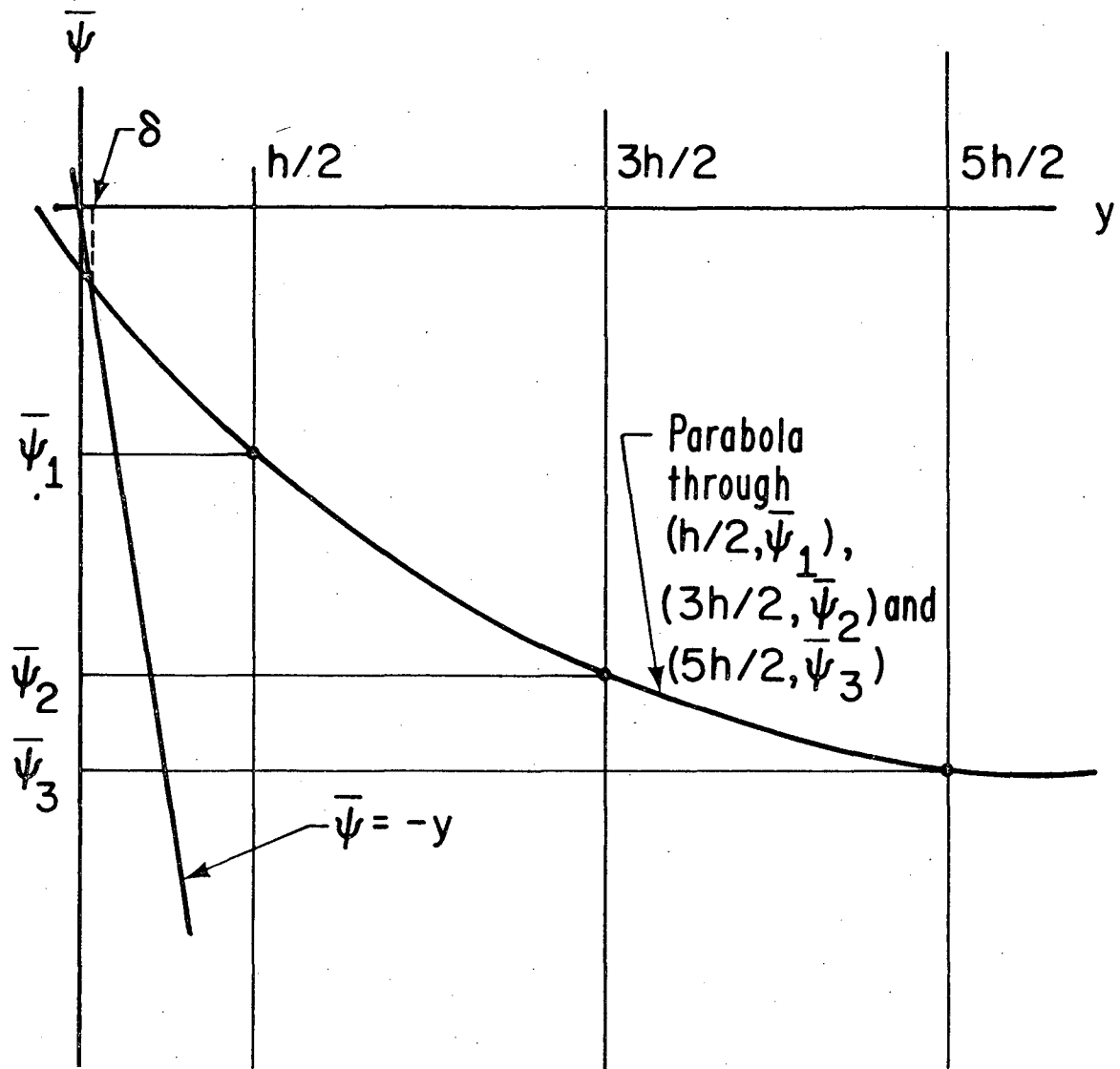


FIGURE 2

XBL 772-263

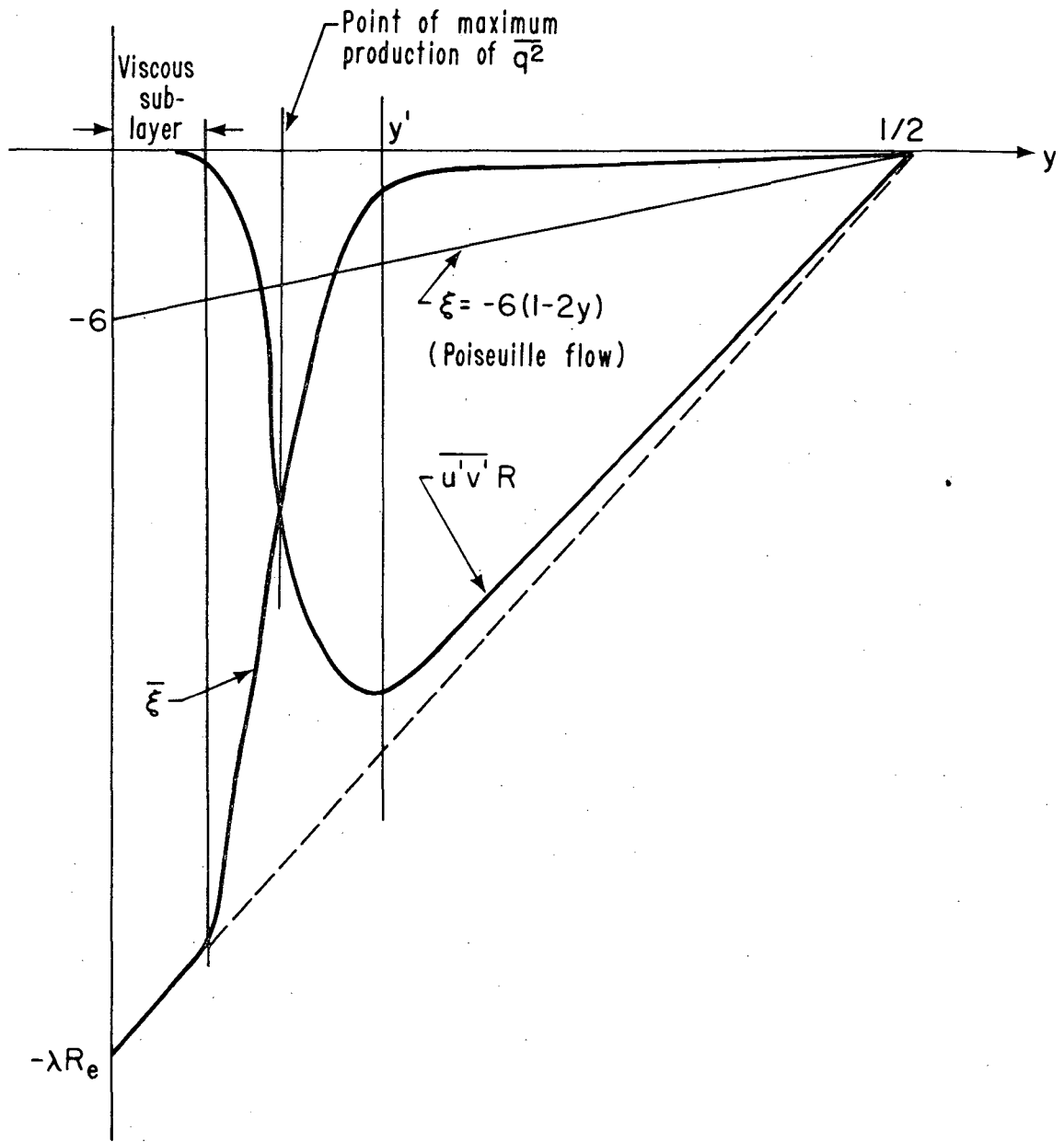


FIGURE 3

XBL 772-267

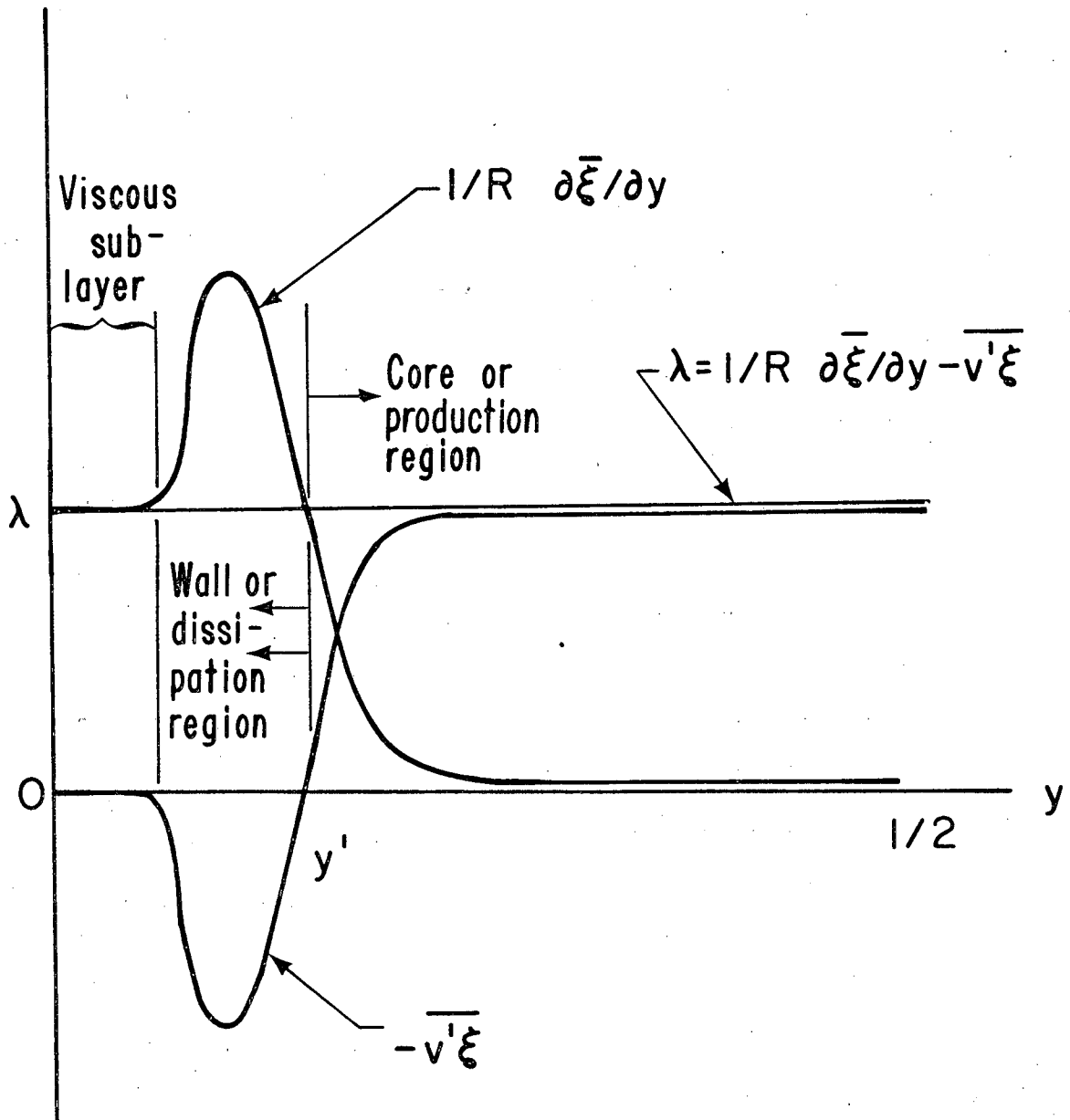


FIGURE 4

XBL 772-259

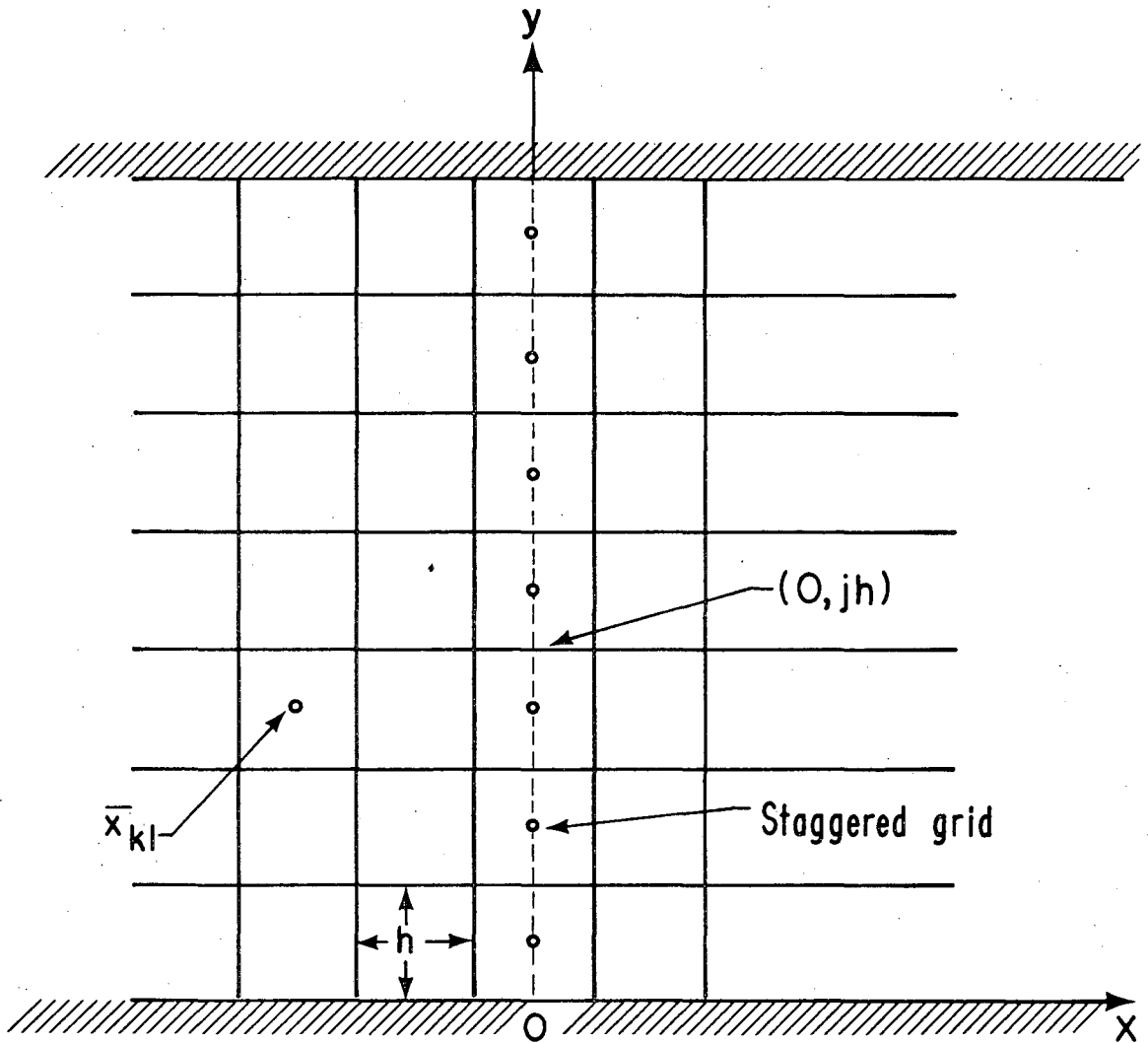


FIGURE 5

XBL 772-269

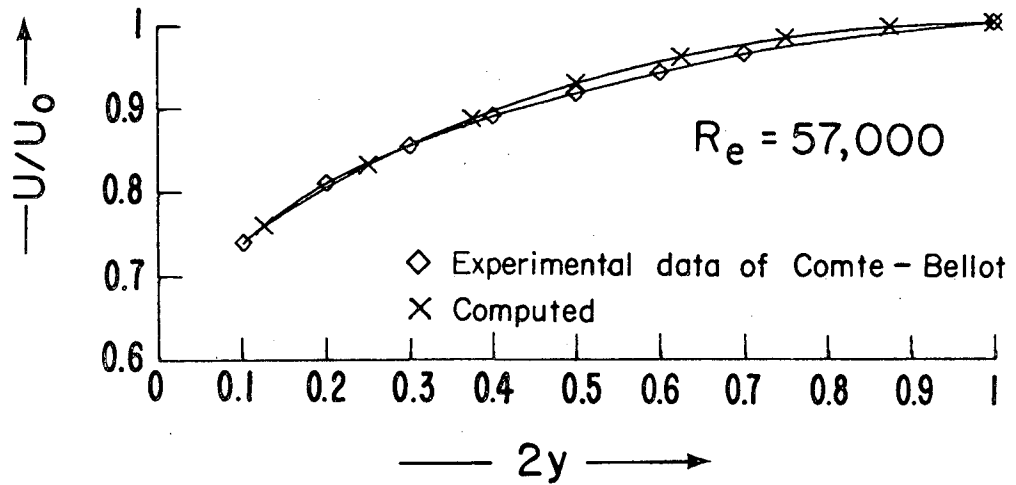
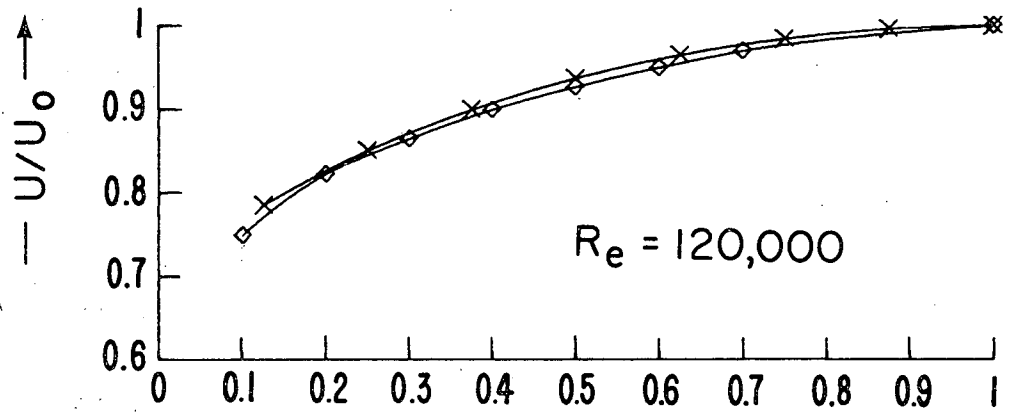
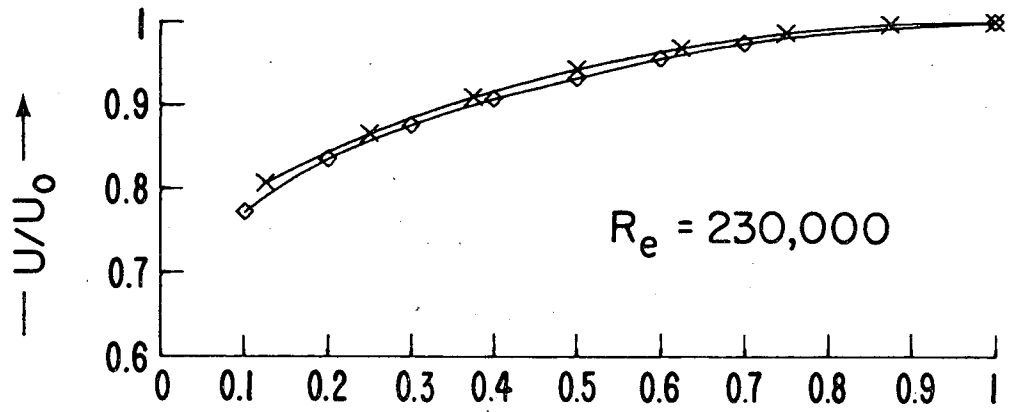
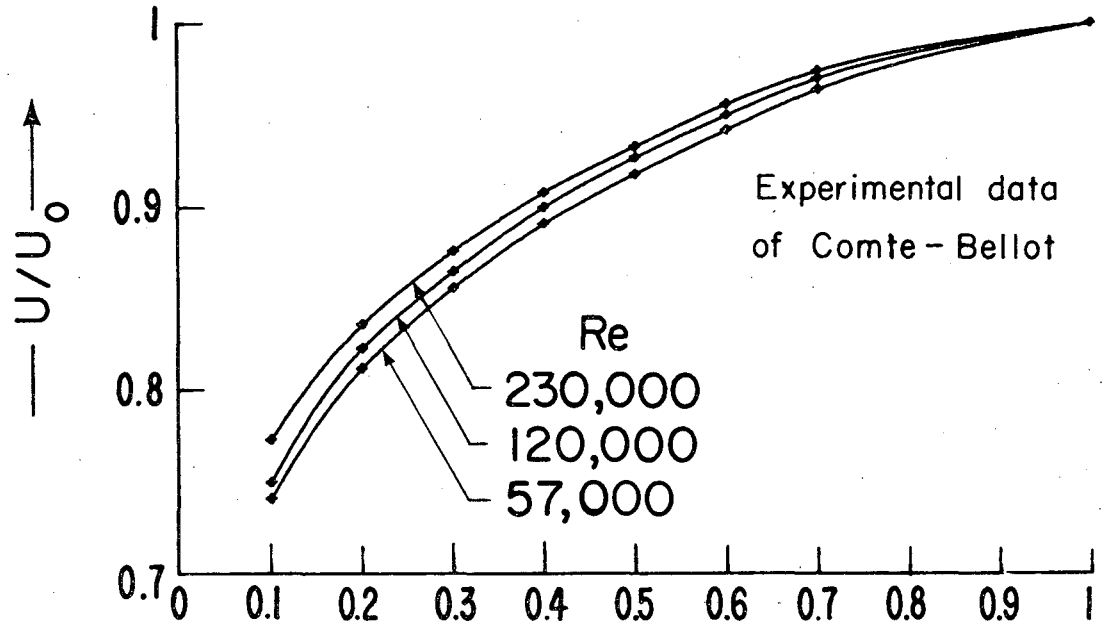
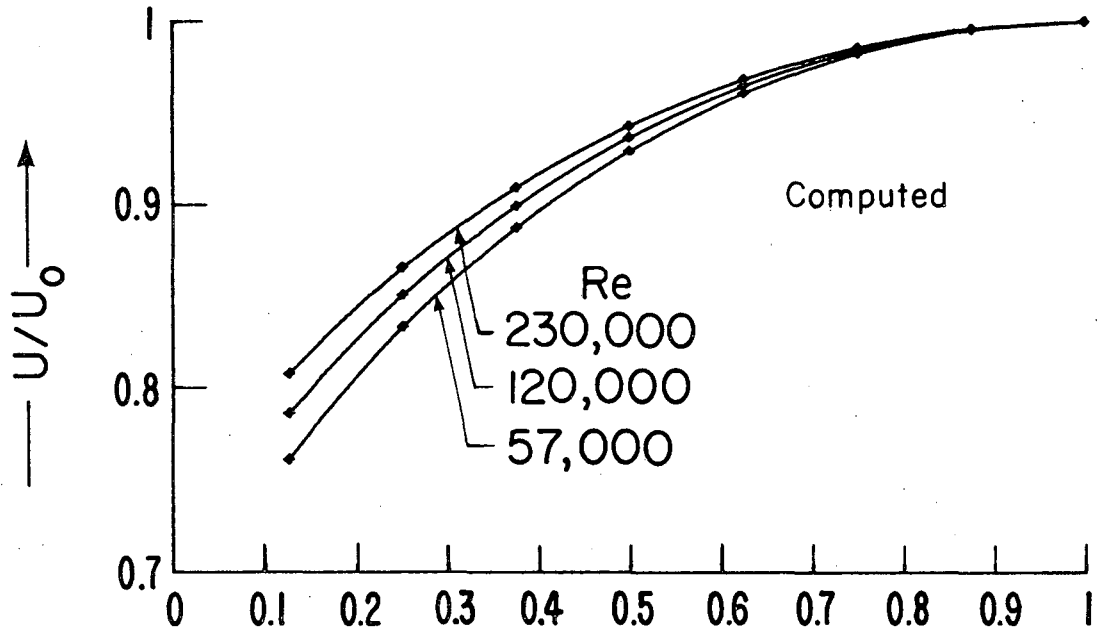


FIGURE 6

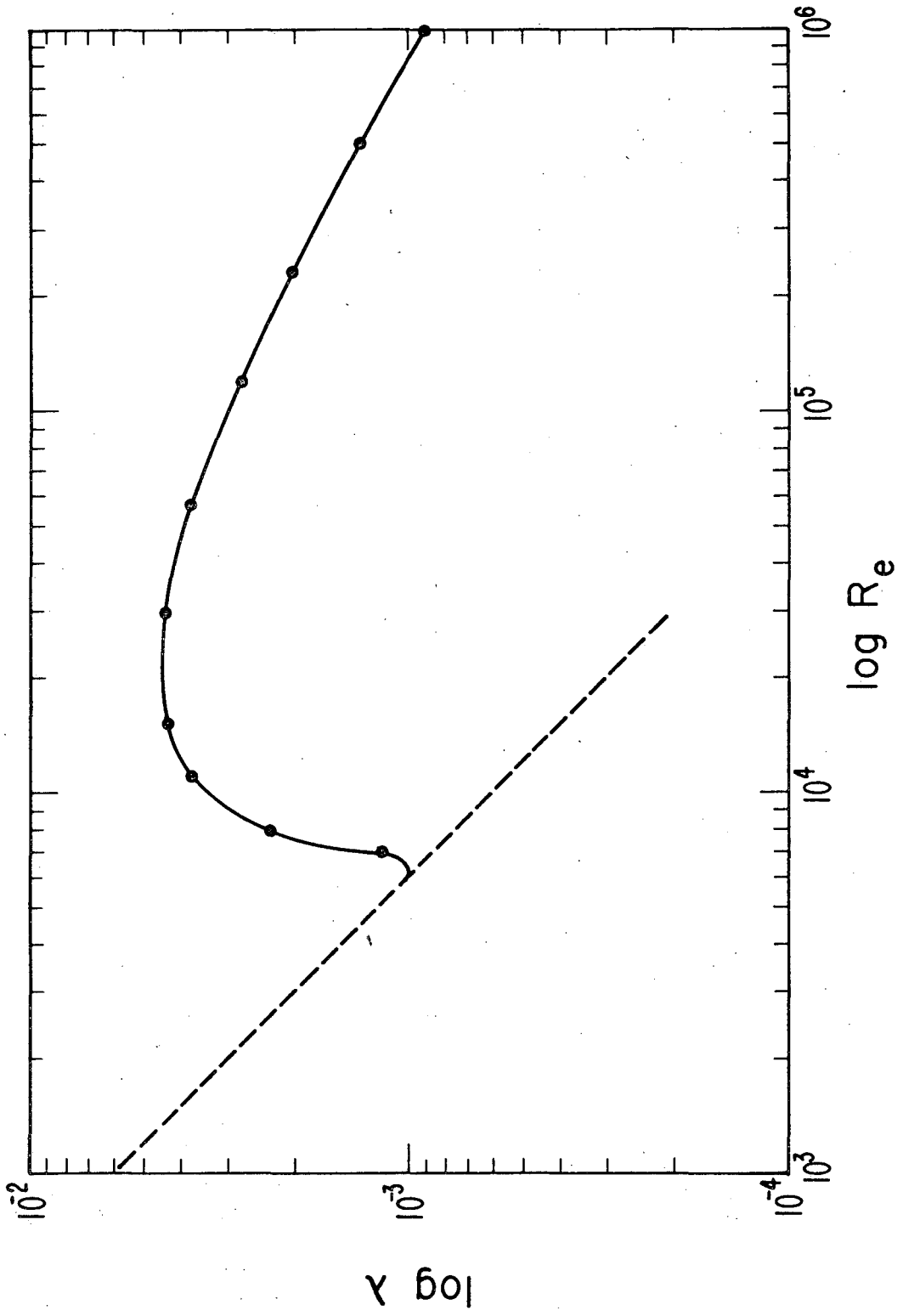
XBL 772-270



$2y$ →

FIGURE 7

XBL 772-271



XBL 772-268

FIGURE 8

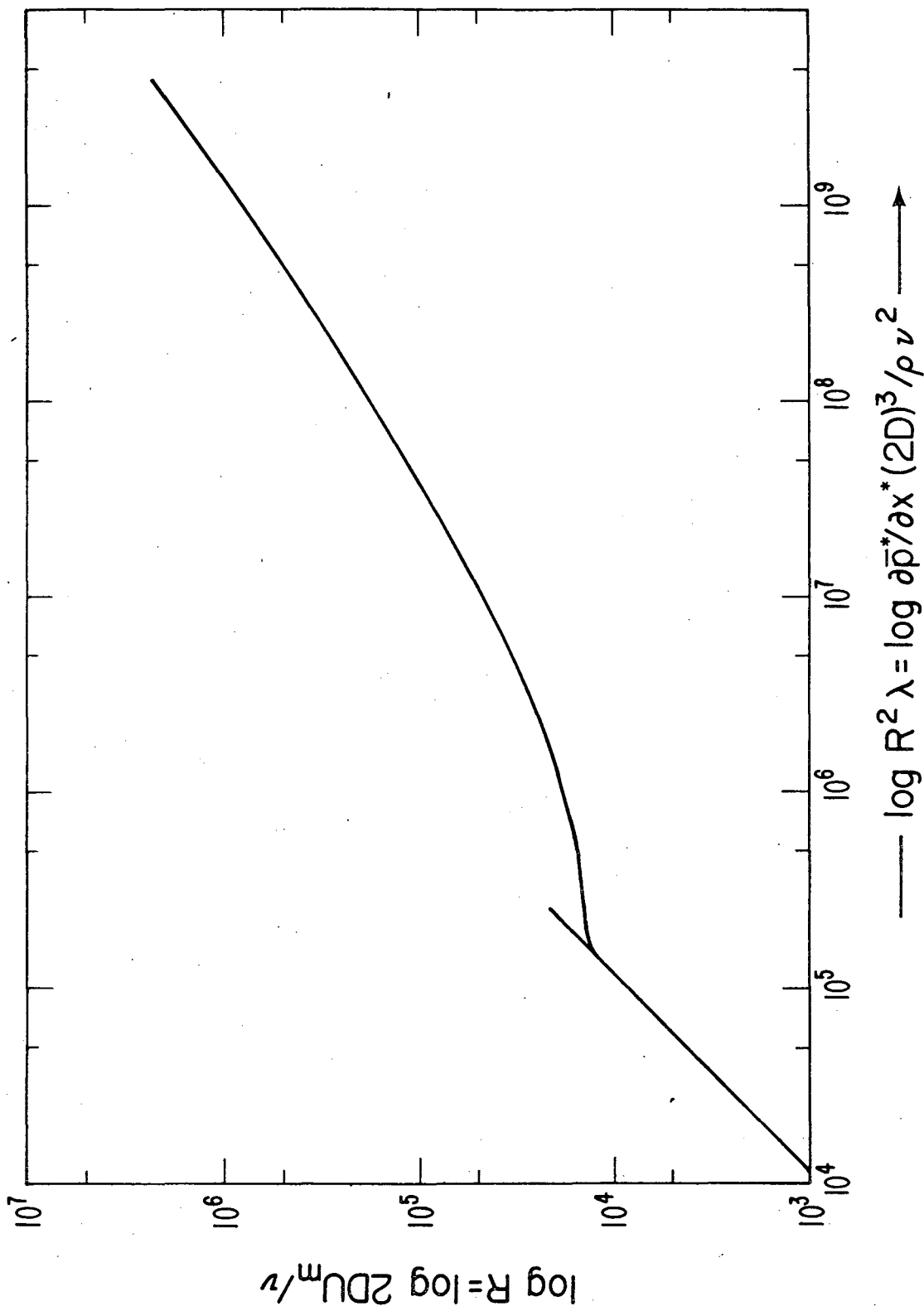


FIGURE 9

XBL 772-261

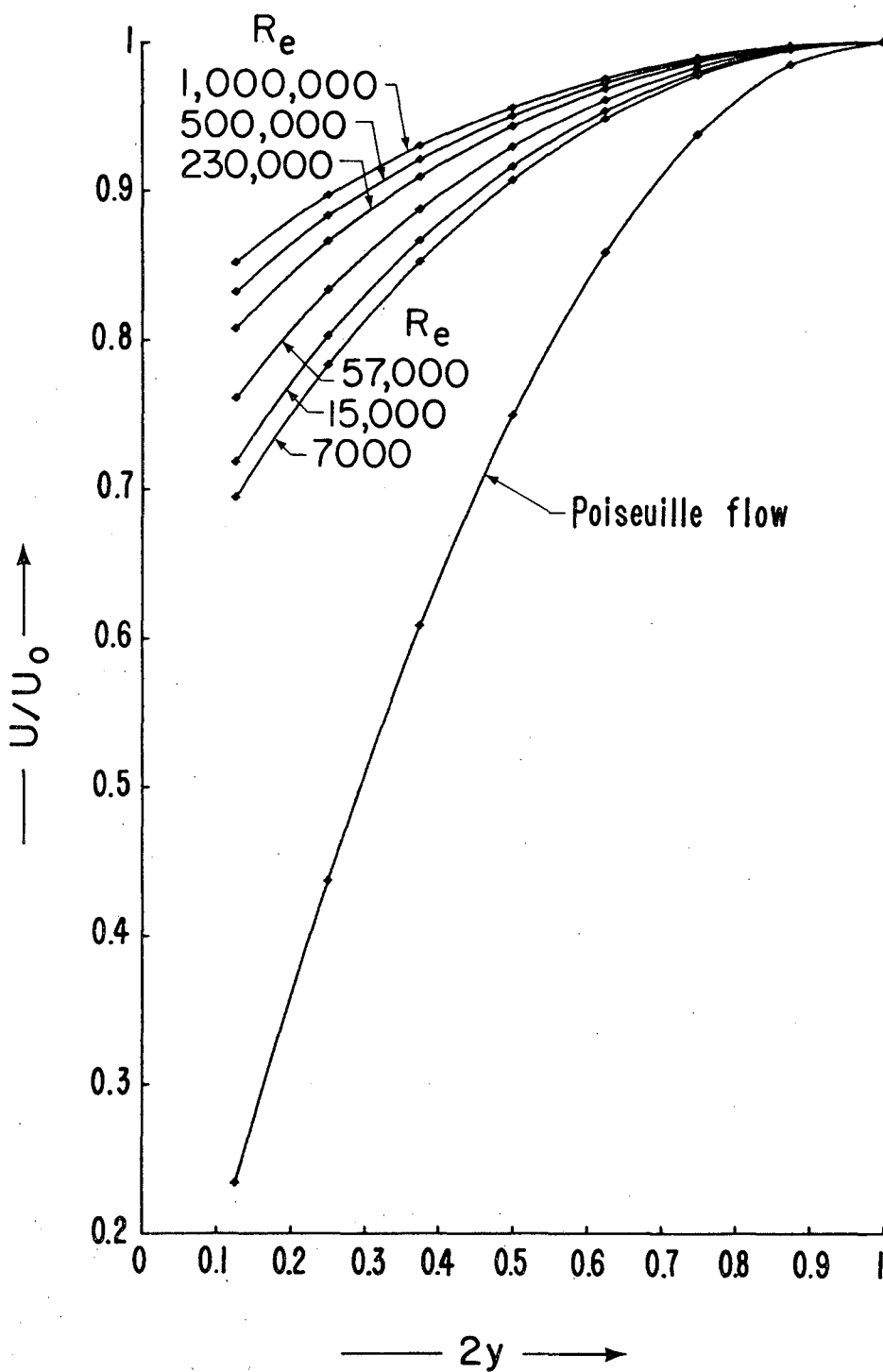


FIGURE 10

XBL 772-272

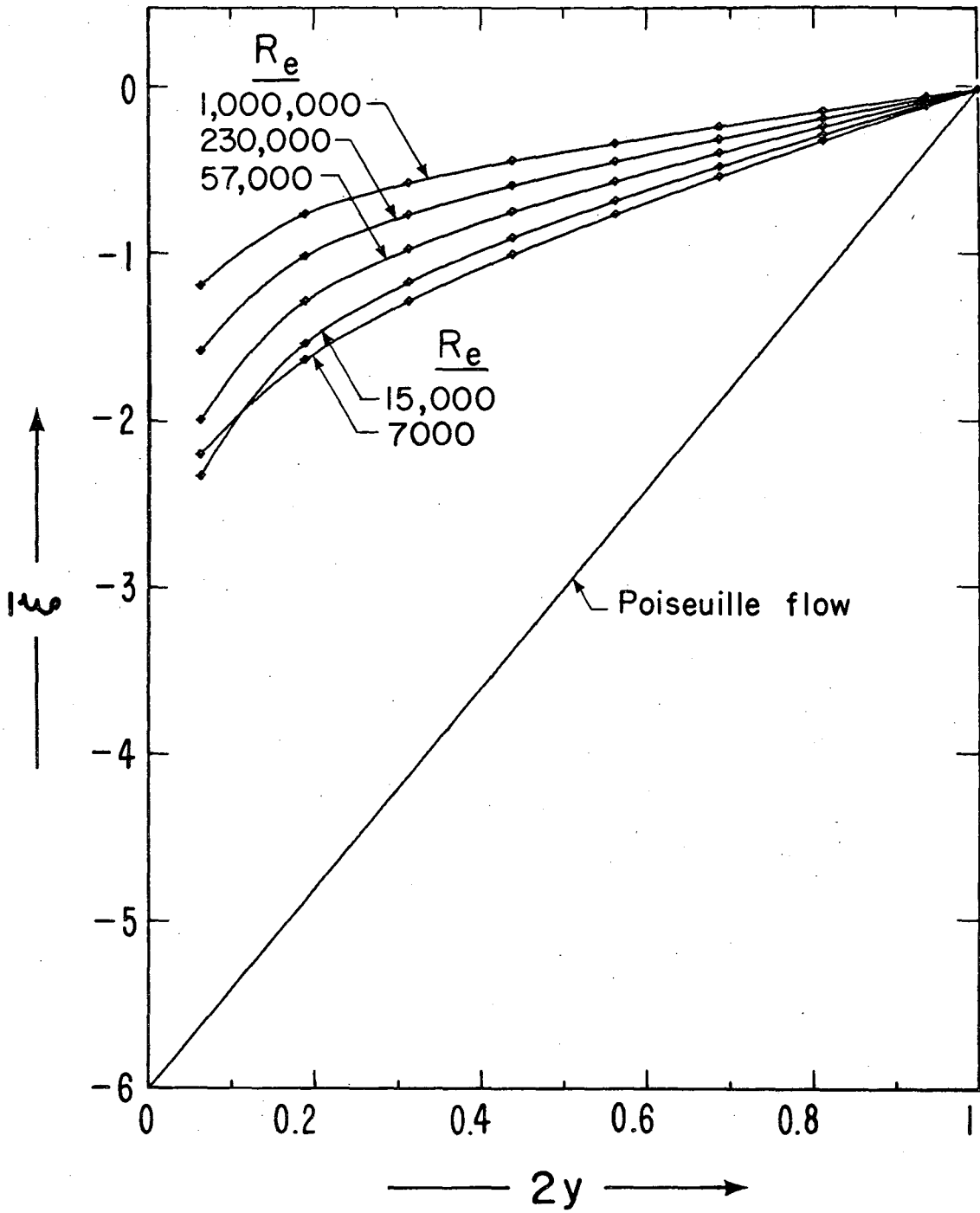


FIGURE 11

XBL 772-266

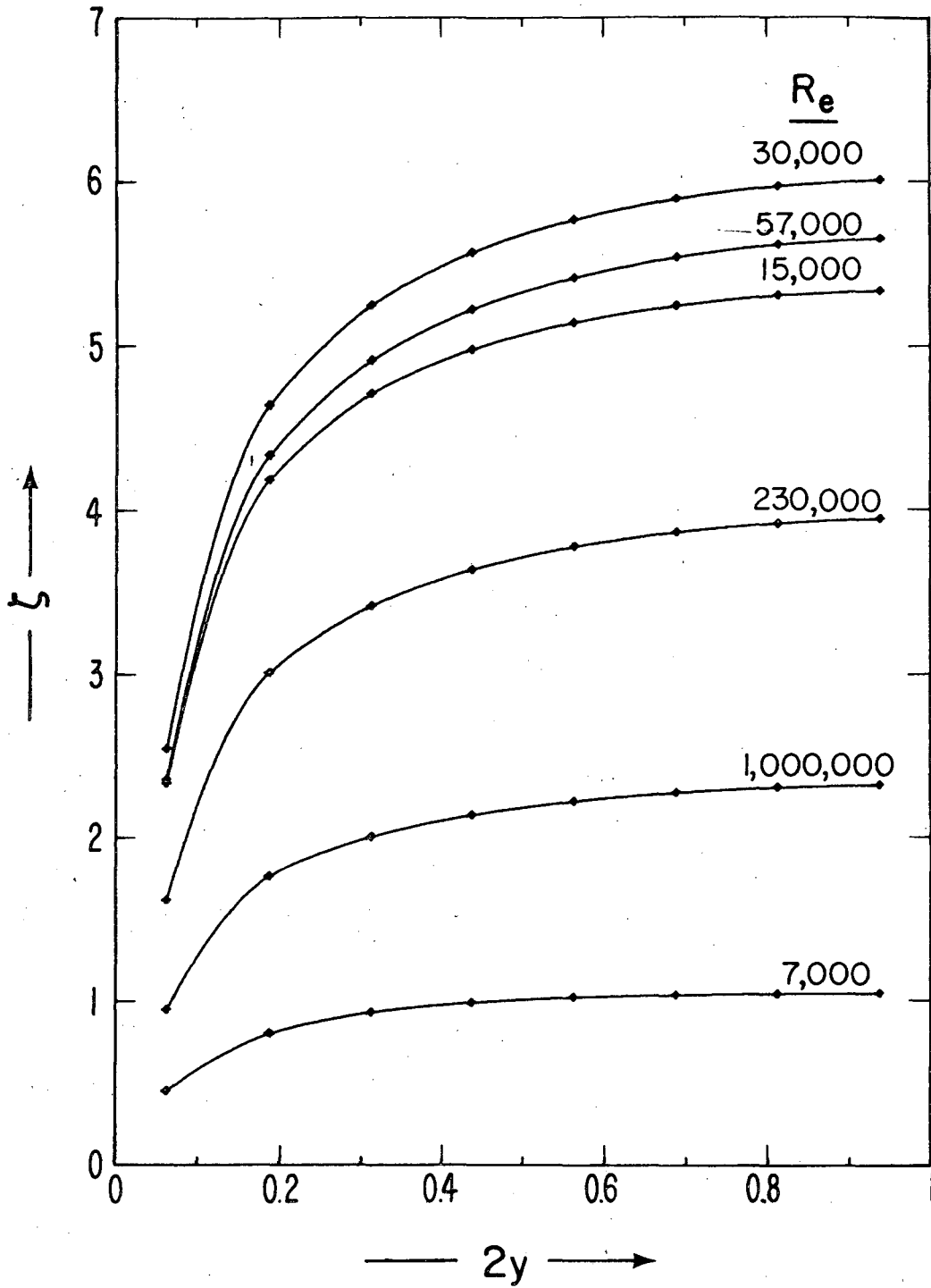


FIGURE 12

XBL 772-265

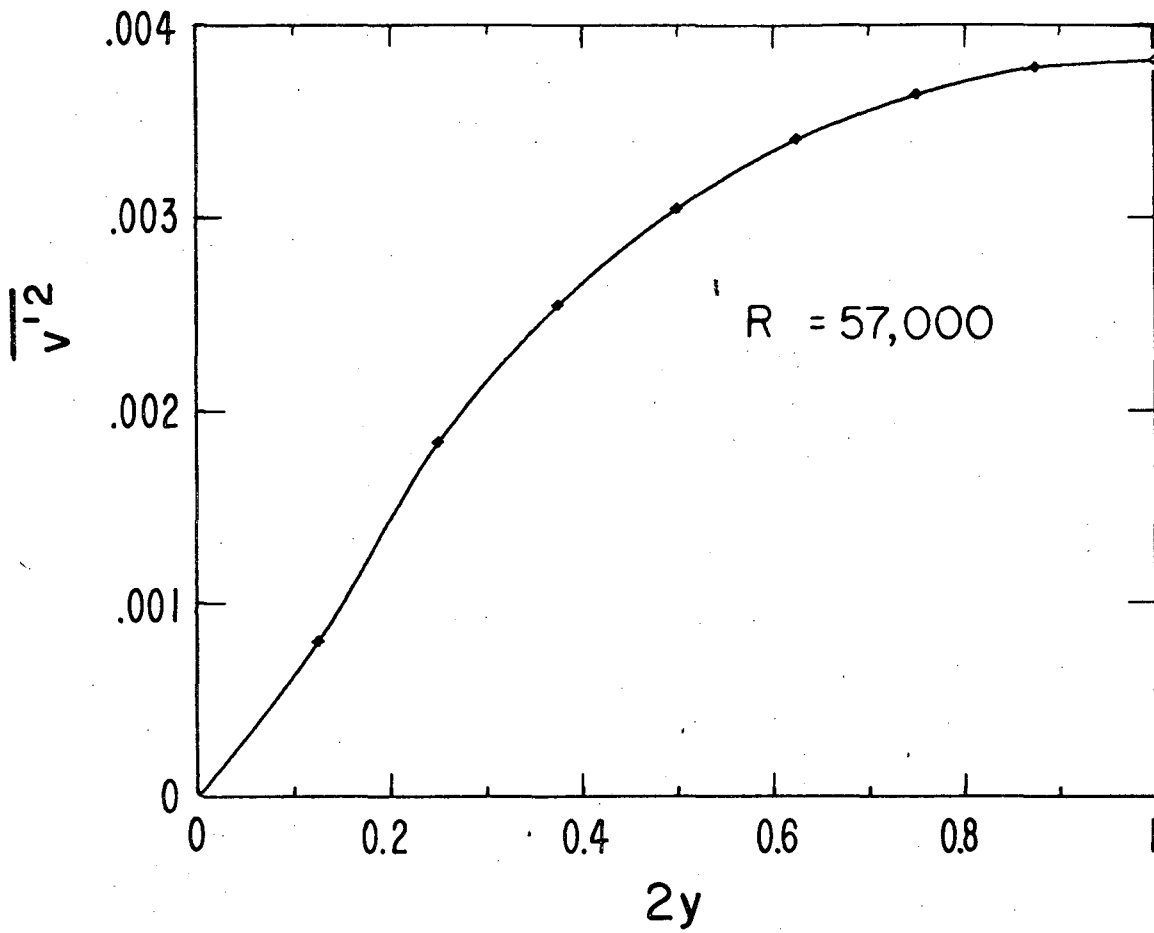


FIGURE 13

XBL 772-264

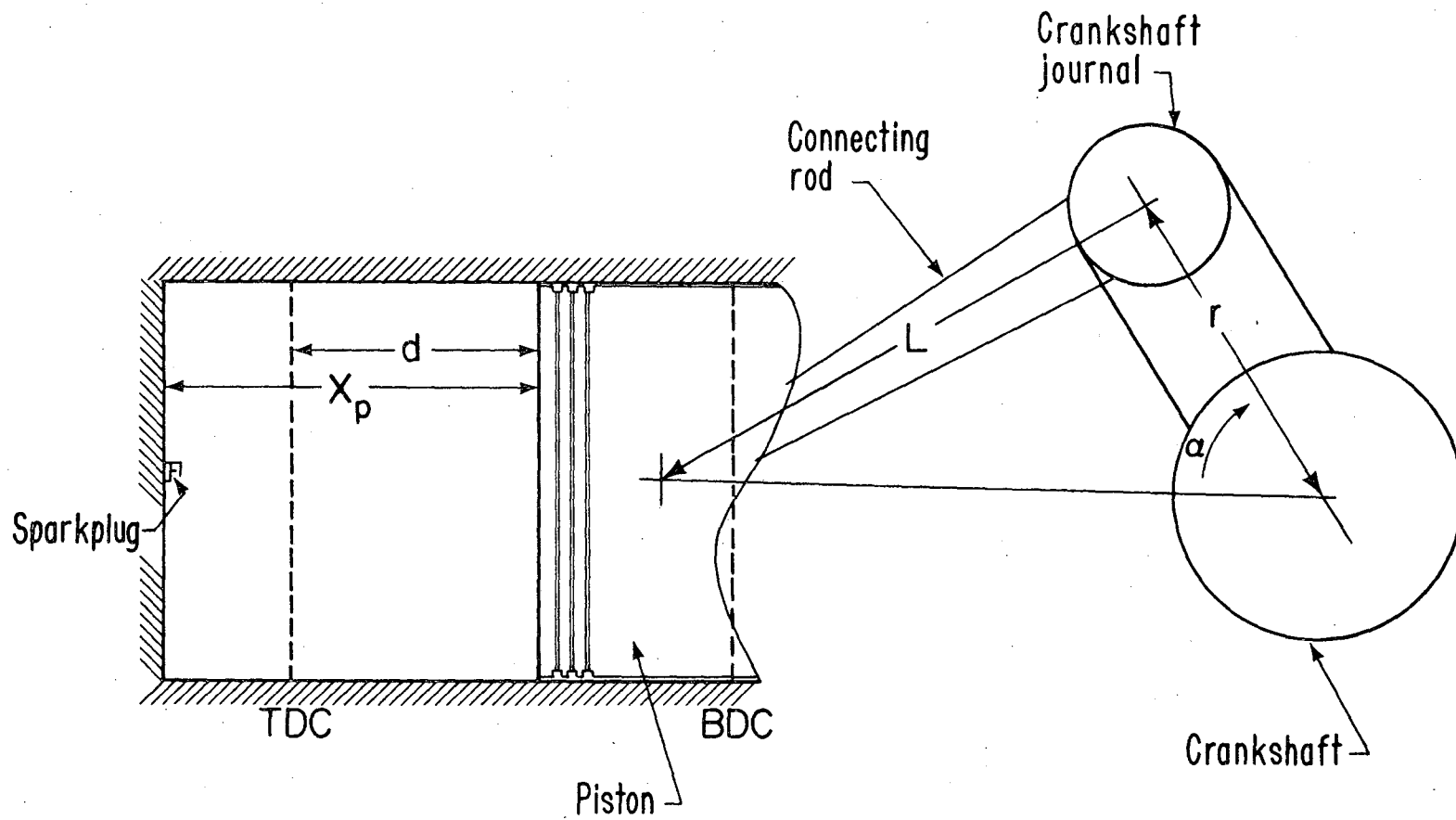


FIGURE 14

XBL 772-262

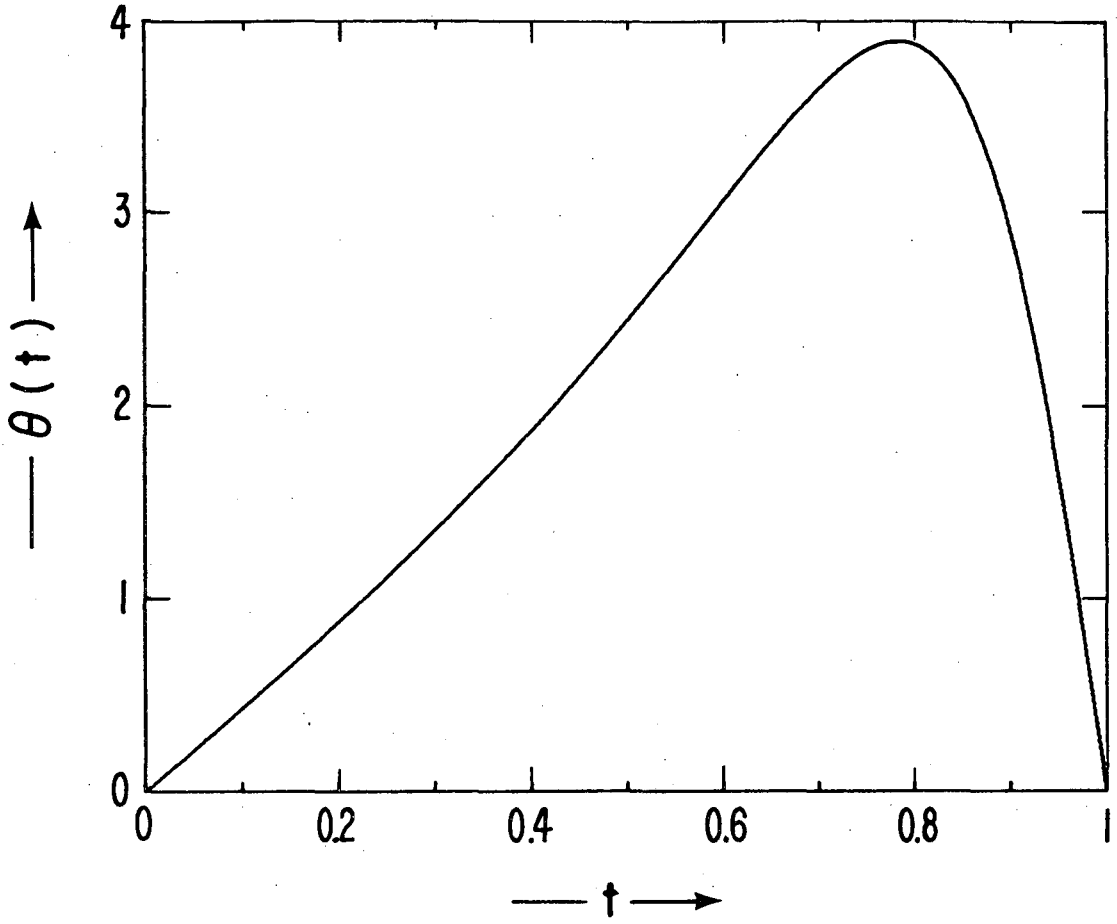
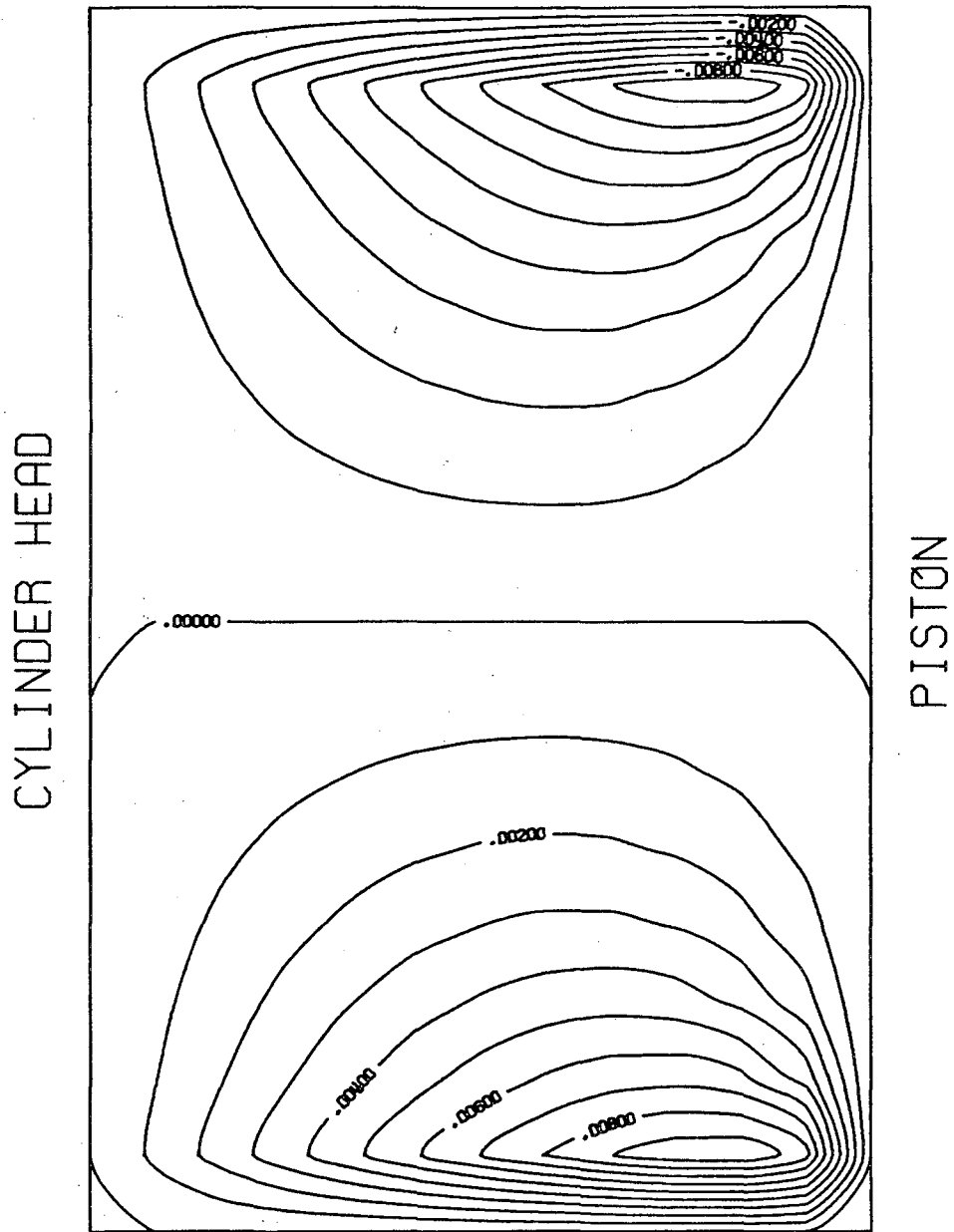


FIGURE 15

XBL 772-258

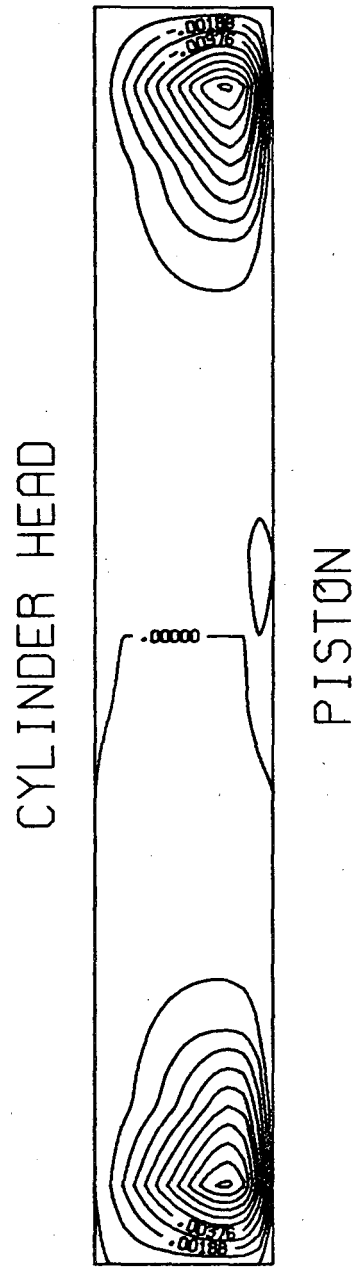


MEAN STREAM FUNCTION

STROKE TO BORE RATIO = 1. TIME = .5

FIGURE 16

XBL 772-273

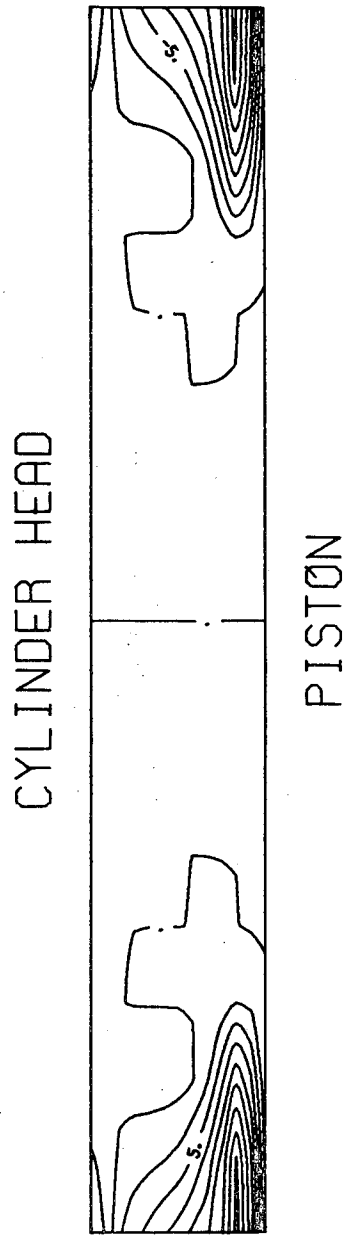


MEAN STREAM FUNCTION

STROKE TO BORE RATIO = 1. TIME = 1.

FIGURE 17

XBL772-274



MEAN. VORTICITY

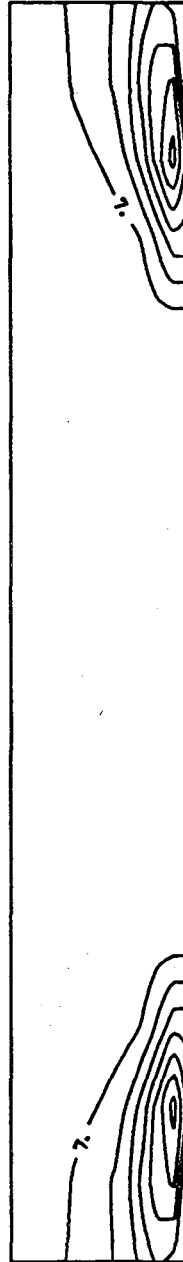
STROKE TO BORE RATIO = 1. TIME = 1.

FIGURE 18

XBL 772-275

CYLINDER HEAD

PISTON



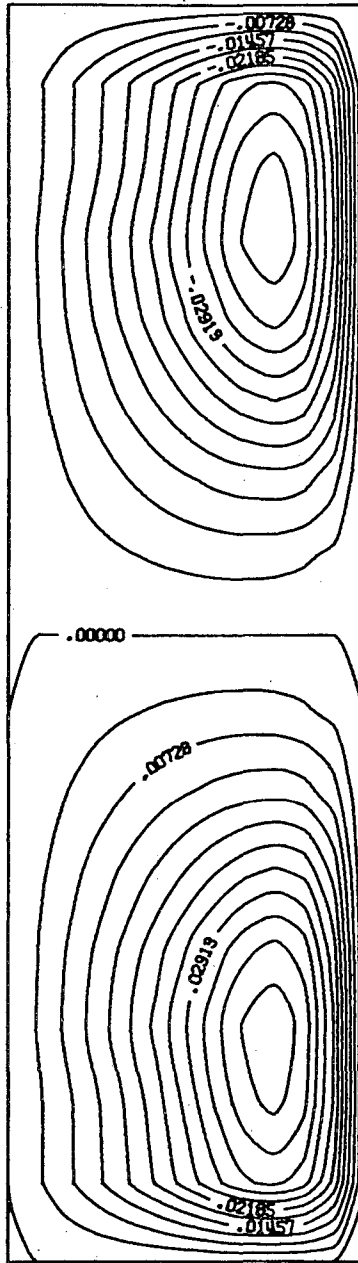
MEAN SQUARED FLUCTUATING VORTICITY

STROKE TO BORE RATIO = 1. TIME = 1.

FIGURE 19

XBL 772-276

CYLINDER HEAD



PISTON

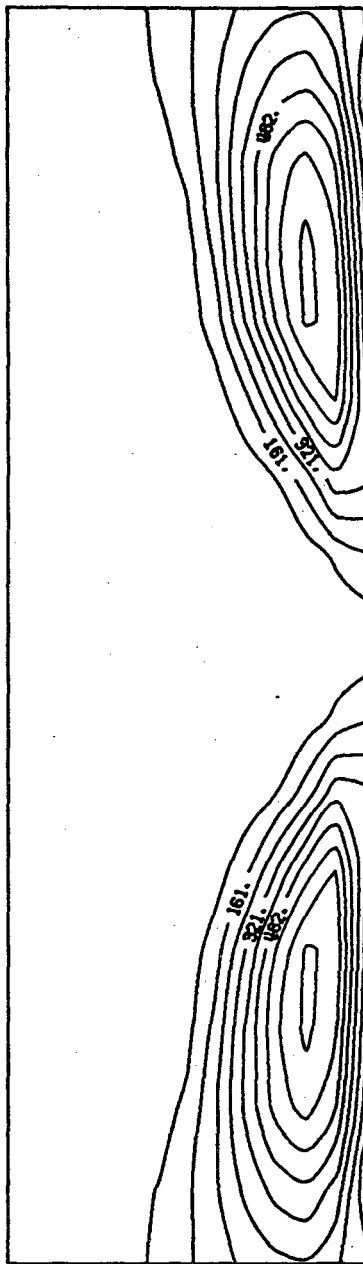
MEAN STREAM FUNCTION

STROKE TO BORE RATIO = 2. TIME = 1.

FIGURE 20

XBL 772-277

CYLINDER HEAD



PISTON

MEAN SQUARED FLUCTUATING VORTICITY

STROKE TO BORE RATIO = 2. TIME = 1.

FIGURE 21

XBL 772-282

This report was done with support from the United States Energy Research and Development Administration. Any conclusions or opinions expressed in this report represent solely those of the author(s) and not necessarily those of The Regents of the University of California, the Lawrence Berkeley Laboratory or the United States Energy Research and Development Administration.

TECHNICAL INFORMATION DIVISION
LAWRENCE BERKELEY LABORATORY
UNIVERSITY OF CALIFORNIA
BERKELEY, CALIFORNIA 94720